# Formation of Key Aroma Compounds Generated in Condensed Wood Smoke for the Flavoring of Foods

DISSERTATION

Presented in Partial Fulfillment of the Requirements for the Degree Doctor of Philosophy in the Graduate School of The Ohio State University

By

Timothy Daniel Vazquez

Graduate Program in Food Science and Technology

The Ohio State University

2022

Dissertation Committee

Devin G. Peterson, Ph.D., Advisor

Christopher T Simons, Ph.D.

Ken Lee, Ph.D.

C. Lynn Knipe, Ph.D.

Rajesh Potineni, Ph.D.

## Abstract

Condensed smoke, also known as liquid smoke, is a popular additive used in meats, sauces, soups, snacks, and meat alternatives. Formed from the aerosol generated during the pyrolysis of wood, condensed smoke offers superior versatility and cost compared to conventional smoke processing. The flavor attributes of condensed smoke are utilized to enhance the quality of food products, however, there is inadequate understanding of the compounds that impact flavor as well as process variables that influence flavor formation, which limits product innovation.

The overall aim of this dissertation was to identify the compounds that contribute to smoke aroma and to characterize the impact of wood structure aroma compound formation during wood pyrolysis.

In phase one Gas Chromatography/Mass Spectrometry/Olfactometry was utilized to identify aroma compounds that contribute to condensed smoke flavor. Twenty-seven odorants with a flavor dilution value $\geq 4$ were identified and quantified by GC/MS/MS in a mixed-hardwood condensed smoke, and four new odor threshold values were determined for 2-methyl-2-cyclopentenone, 3-methyl-2(5H)-furanone, 4-methylsyringol, and acetoxyacetone. Sensory descriptive analysis revealed the condensed smoke consisted of the eight main attributes ashy, burnt-sulfurous, creosote, green-woody, pungent, smoky, spicy-sweet, and woody. No significant differences in the aroma

attributes were reported between the condensed smoke and the corresponding recombination model, indicating that the identified compounds characterized the aroma attributes sufficiently.

In phase two, the impact of hardwood cell-wall structure on the generation of the aroma compound in condensed smoke was investigated utilizing untargeted Nuclear Magnetic Resonance (NMR) chemical profiling analysis. Six hardwood samples were utilized to generate condensed smoke samples, with aroma profiles characterized by a sensory panel and further quantified by GC/MS/MS. The cell-wall structures of the hardwood samples were characterized using Heteronuclear Single Quantum Coherence NMR. Six of the eight aroma attributes significantly varied among the condensed smoke samples, which were ashy, creosote, green-woody, smoky, spice-sweet, and woody. The wood NMR chemical profiles were modeled against the concentrations of 27 aroma compounds by Orthogonal Partial Least Squares Regression (OPLS-R) models with good fit and predictive ability (R2Y: 0.88-0.99, Q2: 0.73-0.97). Predictive NMR spectra revealed changes in hemicellulose, cellulose, and the methoxylation of wood lignin were key components during pyrolysis that impacted the generation of the aroma composition in condensed smoke.

In summary, this work advanced the molecular understanding of the flavor properties of condensed hardwood smoke and supports manufacturing and application strategies to enhance product quality.

## Dedication

To my grandparents who knew the value of education, to my parents for supporting me no matter what, and to Kim who always inspires me to be a better version of myself.

## Acknowledgments

I would like to acknowledge Dr. Devin Peterson for the incredible support and mentorship as my advisor and for creating a lab environment where students like me can grow and learn beyond expectations. I am grateful to Dr. Edisson Tello Camacho for his leadership, mentorship, and uplifting spirit. Thanks also to the rest of the lab who have all made this journey easier. I would also like to extend my gratitude to the rest of my committee: Dr. Ken Lee, who guided me through the beginning of my degree, Dr. Rajesh Potineni, who has generously created this opportunity for me, as well as Dr. Lynn Knipe, who has been an incredible source of expertise and experience on this project, and Dr. Chris Simons whose advice is always full of valuable insight.

## Vita

May 2015 B.S…… Biotechnology, Indiana University

August 2015 to present…….. Graduate Research Assistant, Food Science and Technology Department, The Ohio State University

## Fields of Study

Major Field: Food Science and Technology

## Table of Contents

## List of Tables

## List of Figures

## List of Abbreviations

ANOVA – analysis of variance

GC – gas chromatography

MS – mass spectrometry

GC/O- Gas chromatography olfactometry

NMR – nuclear magnetic resonance

HSQC – heteronuclear single quantum coherence

DA – descriptive analysis

OAV – odor activity value

FD – flavor dilution

AEDA – aroma extract dilution analysis

OPLS-R – orthogonal partial least squares regression

VIPpred- predictive variable influence on projection

PAH – Polycyclic Aromatic Hydrocarbon

TGA – Thermogravimetric Analysis

DSC – Differential Scanning Calorimetry

BET – Best Estimated Threshold

# Chapter 1. Introduction

Humankind has been smoking foods since the first utilization of fire for cooking, and is still one of the most popular methods of preserving and flavoring foods, particularly meats. Smoke is generated by smoldering wood such that a plume of smoke aerosol forms from pyrolyzed material. The aerosol contains char (fully carbonized material), tar (oligomers and anhydrosugars), liquid-phase volatiles, and gases (primarily carbon dioxide and carbon monoxide). Conventionally, the aerosol settles directly on the product, but smoke can also be condensed into a liquid for alternative application. Condensed smoke, also known as liquid smoke allows for more control and consistency,[1,2] which makes it convenient for manufacturers and researchers who study its chemical composition.[3,4]

Most wood pyrolysis occurs between 200 and 500 ˚C, the temperature range at which cellulose, hemicellulose and lignin degrade[5]. Cellulose and hemicellulose are precursors to organic acids, linear and cyclic ketones, aldehydes, furans, and lactones, all common products of pyrolyzed sugar and starch as well[6,7]. Lignin pyrolysis is attributed to the formation of phenolic compounds which are smoky in aroma character[8,9]. The combination of volatiles from the degradation of these three polymers comprise the characteristic aroma of smoke.[4]

The study of smoke aroma has been investigated primarily through the sensory evaluation of condensed smoke fractions or the characterization of the volatile compounds in condensed smoke[2,4,10]. While there have been studies identifying the aroma-active volatile compounds in smoked foods[11–13], there is a lack of literature on the chemical characterization of condensed smoke aroma in isolation.

An additional challenge to understanding smoke aroma is the selection of woods that can be used for smoldering. Commonly, hardwoods are used for their more pleasant flavor as compared to softwoods or non-woody plant species[4]. Smoked products often include a wood species as part of the identity, but little is known about how wood is affecting the flavor. What is known is the confounded by the analysis of a finished food product, and does not consider the sensory character in combination with chemical characterization, which leads to inconsistent conclusions between studies[14,15].

This dissertation aims create a connection from wood structure to final smoke aroma, allowing more control over the generation of smoke flavors. In the Chapter 3, the aroma of a condensed smoke sample from mixed hardwood was characterized. Key aroma compounds were identified and quantified. In Chapter 4, condensed smoke samples from six single-species wood samples were analyzed to investigate the wood structures that were predictive of aroma compound concentration. Condensed smoke samples were characterized by sensory and chemical analysis, and then compared to wood samples to elucidate connections between smoke aroma and wood characteristics.

# Chapter 2. Literature Review

Smoking has been used for thousands of years to add value to foods around the globe. It is one of the oldest methods of food preservation and has inspired whole categories of culinary practice [16]. This dissertation attempts to explain one aspect of smoked foods, the identification of aroma constituents and their formation from wood, by examining one product, condensed liquid smoke, intended to be further processed into any number of different types of foods. Thus, it is important to establish this work in the context of the other published literature available on smoke, particularly liquid smoke. This literature review will be focused on the important functionality that smoke provides, our current understanding of wood structure and pyrolysis to form smoke, and the chemical characterization of smoke itself.

## **2.1** Defining wood smoke and condensed smoke

Wood smoke is ultimately a mixed aerosol containing solid char, liquid tar, semi-volatile liquid organics, and volatile gases. It forms from the pyrolysis of wood under conditions that total combustion is inhibited. If one is a backyard barbecue-er, they might call it “low and slow” conditions, but it can also be formed at high temperatures by limiting oxygen availability. The result is a white-colored aerosol that settles on the food. Any time the smoke is condensing from its aerosol form directly onto the food it is referred to as conventional or traditional smoking, but this smoke can also be condensed directly into a liquid, or dispersed into a matrix such as water or oil. Much of the literature refers to this generically as liquid smoke, liquid smoke flavoring, or condensed smoke, but they are all natural wood smokes.

**2.2** History of smoked foods

The exact origins of smoked foods are unknown, but they likely date back to the paleolithic era [16]. While the process does impart a distinct smoky flavor, it was employed more for its preservation power, especially when combined with salt curing or fermentation. Smoked meats offer a considerably longer shelf-life than meat that was simply dried or cooked normally, and many culturally important foods developed alongside them. With more modern technologies, the use of smoke as a preservative has been made less necessary, but it still contributes flavor, texture, and color changes that all combine to create a highly desirable, unique, and characteristic smoked food. Smoke is not obsolete as a preservative, however, and is still useful as a natural antioxidant and antimicrobial.

**2.3** Antimicrobial properties of smoke

Smoke's antimicrobial and antioxidant properties have been largely attributed to the high quantity of organic acids and phenolics that are present [17]. Liquid smoke and its fractions have been employed to demonstrate and quantify these antimicrobial properties against both gram-negative bacteria such as *Salmonella spp.* and *Escherichia coli* [18,19], as well as the gram-positive *Listeria spp.* [19–24]. Phenolics have been shown to disrupt the cell membranes of both gram-positive and gram-negative bacteria, however, it is more likely that the high level of organic acids present is contributing the most to its inhibitory properties, rather than phenolics[17]. Organic acids, when present in a matrix that is acidic enough to be protonated, can move across bacterial membranes and dissociate, which disrupts the intercellular pH and thus the membrane potential and enzymes that bacteria utilize to produce energy and survive [25]. This functionality has led to numerous organic

acid antibacterial agents that are commonly employed in food such as benzoic acid for beverages, and propionic acid for bread, sometimes naturally occurring in the fruits or yeasts that make these products. Organic acids in liquid smoke have been shown to have a positive correlation with minimum inhibitory concentration tests, even with low phenolic content[26]. Other carbonyls and phenolics have also demonstrated bacterial inhibition. It is suggested that carbonyls can traverse the bacterial cell membrane and react with amino groups to disrupt intracellular activity, while in isolation, phenolics can inhibit bacteria by disrupting the cell membrane itself[27]. These mechanisms are all likely contributing to the numerous studies which demonstrate smoke's antimicrobial properties. In addition, smoke can aid in the prevention of oxidation in foods such as fish and meats. Smoke has a high concentration of phenolics which can sequester free radicals and reduce oxidation in a variety of matrices[28,29]. While this dissertation is focused on aroma, it should not be underestimated that smoke also offers added value in the form of natural antimicrobial and antioxidation functionality.

**2.4** Color development in smoked foods

Smoke also has an important role in the development of color in smoked foods. Carbonyls from wood pyrolysis react with amino acids in Maillard reaction-type pathways to produce dark-colored melanoidins (as well as Maillard-reaction products that contribute flavor)[30,31]. Nitric oxide formed during smoking replaces oxygen in oxymyoglobin to form nitric oxide myoglobin, which contributes a pink color distinct from the normally brown metmyoglobin in cooked meat[32]. Color development from the use of liquid smoke is often

measured as a quality control metric and is typically measured in terms of browning index[33], or the purity of brown color developed with a given portion of liquid smoke.

**2.5** Smoked food market

Condensed smoke was first commercialized by Ernest Wright in 1895, who grew his business to $500,000 by the time he sold it in 1923. Since then, it has grown into a multimillion dollar industry. Smoked foods as a market category are difficult to analyze due to the diversity of products that are related. Liquid smoke had a market size of 56.5 million USD as of 2018[34], which only represents a portion of the overall smoked food market. Liquid smoke is most commonly used for meats such as sausages and fish, as well as in sauces, dairy products such as smoked cheeses, and pet food[34]. While liquid smoke does offer a flavor that can be added across many other categories, such as meat alternatives or soups, its flavor is generally not considered to adequately match authentic conventional smoke, necessitating some improvements in its overall flavor profile. How to best match conventional smoke is a complex in and of itself, however, as the differences in flavor are not well understood.

**2.6** Advantages of condensed smoke over conventional smoke

Conventional smoking is an important process to create all the aforementioned changes in a product, but it is a labor and time-intensive process that can considerably drive up the prices compared to unsmoked products. Smoke condensate has a multitude of advantages over conventional smoke or over using a concocted smoke flavor. First, smoke condensate offers a faster processing time. It can be applied in a variety of ways including drenching, injecting along with the brine, or covering the product in a soaked netting, which

allows the introduction of smoke flavor and color during cooking without the product spending any time in a smokehouse. The smokehouse itself can also be adapted to atomize liquid smoke into a vapor, simulating the conditions of conventional smoke, but even then, the processing time is reduced by up to 25% of a conventional smoke process[35].

These different methods of the introduction of smoke condensate also offer a wider array of tools that can be used for greater control of the final product. Conventional smoking has a multitude of variables that all can differ depending on the shape of the smokehouse, the length of the tubing between the smoldering unit and the smokehouse, or the type of fans that are used to ensure a uniform smoke cloud. Condensed smoke offers a more consistent functionality and a stable flavor that can be more directly scaled up to a production facility from a product development point of view[35,36].

In addition to mimicking a conventionally smoked product, smoke condensate can also be used in applications where conventional smoking is not straightforward or impractical. Condensed smoke has been popular in the pet food industry for many years[17]. It has started to become popular among vegan or plant-based foods where a meat-like smoke flavor is desired, but with plant-based ingredients that would not be practical to conventionally smoke[17]. It can also be easily added to soups, beverages, or sauces without additional processing[36].

Beyond a processing efficiency point of view, the condensed smoke process also lends itself to a few more advantages related to health and environmental impact. Condensed smoke is typically allowed to age for a few days, when the tar, a heavy mix of un-pyrolized lignins or repolymerized, hydrophobic materials, can settle out of the final

aqueous smoke. Polycyclic aromatic hydrocarbons (PAHs), many of which are potent carcinogens, settle out with the tar phase removed in processing[36,37]. No tar phase separation occurs in conventional smoking. A link between processed meats, including smoked meats, and cancer has already been established by the World Health Organization, and it is considered a type 1A carcinogen for colon cancer[38]. Mechanistic studies are still attempting to establish causality, however, the presence of PAHs should be scrutinized, and the ability for condensed smoke to have some control over their removal is an important advantage. As such, the European Food Safety Authority (EFSA) has implemented its regulation of condensed smokes or liquid smoke flavorings as of 2009 to limit the amount of the top 16 carcinogenic PAHs[39]

High-throughput conventionally smoking facilities also more highly impact air quality in the surrounding area, as well as contribute to greater carbon emissions into the atmosphere as compared to condensed smoke. Condensed smoke has the advantage of a closed process, where char and tar can be recycled into the furnaces that are used to smolder, thus reducing the amount of particulate matter that gets released into the atmosphere, which has led to city air quality concerns in the past[40].

With these advantages established, it is also imperative to establish the major disadvantage with condensed smoke, which is that it does not exactly match the flavor quality achieved by a conventional smoking process. Unfortunately, because smoke flavor is poorly understood, there is also not sufficient literature to understand the differences between conventional smoke and condensed smoke flavor quality. Thus, there is a need for studying the exact mechanism by which smoke flavor is formed, and how the condensation

of smoke alters the flavor profile. This begins by discussing and understanding the precursor for all types of wood smoke – wood.

**2.7** Chemical structure and pyrolysis mechanisms of hardwood – cellulose, hemicellulose and lignin

Wood largely serves as vasculature for trees to transport nutrients throughout their other tissues. The vast majority of this secondary xylem is not metabolically active and is essentially an empty plant cell wall that can move water up or down great distances and withstand high pressure [35]. The result is a rigid cell wall structure that is comprised of different ratios of lignin, cellulose, and hemicellulose to provide this function. When the wood is smoldered, these three molecules are primarily responsible for the resultant products [41–43]. These molecules have been of great interest to academic fields concerned with biofuels and sustainable energy, where the goal is to make these processes more efficient [44–47], but the mechanisms of pyrolysis in these areas can also be applied to the formation of flavor compounds.

Hemicellulose and cellulose are both polysaccharides that consist of 25-35% and 40-45% of wood dry mass respectively [48]. Cellulose is a linear polymer of beta-D-glucopyranose units linked by alpha-1,4 glycosidic bonds, whereas hemicellulose consists of a variety of monosaccharide units, mostly xylose and glucuronic acid in hardwoods, with a branching, amorphous structure [49]. Hemicellulose also has varying degrees of modifications, such as acetylated hydroxy groups, and is crosslinked with lignin in a native structure [49]. Both can pyrolyze in a manner consistent with a non-enzymatic process such as caramelization, a radical-driven, high heat, low moisture "cracking" of sugar moieties

[50]. The result is 1 to 4 carbon carbonyls and acids, as well as furans and pyrans. Volatile gases that are released during pyrolysis include carbon monoxide, carbon dioxide, and methane. Non-volatiles include a variety of anhydrosugars and char. Despite their similarity in primary chemical structure, there are a few key differences in how cellulose and hemicellulose pyrolyze that would have an impact on both the yield of aroma compounds and the type of aroma compounds that may form. Briefly, hemicellulose pyrolyzes between 220 and 315 ˚C, whereas cellulose will pyrolyze at a higher temperature, between 315 and 400 ˚C [47,50]. A simple explanation of this difference is that the highly-branched secondary structure of hemicellulose compared to the linear cellulose structure results in a tertiary structure that is much less dense and more labile in hemicellulose. In a Differential Scanning Calorimetry (DSC) experiment, hemicellulose will also degrade exothermically, whereas cellulose exhibits an endothermic behavior in its pyrolysis. It is hypothesized that these behaviors are due to the two main types of competitive reactions that occur during pyrolysis, volatilization/char-formation (exothermic) and depolymerization to form anhydrosugars such as levoglucosan (endothermic) [50,51]. The implications are that during this long, slow-type pyrolysis occurring in DSC, cellulose will tend to form aromatics such as furans and cyclic ketones in a more radical dependent manner through the formation of levoglucosan as a primary product, whereas hemicellulose is forming light gases, small organic molecules, and char that does not contribute as significantly to the aroma. This is supported by studies that show hemicellulose as having a higher overall char yield and lower anhydro-sugar formation [50,52]. It should be stated that the exact mechanisms are complex, multi-dimensional and

only a few broad types of mechanisms have been hypothesized in cellulose. Even less information is known about hemicellulose [5]. This will further be discussed in the context of lignin degradation in this review.

Lignin is less well-characterized, as the compound is much more resistant to degradative methods that have been historically used for analysis. Typically wood is ball-milled and subjected to enzymatic digestion to form lignin that is referred to as milled-wood lignin (MWL) [53]. Klason lignin is also commonly isolated via acid digestion[53,54], but can result in condensation reactions that may alter lignin structure. Both types of lignin can be further fractionated to study their complex polymer structure. Recent methods incorporate nuclear magnetic resonance (NMR) spectroscopy as a means to analyze lignin structure with minimal use of heat, acid, or enzyme that degrade or otherwise alter the structure of lignin[55,56].

In broad terms the lignin polymer consists of three main types of phenyl propane monomer units, p-hydroxyphenyl, syringyl, guaiacyl. Each phenyl ring contains zero, one, or two methoxy groups. These subunits are linked by a variety of ester, ether, and carbon-carbon linkages (Figure 2-1).

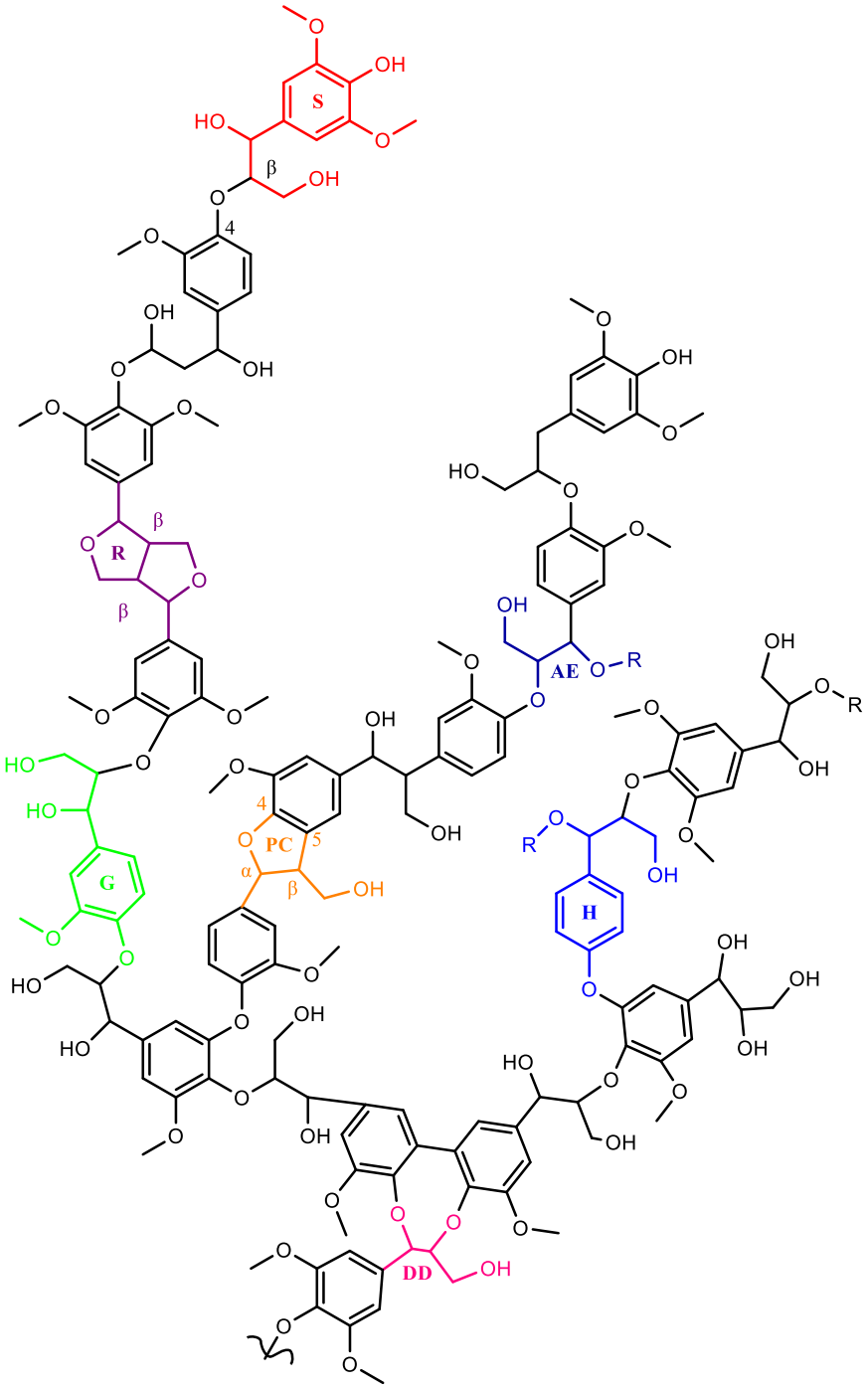


**Figure 2-1**. Basic structure of lignin S: Syringyl unit; G: Guaiacyl unit; H: *p*-Hydroxyphenyl unit; R: Resinol linkage; PC: Phenylcoumaran; AE: Aryl ether; DD: Dibenzodioxocin [56,57]

Lignin's lack of structural characterization due to the complexity in its isolation and the relative novelty of non-destructive methods of lignin characterization, leads to a lack of available information on the mechanism of its pyrolysis. Nevertheless, numerous studies have been conducted on elucidating these mechanisms due to their role in efficient biofuel production and paper processing. Much like hemicellulose, lignin pyrolysis is mostly exothermic[50,51]. Lignin linkages are likely degraded first, and the resultant primary products are substituted phenolic monomers or dimers with intact side chains in the para position. Depending on reacting lignin subunit, the resulting phenolics can also be similarly substituted with one, two, or zero methoxy groups [58]. Secondary reactions can result in oxidation, partial cleavage, or complete loss of the para-substituted side chain, as well as a substitution of the methoxy groups to hydroxy groups, or a methylation of the phenyl ring mostly in the meta or ortho positions [59]. Lignin can also form char through a radical-dependent process, which seems to be influenced by the increased presence of methoxy groups on the original lignin side-chains [60]. These reactions also occur over a much broader range of temperatures as compared to hemicellulose and cellulose as exhibited by its TGA curve (100-900 °C) [5]. The implications could be that lignin pyrolysis is the most sensitive to changes in pyrolysis temperature beyond ~400 °C in terms of final aroma composition. The multitude of secondary and tertiary reactions that all result in differing aroma compounds, due to the change in organoleptic properties that each type of phenol can have, can result in differing aroma impact. Industrial smoking is typically done at a pyrolysis temperature of 300-400 °C, but the actual internal smoldering temperature can be up to 800 °C depending on variables such as particle size and moisture content[37].

Naturally, these compounds do not exist in wood in isolation, but rather they are cross-linked covalently and in proximity due to electrostatic interactions. To study their pyrolysis, previous researchers have isolated these polymers by enzymatic or acid hydrolysis. Isolated cellulose and hemicellulose are then analyzed by thermogravimetric analysis (TGA) and differential scanning calorimetry (DSC), which can then be coupled to a gas chromatograph (GC), mass spectrometer (MS), or infrared spectrometer (IR) [61–63]. These techniques allow comparisons of the pyrolysis of lignocellulosic material in a controlled environment, and thus one can make inferences about the types of products that each of these polymer types can create [5], however, they do not fully represent what may be occurring in the pyrolysis of wood. **Figure 2-2** shows the TGA profile of isolated hemicellulose, cellulose, and lignin, indicating similar pyrolysis ranges as described previously. In **Figure 2-3**, the combined profile is calculated based on isolated material, and it is compared to a whole beechwood sample with comparable lignocellulosic content. The conclusion is that the three types of polymers do not pyrolyze independently, but rather the presence of the others influences the pyrolysis of each, impacting their thermokinetics and thus reaction pathways. In the interest of studying the formation of aroma-active constituents, these studies provide helpful mechanistic insight, but the pyrolysis of woods cannot be exactly modeled by isolated components. The studies that involve the GC or MS coupled to these instruments also are monitoring gasses such as CO2, CO, and methane, rather than compounds that would have an organoleptic impact [5,60].

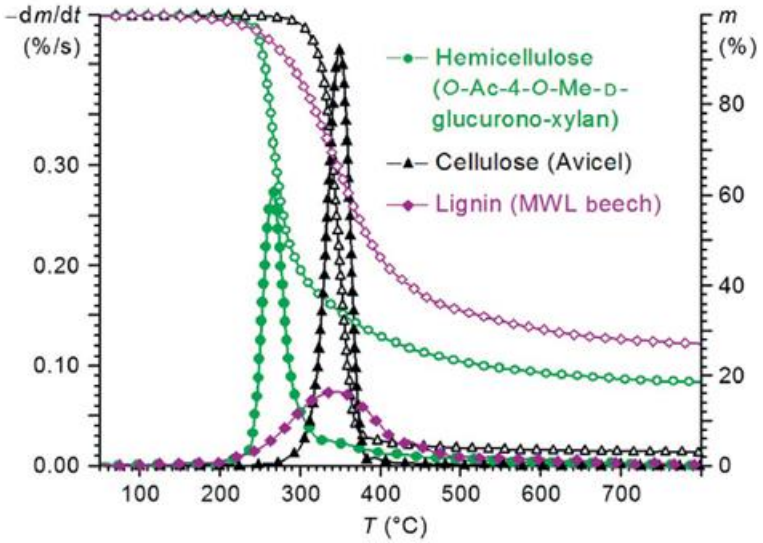


**Figure 2-2.** : Thermogravimetric curves from hemicellulose, cellulose and lignin individually. Open symbols represent weight loss. Closed symbols represent the derivative curve or weight loss over time (Jakab 2015)[5]

.

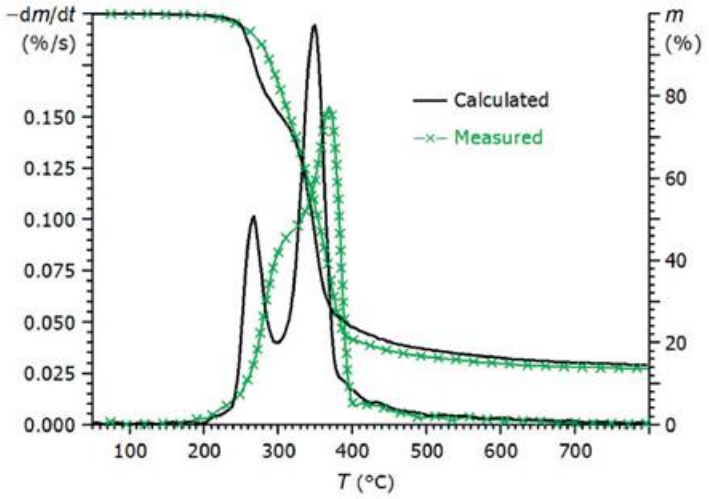


**Figure 2-3.** Calculated thermogravimetric curves from hemicellulose, cellulose and lignin and the actual measured curve from beech wood. (Jakab 2015)[5]

An additional issue with TGA or DSC for the analysis of wood smoke flavor is that these methods involve a slow temperature ramp. A rapid pyrolysis method has been employed for biofuel gasification, and shows that rapid temperature ramping and rapid quenching of these reactions can have vastly different outcomes in the amount of char, tar, or volatile gasses that are produced [64,65]. Reaction kinetics of the competing endothermic reactions and exothermic reactions involved in volatile and char formation as discussed previously can explain these differences but are not yet well characterized because of their complexity.

Pyrolysis-GC can be a useful tool to simulate different thermal conditions and monitor compounds of importance for smoke aroma, and has been employed in the past to measure parameters such as lignin subunit ratios [58,66,66]. For lignocellulosic material characterization, it remains an important tool, however, there are a few limitations. For smoke flavor, the smoke cloud in a conventional smoldering smoker will pyrolyze at 300-800 °C, depending on moisture content and particle size, but then cool to the smokehouse temperature of 30-40 °C over the course of approximately 1-10 minutes [35]. Likewise, a calciner-type smoker to produce condensed smoke may take up to 10 minutes until the smoke is condensed and cooled. Condensed smoke is also aged for at least 1-2 days, which has been shown to improve the organoleptic properties [4]. These types of changes further complicate the use of small-scale techniques such as pyrolysis-GC to characterize all the changes that are occurring which are relevant to smoke flavor. Regardless, it has proven to be a useful technique for general understanding of possible pathways with model polymers or combined wood samples. With the fast pyrolysis of poplar wood done in a pyrolysis-

GC system, Dong and co-authors were able to show the differentiation of the pathways to form hydroxymethylfurfural and furfural as occurring simultaneously during a secondary pyrolysis reaction, rather than the alternative of furfural forming from hydroxymethylfurfural. They also showed that levoglucosan was a stable initial pyrolysis derivative of cellulose, while xylan hemicellulose forms very little of its anhydrosugar, 1,4-anhydroxylpyranose [67].

**2.8** NMR in hardwood cell-wall characterization

NMR has evolved since the early 2000s as a promising method of lignocellulosic structure characterization. NMR offers a nondestructive method of characterization that is a viable alternative to the established methods of plant cell wall analysis. The sample preparation is lower throughput compared to conventional techniques, but quantification is likely to be more accurate[53].

NMR is a spectroscopy technique that relies on the excitation and relaxation of nuclear spins. Briefly, the sample is dissolved in solvent and suspended in an external magnet. Nuclei with a magnetic spin align with the external field. A radiofrequency pulse is then applied to the sample, inverting the spins of aligned nuclei, and then they are allowed to relax back to their lowest energy state, spontaneously realigning to the external magnetic field. This relaxation releases energy in the form of radiofrequency waves and is recorded by the instrumentation. Depending on the electronic environment of nuclei in the sample, there is a unique frequency of energy released. The interpretation of these unique signatures thus allows for the determination of the structure and position of each nucleus of a single element determined by the instrument parameters. Nuclei with a spin number

of 1/2 have a short relaxation time and are the most suitable for NMR experiments. Common nuclei include $^{1}H$, $^{13}C$, $^{31}P$ and $^{15}N$ [68].

The use of NMR for a more accurate determination of lignin subunit ratios is discussed by Bunzel & Ralph who explain that traditional methods may overestimate the lignin occurrence in wheat bran due to systematic bias from conventional digestive analytical techniques [55]. Historically, lignin is isolated with aqueous dioxane (milled wood lignin), and enzymes are used to remove residual carbohydrates [69]. Improvements have been made in this space to better extract lignin that is representative of native lignin, but it is never completely representative. Spectroscopy techniques, however, can analyze lignin natively if sufficient resolution is achieved [53].

NMR spectroscopy of lignin is unparalleled in its ability to obtain structural information of lignocellulosic material [56,70]. While IR and Raman spectroscopy give insight into generally how lignocellulosic material is changing due to a treatment or a TGA experiment, NMR has the potential to directly quantify specific monomer units or linkages. Previously, this was limited by poor resolution, but with recent innovation in instrumentation and software, much of the structural information can be resolved and assigned depending on the type of pulse experiment [53,71].

John Ralph and his co-authors have contributed substantially to creating a standard methodology for the dissolution of wood and other lignocellulosic material for liquid-state NMR analysis. They have developed a method by which cell-wall material can be isolated and dissolved, then analyzed by heteronuclear single quantum coherence (HSQC)[55,56,72]. HSQC is a technique by which the cross-resonant spectra of adjacent $^{13}C$ and $^{1}H$ nuclei are

collected, essentially improving resolution by expanding a 1D experiment into 2D and improving the quality and volume of information that can be collected when cellulose, hemicellulose, and lignin spectra commonly overlap [53].

Critically, Ralph and co-authors have also worked to identify features and provide structural assignments in many different lignocellulosic materials. Other labs have also worked to improve these methods and contributed both native lignocellulosic structure and isolated lignin structure assignments for HSQC [70]. Nonetheless, many regions in the spectra have an overlap that makes it difficult to make structural assignments, particularly the overlap of polysaccharide peaks and important lignin structural linkages between subunits. One way to circumvent this problem is by utilizing a chemometrics approach to highlight important structural differences [72], and then identify only such features that are of importance, a strategy frequently used in untargeted NMR metabolomics [73].

NMR metabolomics is a field of study by which complex mixtures of small molecules are analyzed via NMR. It can be applied to a variety of fields but is commonly used in pathology, nutrition, and other medical research [73]. Recently it has even been used to characterize the activity of gut microbiota [74,75]. Very little untargeted work has been done for wood polysaccharides, but the available methodology, structural assignments, and multivariate analysis techniques for HSQC make the approach a possibility [53].

Through all of these techniques used to characterize lignocellulosic material as well as its pyrolysis, one can begin to understand the general mechanisms that are occurring. They are complex and not thoroughly understood because of the many variables involved, but the general pathways are as follows. Hemicellulose has the least amount of thermal

stability and is first degraded through a loss of its acetylation to form acetic acid and other derivative linear carbonyls [5]. Hemicellulose shares its other pathways with cellulose such as the fragmentation that occurs at higher temperatures to form linear carbonyls or depolymerization reactions, losing water molecules in the process, which result in cyclized furans. Furfural tends to be a dominant furan species formed from hemicellulose degradation [5,52]. The main difference between cellulose and hemicellulose pyrolysis is that cellulose will form anydrosugars much more readily in the form of levoglucosan, while producing less char and initial volatiles early on in pyrolysis [50]. It also requires hotter temperatures overall. Lignin has the longest temperature range of pyrolysis and goes through cleavage of its interunit linkages, followed by a loss of its side chains, demethyoxylation of its methoxy groups located on the phenyl ring, followed by a subsequent alkylation primarily in the 2 and 6 positions of these derivative phenolics [5,66]. Increasing the temperature tends to result in fewer linear carbonyls, more lower molecular weight furans, more alkylated or demethylated phenolics, and more PAH formation [4,5,76].

Most of the aforementioned literature is concerning the degradation of plant cell wall materials for the purpose of understanding pyrolysis to improve biofuel utilization or the generation of industrially useful chemicals. While this is helpful understanding for all fields concerned with pyrolysis there are also those concerned with improving the organoleptic qualities of condensed smoke or smoked products. As was stated previously, smoking also has profound effects on color and microbial stability, but the rest of this review will be focused on the flavor compounds or the generation of condensed smoke intended for use in foods.

**2.9** Chemical characterization of smoke

Much of the early work on smoke condensates was focused on the fractionation of said condensates and a general classification of the component compounds in the 60's and 70's. Fujumaki, Kim and Kurata published on a fractionation of smoke condensates, identifying an acidic, basic, phenolic, carbonyl organic, and non-carbonyl organic fraction, with the phenolic fraction and dicarbonyls being the most differentiating organoleptically [77]. Unfortunately, it was later shown that these fractions were not necessarily pure enough to definitively attribute the sensory properties to a single class of compound, as the fractions frequently contained multiple compound classes [35]. Joseph Maga published a comprehensive review of wood smoke flavor in 1987 which collected 410 volatile compounds over several different published studies including numerous smoke generation techniques and starting materials [4]. This review postulated which compounds might be responsible for the overall flavor of smoked products. An entirely systematic approach is not taken, however, but rather some of the most abundant compounds by GC/FID from the most aromatic fractions are isolated, thresholds are determined and compared to quantified concentrations. Since this was published there have been many more developments in the use of aroma extract dilution analysis (AEDA) as a more systematic approach to prioritizing aroma active compounds in a given sample.

In 1995 there was increased interest in characterizing smoke for the purpose of flavoring food. A series of papers from Maria Guillen and co-authors describe the systematic dichloromethane extraction and identification of both liquid aqueous and solid smoke flavoring preparations via GC-MS and FTIR [10]. In addition to characterizing

commercial preparations, they also smoldered wood and collected the smoke in distilled water on a laboratory scale in order to study the impact of moisture on pyrolysis of beech wood [3]. Similar to previous literature, it was found that smoldering produced higher yields of liquid smoke in intermediate to low moisture ranges (5-15% water by weight). Guillen and co-authors also published on larger phenolics, and lignin dimers and trimers discovered in the non-dichloromethane soluble smoke flavoring phase by GC/MS and confirmed that much of the antioxidant property of smoke could be from these compounds [28]. Likewise, they reported small amounts of pyridines, likely derived from the small quantity of amino acids and alkaloids present in wood, and anhydrosugars for the first time in liquid smoke [78]. In the early 2000s the European Food Safety Authority (EFSA) began regulating liquid smoke in its own category and established guidelines for characterizing smoke for sale in the EU [79]. These requirements led to a few more standardized methods from the European Commission, especially concerning the analysis of PAHs, but also potentially toxicologically relevant volatile compounds [80].

Kostya and Barylko-Pikielna make some interesting comparisons of the sensory profile of smoke flavoring fractions made from the tar phase of smoke condensations to the volatile profile [81]. While the results are correlative, they find that an absence of the carbonyl fraction may be causing a significant flavor change. In addition they found that while the concentrations of syringol-derivative compounds, and most guaiacol-derivatives, including eugenol isomers, varied, there was little sensory effect, with the exception of guaiacol and 4-methylguaiacol [81].

Other characterization studies include Soldera et al in 2008, who characterized phenolics in aqueous smoke flavorings from manufacturers for the purpose of studying their antioxidant activity [29], Montazeri et al in 2012, who characterized volatiles in commercial full-strength liquid smokes as well as more refined derivative flavorings [23], and finally Giri et al in 2017, who are from the European Commission and provided an optimized solid phase micro-extraction (SPME) method for the analysis of commercial liquid smoke flavorings [2]. These studies focused on the compounds present by GC/MS, but they are not concerned with the aroma directly, as they make no effort to correlate the instrumenta data with the sensory profile. The wood-types used to generate these smokes are also not disclosed, except that they are a mix of hardwood varieties.

**2.10** Aroma characterization techniques

A long list of chemicals present in smoke is useful to understand how these compounds could be forming and how pyrolysis reactions are occurring, but when it comes to understanding the flavor, it is only a small piece of the puzzle. An instrument such as a gas chromatograph (GC) coupled to a flame ionization detector (FID) or mass spectrometer (MS) relies on an inherit property of the molecule in order to detect it -- the type of covalent bonds present or the ionization ability of the molecule for example. The human nose detects based on a completely different principle, which is the ability of the odorant to bind to one or more receptors in the olfactory epithelium coated by a relatively hydrophobic mucosal layer [82]. Each odorant has a unique binding affinity to one or more odor receptors and therefore each odorant has a concentration threshold at which it can be detected that has little in common with its response factor on an MS. Even if all of the 400 or more

compounds are quantified, it would be impractical to determine the odor threshold of each of those compounds to determine which ones might be the most significant to the flavor. Charm and aroma extract dilution analysis (AEDA) are techniques that developed in the 1980s as an attempt to address the question of identifying compounds as important to aroma [83,84].

Both techniques rely on GC-Olfactometry (GC-O) which is a technique by which the GC column is attached to an olfactometry port, or a nose piece, which allows the operator to sniff the odorants that are exiting the column. The column flow can be split to another detector such as an MS to allow simultaneous compound identification by mass spectrum. In charm analysis, a panelist will mark the start and stop time of each peak, whereas in AEDA, the analysis is simplified to a single indication that an aroma has been detected [83,85]. Both techniques collect data on samples of increasing dilution factor with the charm analysis having the advantage of retaining peak shape. Otherwise, the techniques are essentially based on similar principles. AEDA is more commonly used, because of its relative ease of operation compared to charm analysis. AEDA is also used in this dissertation, and so the advantages and disadvantages will be discussed here.

AEDA ultimately generates a list of odor-active compounds that are present in any GC appropriate preparation of a sample, most commonly an aroma extract. The raw data from panelists includes only retention time and aroma character. Although the aroma character itself can change in a complex mixture or with concentration, it is still useful to compare data across panelists and dilutions to differentiate two compounds that may have similar retention times. Dilution factors are calculated as the last dilution that assessors

have detected an odorant and are plotted against the retention time to form an "aromagram". An example is shown in Figure 2-4 and clearly exemplifies how the aromagram can reveal potent odorants that may not have had as high of intensity in the FID.

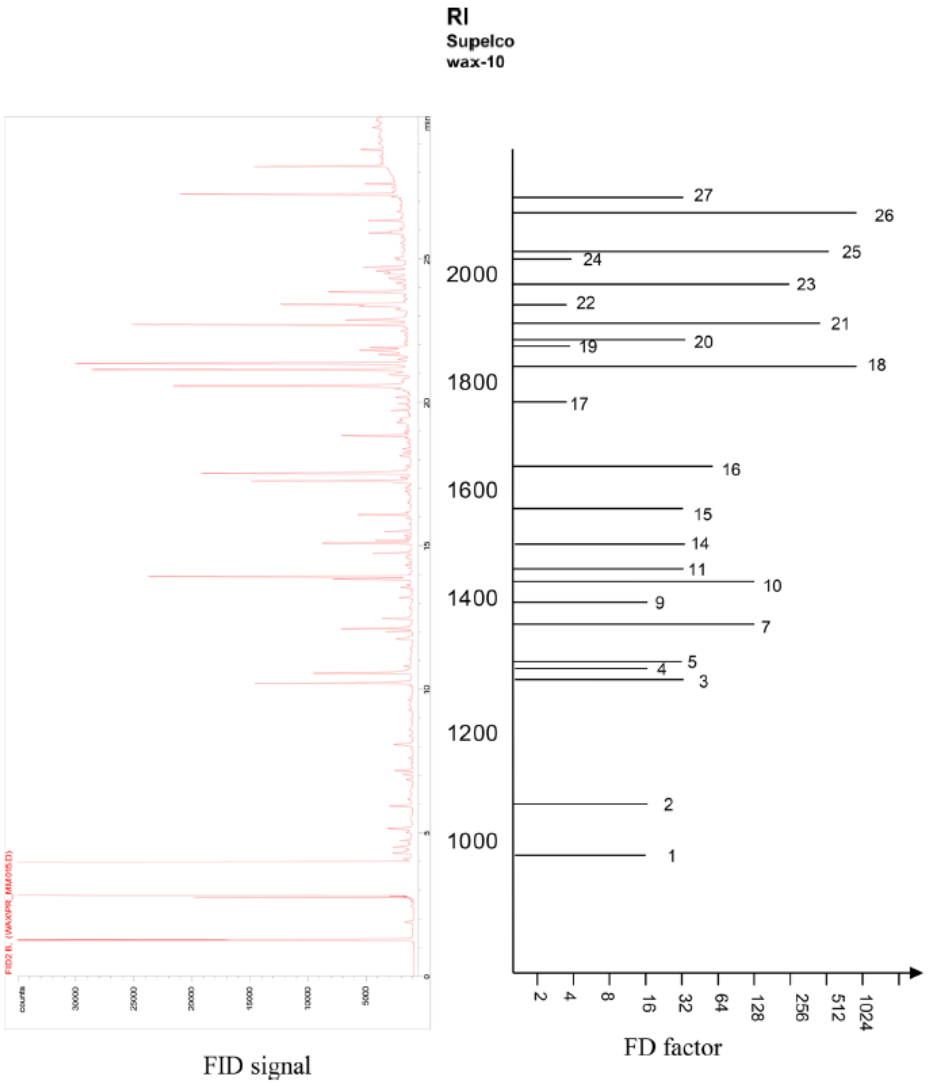


**Figure 2-4.** Example of a typical GC-FID chromatogram (A) contrasted with an "aromagram" from AEDA (B). From Kowoska 2018[86]

Normally, after an aromagram is created, a list of compounds is then generated based on their "intensity", or essentially a subset of compounds are chosen that have the highest dilution factor. In theory, this allows the researcher to prioritize compounds that

are high impact in the sample. Odor activity values (OAV) for each compound are then calculated to take into account the concentration of each compound in the sample as well as the odor threshold[85]. OAV is simply a ratio between the compound concentration and the odor threshold as determined in an appropriate matrix. OAV values greater than 1 are determined to be contributing to the overall aroma[85]. The results are typically verified by recombining all compounds together in a model that should in theory match the original aroma extract[87–89]. Omission experiments, experiments that remove some of the low-dilution factor compounds in the recombinant model, can inform whether these compounds are contributing to the aroma.

AEDA is useful for determining which volatile compounds might be responsible for the aroma or retronasal flavor. As a tool its strength is the systematic determination of aroma composition, but it is not perfect, and the recombinant models can sometimes fail to match the original extract for a variety of reasons[11,90,91]. AEDA relies on the detection of single compounds, when it is now known that the detection of aroma is dependent on the simultaneous binding of many individual compounds to odor receptors in the olfactory epithelium. Competitive binding, additive effects, or synergistic effects can greatly affect the aroma perception, which means that compounds that are sub-threshold may have a significant impact on the flavor[92,93], or likewise some reported compounds may not be significant. Regardless, it does provide a simple and systematic solution to assessing which compounds may be important to monitor, and thus it still frequently used today.

While AEDA is the most commonly used systematic aroma identification tool, it has only partially been applied to condensed smoke or pure smoke made from hardwood

in one instance. Cadwallader published a table of high impact odorants from commercial hickory and mesquite liquid smokes that was originally presented at the 1996 Institute of Food Technologists meeting, but a recombination model or OAV values were not published for validation[37]. Pino in 2014 published on AEDA of an aqueous smoke flavoring made from rice husk[94]. These high-impact odorants are reported in Table 2-1. Otherwise, AEDA analyses are typically performed on finished products such as smoked pork[86,95] or smoked and fermented salami[11]. While it is generally impossible to differentiate aroma compounds that would arise from the smoking process specifically, it can be assumed that the phenolic compounds most likely are due to smoke.

**Table 2-1.** High impact odorants as reported from AEDA studies on condensed wood smoke and rice hull smoke.[37,94]

| Compound | Odor Description |
|---|---|
| 2,3-Butanedione | Buttery |
| 1-Pentene-3-one | Plastic |
| 2,3-Pentanedione | Buttery |
| 3-(Methylthio)propanal | Potato |
| 2-Furfural | Caramel-like |
| 2-Acetylfuran | Balsalmic, sweet |
| Acetic acid | Vinegar, acid |
| 5-Methyl-2-furfural | Sweet-spicy, caramel |
| Butanoic acid | Spoiled mlik |
| 3-Methylbutanoic acid | Dried fruit |
| 2-Methoxyphenol | Smoky |
| 4-Methylguaiacol | Smoky, vanilla |
| 2-Methylphenol | Ink, phenol |
| 4-Ethylguaiacol | Cloves, smoky |
| 4-Methylphenol | Stable, fecal |
| Eugenol | Cloves, smoky |
| 4-Propylguaiacol | Cloves, smoky |
| 4-Vinylguaiacol | Cloves, spicy |
| 4-(2-Propenyl)-2-methoxyphenol | Woody |
| Phenol | Pungent |
| 2,6-Dimethoxyphenol | Smoky |
| Isoeugenol | Cloves |

To conclude, smoke is truly an ancient method of food preservation and flavoring that is of significant importance to many cultures across the globe. Yet, its flavor is not well understood outside of some trends from fractionation and characterization experiments. A more systematic approach, such as AEDA in combination with OAV and recombination analysis, has never been applied to any form of pure wood smoke in the literature, which highlights a need for this type of analysis to better understand the compounds driving flavor. In addition, while pyrolysis studies have begun to understand

the general pathways of volatile formation, these types of analyses have not yet been applied to optimize the flavor of smoke from wood pyrolysis.

There is a distinct gap in the literature that can be fulfilled with modern characterization and multivariate methods, and new instrumentation that did not allow these types of analyses previously. This dissertation aims to bridge that gap and create a connection from wood structure to final smoke aroma, allowing more control over the generation of smoke flavors in the future.

## **2.11** Objectives

There are two main research objectives of this thesis:

1. Characterize the most important aroma constituents of condensed smoke for the use of flavoring foods
2. Investigate the impact of wood structure on the formation of aroma constituents in condensed smoke

# Chapter 3. Characterization of the aroma of condensed hardwood smoke by gas chromatography/mass spectrometry/olfactometry

*Vazquez T., Tello E., and Peterson D.G. 2022.*
*Manuscript in preparation.*

## **3.1** Abstract

The aroma composition of condensed hardwood smoke generated from a mixed hardwood was characterized by Gas Chromatography/Mass Spectrometry/Olfactometry (GC/MS/O) analysis. Twenty-seven odorants with a flavor dilution value ≥4 were identified and quantified by GC/MS/MS. The odor thresholds for each compound were compiled, and new aroma thresholds for four compounds (2-methyl-2-cyclopentenone, 3-methyl-2(5H)-furanone, 4-methyl-2,6-dimethoxyphenol, and acetoxyacetone) were determined. Sensory descriptive analysis revealed the condensed smoke consisted of the eight main attributes ashy, burnt-sulfurous, creosote, green-woody, pungent, smoky, spicy-sweet, and woody. No significant differences for the aroma attributes were reported between the condensed smoke and the corresponding recombination model, indicating that the identified compounds sufficiently characterized the aroma attributes.

Key Words: gas chromatography-olfactometry, liquid smoke, condensed hardwood smoke, odor threshold, aroma recombination model

## **3.2** Introduction

Smoking foods has been in practice for thousands of years to increase shelf-life and enhance flavor in a wide variety of different products. The functionality of smoke has been

attributed to the complex composition of chemical compounds that adsorb and react with the food during the smoking process. Conventional smoke is an aerosol that forms from the pyrolysis of wood, usually hardwood[4]. Most pyrolysis occurs between 200 and 500 ˚C, which is attributed to the thermal degradation temperatures of the main components of hardwoods, specifically cellulose, hemicellulose, and lignin[5]. Cellulose and hemicellulose form the majority of organic acids, linear and cyclic ketones, aldehydes, and furans, similar to products formed by heating sugar and starches[6,7,18]. On the other hand, lignin pyrolysis generates primarly phenolic compounds [59]. In addition numerous other large organic molecules are produced including anhydrosugars, oligomers, and hydrocarbons that comprise the complex tar-phase.[96,97]

Conventionally, smoke is produced in or adjacent to the smokehouse under dynamic conditions that can challenge uniform application. Consequently, manufacturers more commonly rely on smoke that has been condensed, known as condensed smoke or liquid smoke, which allows for more control and consistency[1,2] and also typically used to study the chemical composition[3,4].

Commonly condensed smoke has been fractionated into different chemical classes for characterization and the phenolic fractions are reported to have the strongest perceived aroma intensity[4]. The phenolic compounds guaiacol, 4-methylguaiacol, and syringol are considered to be important contributors of smoke flavor, although other phenolics such as *o*-cresol, *p*-cresol, and 4-ethylguaiacol have been shown to modulate smoke intensity and character[12]. Further studies have enabled the identification of over 400 volatile compounds

in smoke materials[2,10,23,35], but lack an understanding the contribution to the aroma component. Currently there is an inadequate understanding of the compounds that contribute to the aroma character of smoke materials. The aroma of numerous smoked foods such as pork loin[86], fermented sausages[11], cheese[98], fish[12], and cured pork[95] have been investigated, but the ability to define the compounds originating from the smoke is confounded by the analysis of the food product.

The objective is to identify the compounds that contribute to condensed hardwood smoke aroma. Condensed smoke was obtained from a pilot-scale rapid thermal pyrolysis generator and analyzed by Aroma Extract Dilution Analysis (AEDA) using Gas-Chromatography/Mass Spectrometry/Olfactometry (GC-MS/O). Identification of aroma-active components in condensed smoke will enhance the understanding of smoke flavor in finished products.

## **3.3** Materials and Methods

### **3.3.1** Condensed Smoke Samples

A condensed smoke sample was generated by Red Arrow Products (Manitowoc, WI). A mixture of hardwood sawdust was pyrolyzed on a lab-scale rapid thermal pyrolysis smoke generator. The condensed smoke sample was collected without any other further dilution or processing as an aqueous pyrolysis product of 70˚ Brix with a pH of 3.4. Samples were stored at 4˚ C until analysis in opaque high-density polyethylene bottles.

### **3.3.2** Chemicals

Compounds 2,3-butanedione, 2,3-pentanedione, hydroxyacetone, 2-methyl-cyclopentenone, acetic acid, 1-acetoxyacetone, 2-furaldehyde (furfural), 2-acetylfuran, butyric acid, 3-methyl-2(5H)-furanone, 2-methoxyphenol (guaiacol), 2,6-dimethylphenol, 2-methoxy-4-methylphenol (creosol), maltol, 2-methylphenol (o-cresol), 2-methoxy-4-ethylphenol, 2-ethylphenol, 2,5-dimethylphenol, 2,4-dimethylphenol, 4-methylphenol (p-cresol), 3-methylphenol (m-cresol), 4-ethylphenol, 3-ethylphenol, 3,4-dimethylphenol, 2,6-dimethoxyphenol (syringol), 3,5-dimethoxytoluene (4-methyl-syringol), and acetovanillone were purchased from Sigma Aldrich (St. Louis, MO). Dichloromethane was obtained from Thermo Fisher Scientific (Waltham, MA). Alkane ladder (C7-C30) was purchased from Agilent Technologies (Santa Clara, CA).

### **3.3.3** Preparation of condensed smoke samples

Condensed smoke (0.250 g) was diluted into to 10 mL of dichloromethane and sonicated for 30 minutes until a clear amber-colored solution was formed. This solution was then directly transferred into 2 mL amber glass GC-vials and stored at -80 C until analysis.

### **3.3.4** Analysis of odor active compounds by Gas Chromatography-Olfactometry/Mass Spectrometry (GC/MS-O)

Volatile analyses were carried out on an Agilent 6890N gas chromatograph system (Agilent Technologies, Santa Clara, CA) coupled with an Agilent 5973 series

Mass Spectrometer Detector (MSD)(Agilent Technologies, Santa Clara, CA) and an Olfactometry Detection Port (ODP 2)(Gerstel, Linthicum Heights, MD). Helium was used as a carrier gas and held at a constant flow of 1.6 mL/min and the effluent was split 1:1 after the GC column between the MSD and sniffing port using a capillary splitter and two deactivated fused silica columns (1 m x 0.1 mm i.d. for MS and 1 m x 0.15 mm i.d. for ODP). ODP and MS transfer line heaters were held at 250˚C. One uL of the condensed smoke sample was injected into a 250 ˚C split/splitless injector within a 1:10 split ratio. The system was equipped with a DB-5MS capillary column (30 m x 0.25 mm i.d. x 0.25 μm) (Agilent, Santa Clara, CA) or a DB-WAX column (60 m x 0.25 mm i.d. x 0.25 μm) (Agilent, Santa Clara, CA). For the DB-5 column, the oven temperature program was as follows: initial oven temperature was set at 40 ˚C for 2 min, then ramped to 100 ˚C (15 ˚C/min), 150 ˚C (10 ˚C/min), 250 ˚C (5 ˚C/min), and held for 8 min. For the DB-Wax column, the oven temperature was set at 40 ˚C for 2 min, then ramped to 180 ˚C (7 ˚C/min), ramped to 225 ˚C (3 ˚C/min), ramped to 250 ˚C (10 ˚C/min) and held for 5 min. Mass spectra were recorded at 70 eV ionization energy. MS source temperature was set at 280 °C, mass range 30-350 amu, and the MS quadrupole temperature was held at 150 ˚C. Identification of the odor active compounds was confirmed by comparing the mass fragmentation patterns, linear retention indices (LRI) in two columns, and odor descriptors with those exhibited by authentic standards. LRI values for the compounds were calculated from the retention times of n-alkanes from a C7 to C30 mixture as an external reference.

**3.3.5** Aroma Extract Dilution Analysis (AEDA)

The condensed smoke was serially diluted by half-volume in dichloromethane until no further aromas were detected by GC-O to perform the AEDA. Each dilution was submitted to GC-O analysis by four trained panelists in duplicate using a DB-5 MS column (30 m x 0.25 mm i.d. x 0.25 μm) according to the parameters listed in section 3.3.4. The odor-active compounds were located in the chromatograms, and flavor dilution (FD) factors were assigned to each odorant detected. The FD factors were determined as the last dilution at which at least two assessors were able to detect the odorant in both replicates. Compounds that co-eluted during AEDA are indicated in Table 3-3.

**3.3.6** Quantification of odor-active compounds

Quantification of all odorants with FD ≥ 4 was achieved by standard addition. Condensed smoke was diluted by adding 0.250 g to 10 mL of dichloromethane spiked with authentic standards for each of the analytes ranging from 1 to 5 times the approximate concentration determined in preliminary testing (See ). The internal standard 2-methyl-3-heptanone (1 μl, 10 mg/L) was added to each sample. Each concentration level was analyzed in triplicate. Samples were held at 4 ˚C until analysis. One uL of each sample was injected onto an Agilent 7890B GC system equipped with a DB-5MS or DB-WAX column using a split/splitless injector set to split 10:1. The inlet temperature was set to 250 ˚C. Helium gas was used as a carrier with a flow rate of 1.2 mL/min. To accommodate differences in compound concentration ranges and avoid saturation at the detector, samples were diluted from 1:10 to 1:100 in dichloromethane before injection.

For the DB-5 MS capillary column (60 m x 0.25 mm i.d.; 0.25 μm film thickness) (Agilent, Santa Clara, CA), the temperature program was as follows. The initial oven temperature was set at 40 ˚C then ramped to 70 ˚C (3 ˚C/min), 120 ˚C (5 ˚C/min), 300 ˚C (10 ˚C/min), and held for 4 min, and the capillary transfer line to the MSD was set to 300 ˚C. The second column used was a DB-WAX capillary column (60 m x 0.25 mm i.d.; 0.25 μm film thickness; Agilent, Santa Clara, CA) and temperature program was as follows. The oven temperature was set at 40 ˚C, then ramped to 180 ˚C (7 ˚C/min), 225 ˚C (3 ˚C/min), 250 ˚C (10 ˚C/min), and held for 5 min and the capillary transfer line to the MSD was set to 250 ˚C.

The MS was operated in MRM mode (Agilent 7010B GC-QQQ). Quadrupole temperatures were set at 150 ˚C and source temperature was 250 ˚C. MRM methods were optimized by injection of pure standards by the following procedure. Each standard first was analyzed in scan mode (30-350 *m/z*) to identify precursor ions. Then, each precursor ion was fragmented in the second quadrupole using variable collision energies (5, 10, 15, 20, and 25 eV). Optimal product ions and collision energies were selected based on abundance and selectivity for each standard **Table 3-1**). In the case of 2,3-butanedione, a single ion monitoring method was used because of a lack of unique product ions. Compounds were quantified using a 5-point standard addition curve in triplicate ($r^2$ > *0.97).* Standard addition curves are given in .

**Table 3-1.** Aroma-active compounds identified in condensed smoke with experimentally determined LRI and optimized MRM parameters used in quantitation.

| Compound | Precursor Ion (*m/z*) | Product Ion (*m/z*) | | CE (eV) |
|---|---|---|---|---|
| | | Quantifier | Qualifier | |
| 2,3-Butanedione* | - | 86 | 43 | - |

| | | | | |
|---|---|---|---|---|
| 2,3-Pentanedione | 100 | 57 | 43 | 5 |
| Acetol | 74 | 43 | - | 5 |
| 2-Methyl-2-cyclopentenone | 96 | 67 | 53 | 5 |
| Acetic acid | 60 | 45 | 43 | 10 |
| Acetoxyacetone | 86 | 43 | - | 5 |
| Furfural | 96 | 39 | 67 | 25 |
| 2-Acetylfuran | 110 | 95 | 39 | 5 |
| Butyric acid | 73 | 55 | 45 | 5 |
| 3-Methyl-2(5H)-furanone | 98 | 69 | 41 | 5 |
| Guaiacol | 124 | 109 | 81 | 15 |
| 2,6-Dimethylphenol | 122 | 107 | 77 | 15 |
| 4-Methylguaiacol | 138 | 123 | 95 | 15 |
| Maltol | 126 | 71 | 97 | 25 |
| o-Cresol | 108 | 107 | 79 | 15 |
| 4-Ethylguaiacol | 152 | 137 | 122 | 15 |
| 2-Ethylphenol | 107 | 77 | 79 | 15 |
| 2,5-Dimethylphenol | 122 | 107 | 77 | 15 |
| 2,4-Dimethylphenol | 122 | 107 | 77 | 15 |
| p-Cresol | 108 | 107 | 79 | 15 |
| m-Cresol | 108 | 107 | 79 | 15 |
| 4-Ethylphenol | 107 | 77 | 79 | 15 |
| 3-Ethylphenol | 107 | 77 | 79 | 15 |
| 3,4-Dimethylphenol | 122 | 107 | 77 | 15 |
| Syringol | 154 | 139 | 111 | 15 |
| 4-Methyl-syringol | 168 | 153 | 125 | 5 |
| Acetovanillone | 166 | 151 | 123 | 15 |

*2,3-Butanedione was quantified in single-ion monitoring (SIM) mode

### **3.3.7** Odor threshold determination of selected aroma compounds

Sensory odor threshold values in water for 23 of the 27 compounds were found in the literature (**Table 3-3**). The odor threshold values for 2-methyl-2-cyclopentenone, acetoxyacetone, 3-methyl-2-(5H)-furanone, and 4-methyl-syringol were determined experimentally using a forced-choice ascending concentration series method of limits from

ASTM E679-19[99]. Twelve to fifteen panelists (ages 22-45, 5 males, 10 females) were recruited from The Ohio State University Department of Food Science and Technology (IRB # 2021E0700). Panelists evaluated a series of triangle tests that contained the compound of interest in water alongside two distilled water blanks. Five mL of each sample or water was presented in 60 mL amber bottles which were prepared not more than 24 hours before assessments, and then stored at 4 ˚C. Two hours before analysis, bottles were placed at room temperature to equilibrate. The compound was presented in ascending order, seven dilutions were assessed for each series. Standards were diluted such that in the final set, the sample aroma was obvious to all panelists, and the first set was indiscernible. Highest concentrated standards were 33 μg/g for 4-methyl-syringol, 100 μg/g for 2-methyl-2(5H)-furanone, 33 μg/g for acetoxyacetone, and 300 μg/g for 2-methyl-2-cyclopentenone. Samples underwent serial dilution by a factor of 3 (1:3, 1:9, 1:27, … 1:2187). Panelists were instructed to smell each sample set, identify the different sample, and comment on any aroma perceived. All samples were evaluated in duplicate over two sessions during the same day.

The best estimated threshold (BET) for each panelist was calculated as the geometric mean of the concentration of the last incorrect set and the subsequent correct set. Overall BET was reported as the geometric mean of all panelists' individual BETs.

**3.3.8** Sensory Descriptive Analysis

**3.3.8.1** Lexicon development and panel training

Descriptive analysis was completed by an external panel at Kerry Ingredients (Beloit, WI) with over 1000 hours of sensory evaluation experience and over 100 hours

focused on condensed smoke and smoked products (ages 28-65, 1 male and 6 females). The panel had previously established a lexicon based on Jaffe et al [100]. for smoked products and reduced the list of attributes to 7 descriptors that were appropriate for the condensed smoke sample (**Table 3-2**) over three, 3-hour training sessions. Lexicon was validated via a correlation matrix to ensure no overlap between attributes in XLSTAT (Addinsoft, Paris, France).

**3.3.8.2** Sample Preparation and Evaluation

A recombinant model was created by dissolving authentic standards in dichloromethane at the concentrations reported in **Table 3-3**. The condensed smoke sample was prepared as described in section 3.3.3. Both the condensed smoke and the recombinant samples were diluted in dichloromethane to equal concentration for sensory evaluation, which is 1:40 of the original condensed smoke.

Twenty uL of each sample was portioned on a paper aroma strip, which was subsequently air-dried for 15 seconds to remove residual dichloromethane before placing in a 50 mL amber bottle. Samples were kept in the dark at 4 ˚C for less than 24 hours and then equilibrated at room temperature for 20 minutes before evaluation. Samples were labeled with three-digit codes and serving order was randomized. All references were available to panelists during the evaluation. Panelists rated the intensity of each attribute using a 15-point scale anchored with 1 as “just recognizable” and 15 as “extremely intense”. The samples were evaluated in duplicate over two days. Responses were recorded using EyeQuestion (Logic8 B.V., Elst, Netherlands).

**Table 3-2**. Aroma attributes with definitions and references used for descriptive analysis of condensed smoke samples.

| Attribute | Definition | Reference |
|---|---|---|
| Ashy | The aromatics associated with the residual of burnt products and dirty ashtrays. | Ghirardelli 100% cocoa |
| Burnt- sulfurous | The dark, heavy, slightly sharp and pungent notes of burning, skunk, or rubber or with the charring or burning of food. | Starbucks dark roast whole bean coffee, espresso roast, 100% arabica |
| Creosote | Tarry and phenolic aroma associated with smoke and solvents. | Medicasp coal tar gel shampoo |
| Green-woody | The aromatics associated with green wood, unseasoned wood, young branches or saplings. | Grape stems, red seedless table grapes |
| Pungent | A strong, penetrating aroma or flavor resulting in a physically penetrating sensation in the nasal cavity. | Nakano rice vinegar |
| Smoky | Mellow and well-balanced, hardwood smoke notes. | McCormick Grill Mates mesquite seasoning |
| Spice-sweet | Brown spice or sweet spice; sweet, brown, such as clove, cinnamon, nutmeg, and allspice; baking spices. | Tones ground allspice |
| Woody | Wood notes characteristic of bark, pits, seeds, or trees. | Great Value chopped walnuts |
| Overall | Intensity of overall aroma from the sample. | None |

**3.3.8.3** Sensory data analysis

Panelist performance and data analysis were evaluated using a linear regression model to investigate the three independent variables (samples, panelists, and replicates) as well as interactions for each attribute (sample*panelist, sample*replicate, and panelist*replicate) using IBM SPSS Statistics program version 28 (IBM, Armonk, NY).

## **3.4** Results and Discussion

### **3.4.1** Identification of Aroma-Active Compounds

A total of thirty-nine odor-active regions were detected in the condensed smoke by GC-O analysis. Twenty-four regions showed FD factors $\geq$ 4, with the most frequent descriptors for these regions reported as buttery, floral, sweet-smoky, phenolic, and ashy. Further MS analysis revealed all the odor active regions were assigned to one compound, confirmed by authentic standards, except for two regions that contained co-eluting alkylated phenolic isomers that were not distinguished during GC-O analysis due to similar LRI and odor quality, which also reported similar mass fragmentation patterns (**Table 3-1**). These two regions were further confirmed to contain five isomers, resulting in twenty-seven odorants.

All compounds identified in the current study have been previously reported as chemical components of wood smoke. In comparison to previous GC-O analysis conducted in smoke or in smoked foods,[1,2,4,10,23,28,78] the current study revealed ten additional compounds that included acetol, 2-methyl-2-cyclopentenone, acetoxyacetone, 3-methyl-2(5H)-furanone, 2,6-dimethylphenol, maltol, 2-ethylphenol, 2,5-dimethylphenol, 2,4-dimethylphenol, 3,4-dimethylphenol, and acetovanillone as odor-active (Table 3-3). Some of these compounds have been reported in GC-analysis of other matrices such as char-barrel aged whisky[87], toasted rice[7], caramel[6], and vanilla[101].

**Table 3-3**. Aroma compounds in condensed smoke with flavor dilution of $\geq$ 4.

| Compound | Aroma Descriptor | LRI | | FD | Conc. (µg/g smoke) | Typical Application Concentration of 0.3% (µg/g)[a] | Odor Threshold in water (µg/g) | Theoretical OAV[b] (0.3% application) |
|---|---|---|---|---|---|---|---|---|
| | | DB-WAX | DB-5 | | | | | |
| 2,3-Butanedione | buttery | 977 | 595 | 64 | 1377 ± 130 | 4.2 ± 0.39 | 0.004[d] | 1050 |
| 2,3-Pentanedione | toasted, buttery, caramel | 1055 | 708 | 8 | 159 ± 18 | 0.48 ± 0.054 | 0.02[e] | 24 |
| Acetol | sweet caramel | 1315 | 690 | 32 | 92776 ± 5559 | 278.4 ± 16.8 | 100[e] | 3 |
| 2-Methyl-2-cyclopentenone | floral, fruity, medicinal | 1394 | 905 | 8 | 823 ± 62 | 2.46 ± 0.186 | 4.4[c] | <1 |
| Acetic acid | vinegar | 1442 | 653 | 4 | 273890 ± 18513 | 821.7 ± 55.5 | 22[f] | 37 |

| | | | | | | | | |
|---|---|---|---|---|---|---|---|---|
| Acetoxyacetone | sour, dairy | 1466 | 862 | 64 | 2204 ± 135 | 6.6 ± 0.39 | 20[c] | <1 |
| Furfural | nutty, brothy, caramel | 1477 | 831 | 16 | 31650 ± 1605 | 95.1 ± 4.8 | 3[e] | 32 |
| 2-Acetylfuran | buttery, sweet | 1523 | 910 | 16 | 362 ± 29 | 1.08 ± 0.087 | 10[f] | <1 |
| Butyric acid | cheesy | 1661 | 805 | 32 | 837 ± 76 | 2.52 ± 0.228 | 0.05[f] | 50 |
| 3-Methyl-2(5H)-furanone | green, woody, soap | 1750 | 972 | 8 | 1161 ± 73 | 3.48 ± 0.219 | 3.1[c] | 1.1 |
| Guaiacol | clove, vanilla | 1880 | 1088 | 128 | 2652 ± 113 | 8.1 ± 0.33 | 0.012[d] | 675 |
| 2,6-Dimethylphenol | burnt, phenolic, ashy | 1923 | 1108 | 4 | 119 ± 8 | 0.36 ± 0.0237 | 0.4[g] | <1 |
| 4-Methylguaiacol | toasted, vanilla, ashy | 1977 | 1191 | 32 | 1481 ± 79 | 4.5 ± 0.237 | 0.021[f] | 214 |
| Maltol | sweet, cooked sugar | 2027 | 1111 | 32 | 1139 ± 82 | 3.3 ± 0.246 | 2.5[e] | 1.3 |
| o-Cresol | green, pine, phenolic | 2012 | 1051 | 4 | 1063 ± 74 | 3.3 ± 0.222 | 0.65[f] | 5 |
| 4-Ethylguaiacol | smoky, creosote | 2050 | 1277 | 8 | 582 ± 42 | 1.74 ± 0.126 | 0.05[h] | 35 |
| 2-Ethylphenol | ashy | 2078 | 1134 | 4 | 85 ± 5 | 0.255 ± 0.0156 | 0.3[i] | <1 |
| 2,5-Dimethylphenol | sweet burnt | 2088 | 1146 | 4 | 32 ± 4 | 0.096 ± 0.0117 | 0.4[g] | <1 |
| 2,4-Dimethylphenol | burnt, smoky | 2090 | 1154 | 8 | 692 ± 22 | 2.07 ± 0.066 | 0.5[j] | 4 |
| p-Cresol | burnt, plastic, clove | 2094 | 1072 | 32* | 869 ± 47 | 2.61 ± 0.141 | 55[f] | <1 |
| m-Cresol | burnt, plastic, clove | 2103 | 1072 | 32* | 466 ± 30 | 1.41 ± 0.09 | 0.19[f] | 7 |
| 4-Ethylphenol | ashy | 2187 | 1163 | 32* | 226 ± 17 | 0.69 ± 0.051 | 0.021[j] | 33 |
| 3-Ethylphenol | ashy | 2195 | 1165 | 32* | 76 ± 7 | 0.228 ± 0.0198 | 0.0017[j] | 134 |
| 3,4-Dimethylphenol | sweet, ashy | 2235 | 1191 | 32* | 59 ± 5 | 0.177 ± 0.0144 | 1.2[g] | <1 |
| Syringol | ashy, smoky | 2283 | 1349 | 4 | 11911 ± 575 | 35.7 ± 1.71 | 1.85[f] | 19 |
| 4-Methylsyringol | woody, vanilla, ashy | 2369 | 1443 | 64 | 3353 ± 71 | 10.2 ± 0.213 | 0.22[c] | 46 |
| Acetovanillone | sweet, vanilla | 2677 | 1487 | 16 | 2248 ± 148 | 6.6 ± 0.45 | 1[k] | 7 |

*a* – 0.3% application rate represents a reasonable usage level in a final application such as brine, soup, or sauce; *b* – OAV is calculated by dividing the concentration by the odor threshold; *c* – threshold level was determined experimentally; d – Rychlik et al 1998; e – Buttery et al 1999; f – Leffingwell and associates; g – Fenaroli 1971; h – Van Gemert 2011; i – Pang et al 2019; j – Czerny 2008; k – Marcq and Schieberle 2015;*two or more compounds were represented in the same odor active region and share the same FD.

In general, the smoke compounds identified consisted of aldehydes, ketones, lactones, acids and phenolics, which would originate from the thermal degradation of cellulose, hemicellulose, and lignin[66]. Dry hardwood is containing primarily carbon, hydrogen, and oxygen in its molecular structure[102,103], which would not favor the generation of nitrogen or sulfur-containing compounds, and which was in alignment with the compounds identified (Table 3-3).

### **3.4.2** Quantification of odorants

The concentrations of twenty-seven odorants ranged from 32 µg/g for 2,5 dimethylphenol to 270,000 µg/g for acetic acid (Table 3-3). The next most abundant compounds were acetol (92,000 µg/g), furfural (31,000 µg/g), and syringol (12,000 µg/g). Taking into account the typical dosage of condensed smoke in a finished product such as a soup or a brine is approximately 0.3% w/w[104–113], the concentration range at this dosage would be between 0.0017 and 800 µg/g. This compound composition was in general agreement with those reported in smoke food products[2], with the exception of relatively higher amounts of low molecular weight carbonyl compounds such as 2,3-butanedione, 2,3-pentanedione, and 2-methyl-2-cyclopentenone, and higher molecular weight phenolics such as acetovanillone. Condensed smoke ingredients typically undergo different processing steps, for example concentration under vacuum, which could result in the loss

of low molecular weight compounds and explain some of the noted differences observed in chemical composition with prior findings.

### **3.4.3** Formation of aroma compounds from hardwood

Phenolic compounds are formed from the pyrolysis of lignin, which consists of three types of phenylpropane monomer units, guaiacyl, syringl, and hydroxyphenyl[103]. Monomer lignin units are bonded by a majority of β-ether linkages in hardwood[54] in the para-position to the hydroxyl group, as well as α-ether, β-aryl, and biphenyl linkages[59]. Ether linkages are the most susceptible to thermal degradation and can form a variety of side-chains such as the ethyl ketone found in acetovanillone (2248 μg/g), and the alkyl-substitutions[59] found in 4-methylguaiacol (1481 μg/g), 4-ethylguaiacol (1277 μg/g), 4-methylsyringol (3353 μg/g), 4-ethylphenol (226 μg/g) and p-cresol (869 μg/g). Further removal of the side-chain[59] results in the other guaiacyl and syringyl derivatives, guaiacol (2652 μg/g) and syringol (11,911 μg/g).

A secondary reaction occurs during pyrolysis that results in the conversion of guaiacol and syringol methoxy groups to methyl-groups via a quinone methide intermediate[59]. This more favorably occurs in the ortho-position and is responsible for the higher abundance of methyl-substitutions in the ortho-position found in *o*-cresol (1063 μg/g), 2,6-dimethylphenol (119 μg/g), and 2,4-dimethylphenol (692 μg/g), as opposed to the meta-position substitutions to form *m*-cresol (466 μg/g), 3-ethyphenol (76 μg/g), and 2,5-dimethylphenol (32 μg/g).

Carbohydrates in the cellulose and hemicellulose of wood cell-walls primarily form the carbonyl compounds found in condensed smoke. Carbohydrate degradation is evident from the large quantity of sugar fractions such as acetol (92,776 μg/g), acetoxyacetone (2204 μg/g)[114], as well as acetic (273,890 μg/g) and butyric (837 μg/g) acids[115]. Additionally 2,3-butanedione (1377 μg/g) and 2,3 pentanedione (159 μg/g) can form from the reaction of the sugar degradation products hydroxypropanone or hydroxybutanone with formaldehyde[116]. Cyclic compounds such as furfural (31,650 μg/g), 2-acetylfuran (362 μg/g), and 3-methyl-2-(5H)-furanone (1161 μg/g), as well as maltol (1139 μg/g), and 2-methyl-2-cyclopentenone (823 μg/g) can form from the thermal dehydration of sugars during pyrolysis[114].

**3.4.4** Determination of odor thresholds and calculation of a theoretical OAV

Odor threshold values are used in combination with compound concentration to determine the odor activity value (OAV) to estimate an odorants contribution to the aroma of food products[85]. The odor thresholds in water for the twenty-seven compounds are reported in Table 3-3, four were experimentally determined, including 2-methyl-2-cyclopentenone (4.4 μg/g), 3-methyl-2(5H)-furanone (3.1 μg/g), 4-methyl-syringol (0.22 μg/g), and acetovanillone (1.0 μg/g). Based on a typical food application usage level (0.3% w/w), the corresponding concentration of the twenty-seven odorants were compared with the corresponding threshold values, and revealed 2,3-butanedione (buttery), guaiacol (clove, vanilla), 4-methylguaiacol (toasted, vanilla, ashy), and 3-ethylphenol (ashy) had the highest OAVs, followed by 4-methylsyringol (burnt, plastic, clove) and butyric acid

(cheesy). This calculation suggests these compounds have a high contribution to the aroma profile of condensed smoke or aqueous smoke flavorings. With the exception of 3-ethylphenol, these compounds are all frequently reported with high OAVs in other foods including coffee[117,118], cheese[13,85], and meats[11,86]. Among the twenty-seven compounds, eight compounds (2-methyl-2-cyclopentenone, acetoxyacetone, 2-acetylfuran, 2,6-dimethylphenol, 2-ethylphenol, 2,5-dimethylphenol, p-cresol) were reported to be below the OAV, suggesting negligible contribution to the aroma profile.

Interestingly, the compound 3-ethylphenol (ashy) has only been reported once in hardwood smoke[2], and once in other smoked foods[11]. The low concentration of 3-ethylphenol and coelution with the more abundant 4-ethylphenol (DB-5 column), and the indistinguishable MS fractionation pattern likely contributed to the low detection in prior literature.

### **3.4.5** Sensory Descriptive Analysis

The sensory panel revealed the condensed smoke consisted of eight main attributes (ashy, burnt-sulfurous, creosote, green-woody, pungent, smoky, spice-sweet, woody) which are illustrated in Figure 3-1, along with the comparative analysis of the aroma recombination model. All eight attribute ratings were reported any significant differences between the samples ($\alpha$=0.05), indicating that the condensed smoke was adequately characterized by the 27 compounds included in the recombinant model. Replicates were not significant, and the panelist*sample interactions were not significant, indicating good reproducibility and attribute concept alignment (Table 3-4).

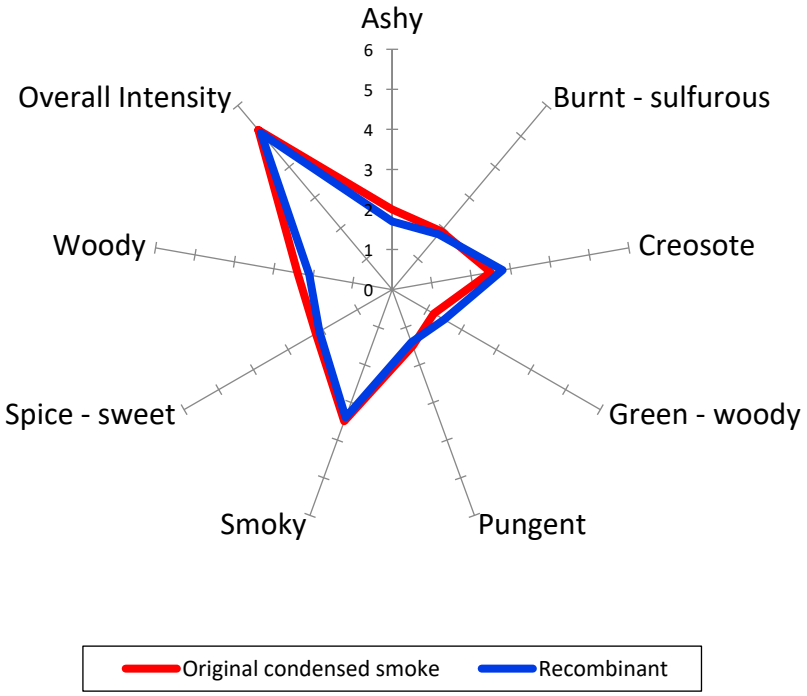


**Figure 3-1**. Sensory profile of condensed smoke and recombination model (N=7, in duplicate). No significant differences were found between samples for all attributes ($\alpha$ = 0.05, linear discriminant analysis model with replicate and panelist interactions)

Table 3-4. Panelist main effects and interaction terms

| | | Ashy | Burnt - sulfurous | Creosote | Green - woody | Pungent | Smoky | Spice - sweet | Woody | Overall |
|---|---|---|---|---|---|---|---|---|---|---|
| P-values | Sample | 0.088 | 0.917 | 0.083 | 0.213 | 0.308 | 0.478 | 0.842 | 0.207 | 0.638 |
| | Replicate | 0.697 | 0.086 | 0.083 | 0.955 | 0.269 | 0.666 | 0.434 | 0.293 | 0.336 |
| | Sample by Rep | 0.192 | 0.66 | 0.021 | 0.165 | 0.060 | 0.603 | 0.174 | 0.203 | 0.296 |
| | Sample by Panelist | 0.603 | 0.855 | 0.083 | 0.414 | 0.218 | 0.798 | 0.253 | 0.909 | 0.506 |
| | Panelist by Rep | 0.199 | 0.368 | 0.754 | 0.955 | 0.897 | 0.885 | 1.000 | 0.293 | 0.958 |

N=7 in duplicate. Statistics are based on a linear discrimination model incorporating the sample, the replicate, and the panelist as main effects as well as interactions. Significance was assessed at $\alpha$=0.05.

The aroma attributes of phenolic compounds are known to be complex, consisting of multiple attributes that can impact the overall smoke aroma beyond additive

relationships that contribute to the flavor character, as demonstrated in model solutions.[9,119] Methoxylated phenolics such guaiacol (clove, vanilla), 4-methylguaiacol (woody, vanilla, ashy), 4-ethylguaiacol (smoky, creosote), syringol (ashy, smoky), and 4-methylsyringol (woody, vanilla, ashy) are likely contributing to the smoky character. Burnt-sulfurous, ashy, and creosote notes were based on the alkyl phenols such as 3-ethylphenol (ashy), 4-ethylphenol (ashy), 2,4-dimethylphenol (burnt, smoky), and *m*-cresol (burnt, plastic, clove). Green woody and woody were likely attributed to several classes of compounds such as 2-methyl-2-cylopentenone (floral, fruity, medicinal), 3-methyl-2(5H)-furanone (green, woody, soap), *o*-cresol (green, pine, phenolic), and 4-methyl-syringol (woody, vanilla, ashy). Likewise, spice-sweet aroma was suggested to be from a mixture of compound classes that add the sweet-character associated with brown spices and brown sugar such as furfural (nutty, brothy, caramel), 2,3-butanedione (buttery), 2,3-pentanedione (toasted, buttery, caramel), maltol (cooked sugar, sweet), guaiacol (clove, vanilla), and acetovanillone (sweet, vanilla). Acids, especially acetic acid, are likely contributing to the pungency of the samples.

### **3.4.6** Limitations and future research

Analyzing condensed smoke smoke, rather than smoke applied in food, allows for the understanding of compounds that might change during processing or may react with the food product. However, isolating smoke for analysis does introduce some matrix limitations, such as relying on a dichloromethane extract. A mixed hardwood blend was chosen to be generic, but there are a variety of aroma-active smoke compounds that could

be generated using other smoking techniques or wood sources, which might warrant further investigation. Additionally, omission analysis, omitting specific compounds to see how or if the aroma character might change, would help understand the contribution of individual compounds to overall smoke aroma changes.

## **3.5** Conclusion

Twenty-seven odorants in condensed smoke were reported to characterize the flavor profile that consisted of sweet-spice, smoky, creosote, ashy, burnt-sulfurous, green-woody, woody, and pungent aroma attributes. These findings provide an improved molecular basis to optimized smoke flavoring materials for food applications.

**3.6** Supplemental Figures

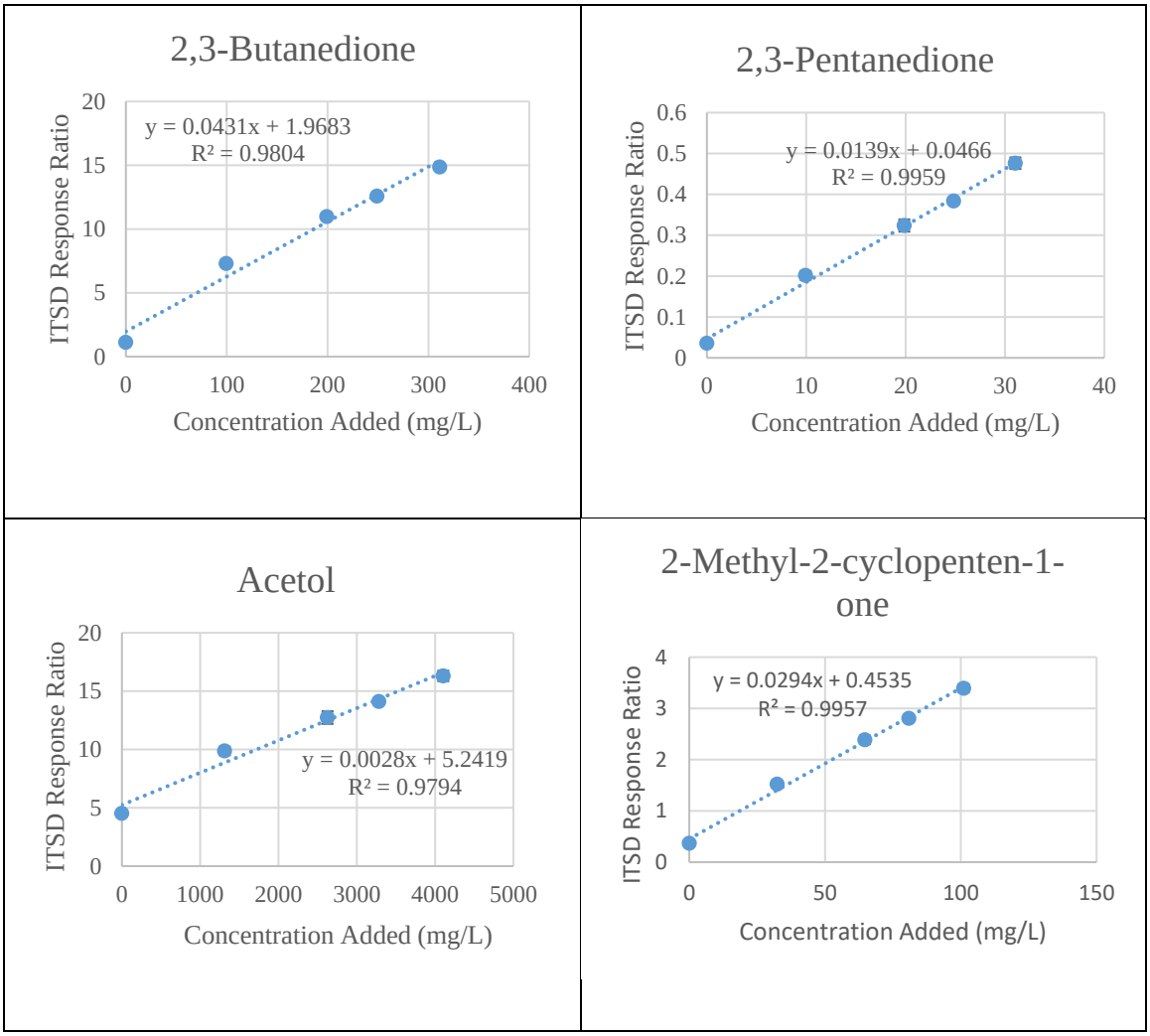


**Supplemental Figure 1.** Standard addition curves built in condensed smoke for selected aroma compounds. Values are represented as average of triplicate

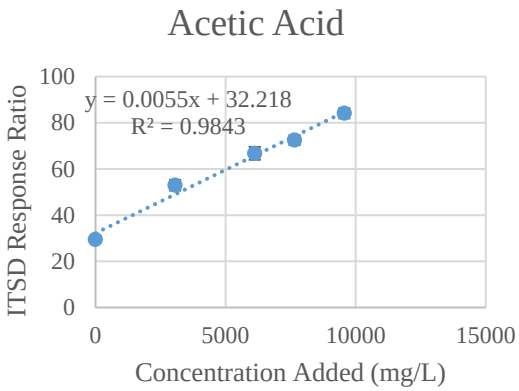
Acetic Acid
y = 0.0055x + 32.218
R² = 0.9843
ITSD Response Ratio
Concentration Added (mg/L)
0
20
40
60
80
100
0
5000
10000
15000

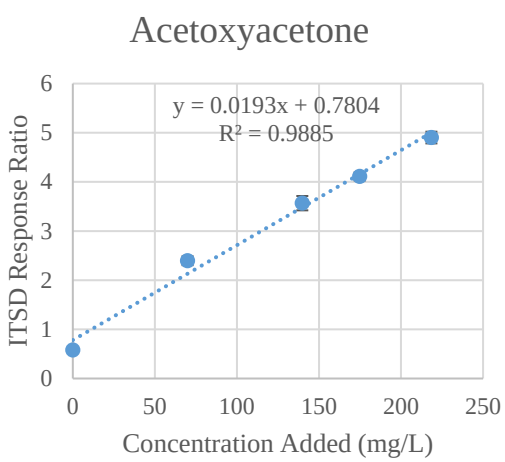
Acetoxyacetone
y = 0.0193x + 0.7804
R² = 0.9885
ITSD Response Ratio
Concentration Added (mg/L)
0
1
2
3
4
5
6
0
50
100
150
200
250

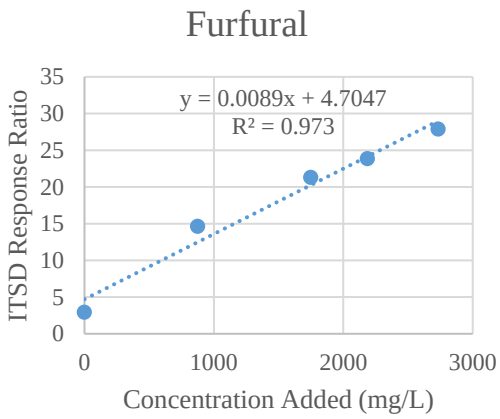
Furfural
y = 0.0089x + 4.7047
R² = 0.973
ITSD Response Ratio
Concentration Added (mg/L)
0
5
10
15
20
25
30
35
0
1000
2000
3000

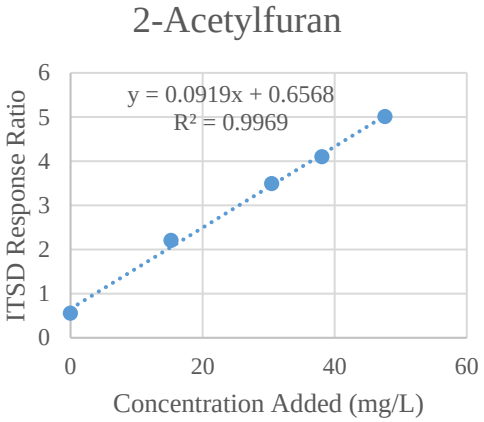
2-Acetylfuran
y = 0.0919x + 0.6568
R² = 0.9969
ITSD Response Ratio
Concentration Added (mg/L)
0
1
2
3
4
5
6
0
20
40
60

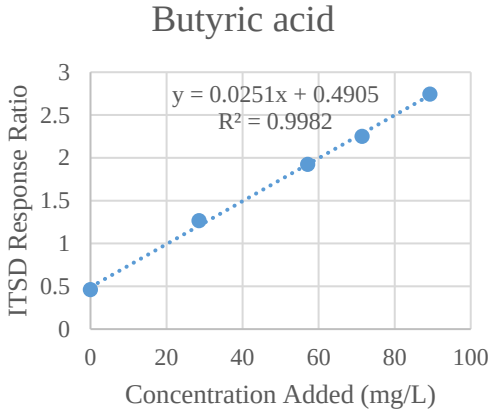
Butyric acid
y = 0.0251x + 0.4905
R² = 0.9982
ITSD Response Ratio
Concentration Added (mg/L)
0
0.5
1
1.5
2
2.5
3
0
20
40
60
80
100

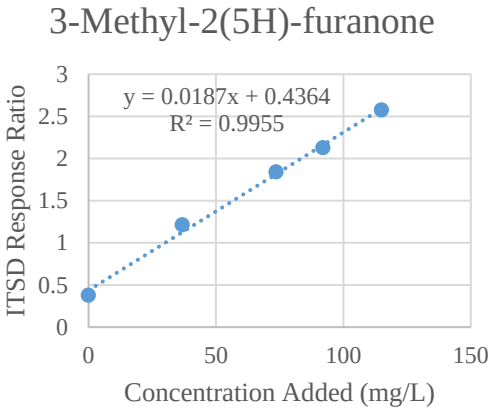
3-Methyl-2(5H)-furanone
y = 0.0187x + 0.4364
R² = 0.9955
ITSD Response Ratio
Concentration Added (mg/L)
0
0.5
1
1.5
2
2.5
3
0
50
100
150

Continued

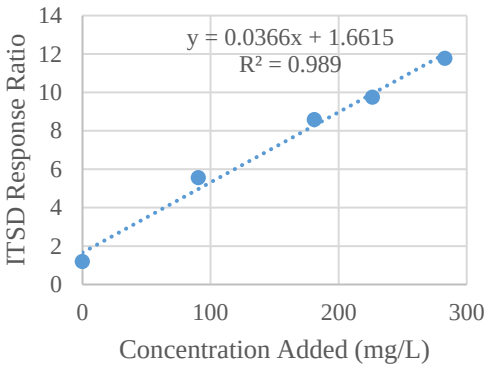
Guaiacol
y = 0.0366x + 1.6615
R² = 0.989
ITSD Response Ratio
Concentration Added (mg/L)
0
2
4
6
8
10
12
14
0
100
200
300

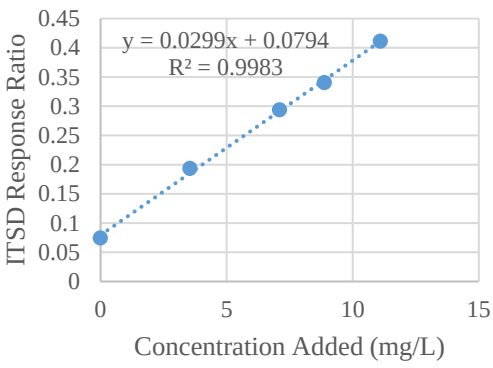
2,6-Dimethylphenol
y = 0.0299x + 0.0794
R² = 0.9983
ITSD Response Ratio
Concentration Added (mg/L)
0
0.05
0.1
0.15
0.2
0.25
0.3
0.35
0.4
0.45
0
5
10
15

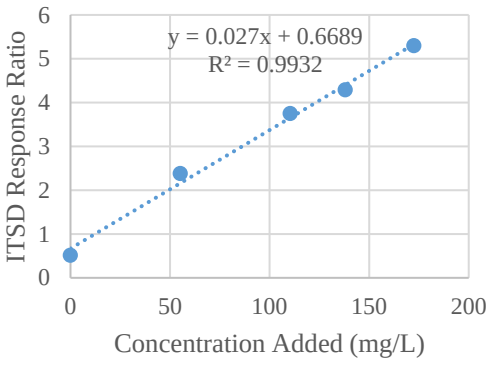
4-Methylguaiacol
y = 0.027x + 0.6689
R² = 0.9932
ITSD Response Ratio
Concentration Added (mg/L)
0
1
2
3
4
5
6
0
50
100
150
200

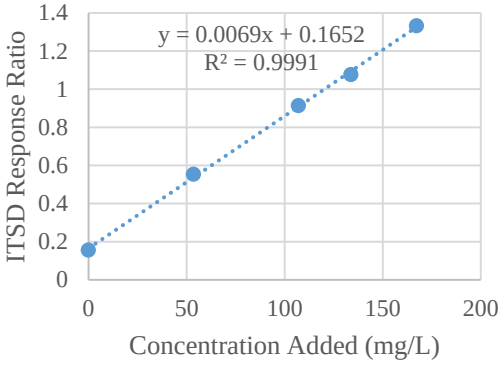
Maltol
y = 0.0069x + 0.1652
R² = 0.9991
ITSD Response Ratio
Concentration Added (mg/L)
0
0.2
0.4
0.6
0.8
1
1.2
1.4
0
50
100
150
200

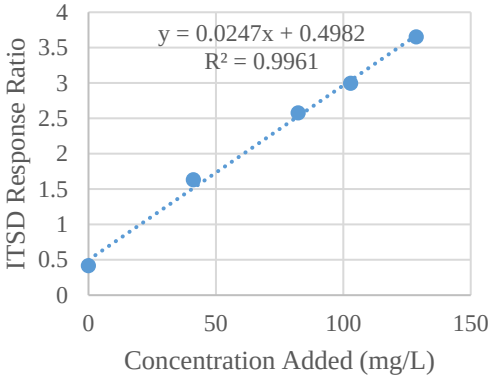
o-Cresol
y = 0.0247x + 0.4982
R² = 0.9961
ITSD Response Ratio
Concentration Added (mg/L)
0
0.5
1
1.5
2
2.5
3
3.5
4
0
50
100
150

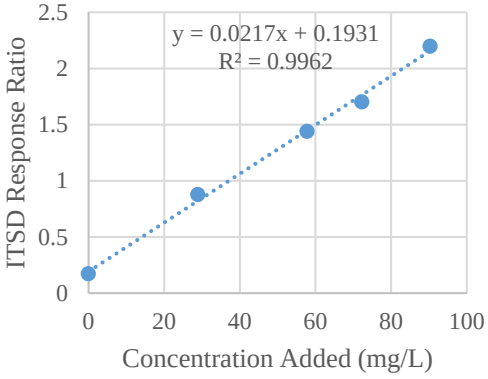
4-Ethylguaiacol
y = 0.0217x + 0.1931
R² = 0.9962
ITSD Response Ratio
Concentration Added (mg/L)
0
0.5
1
1.5
2
2.5
0
20
40
60
80
100

Continued

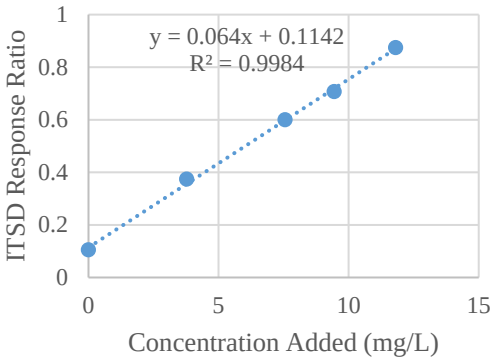
2-Ethylphenol
y = 0.064x + 0.1142
R² = 0.9984
ITSD Response Ratio
Concentration Added (mg/L)

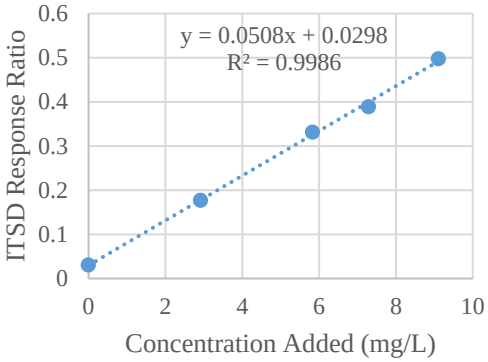
2,5-Dimethylphenol
y = 0.0508x + 0.0298
R² = 0.9986
ITSD Response Ratio
Concentration Added (mg/L)

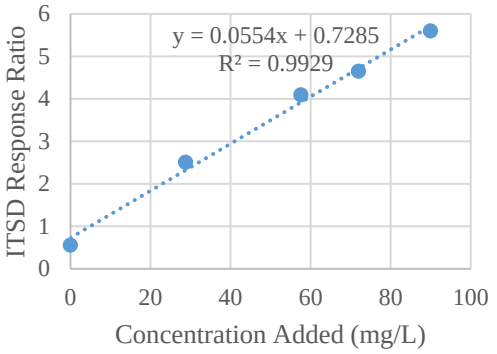
2,4-Dimethylphenol
y = 0.0554x + 0.7285
R² = 0.9929
ITSD Response Ratio
Concentration Added (mg/L)

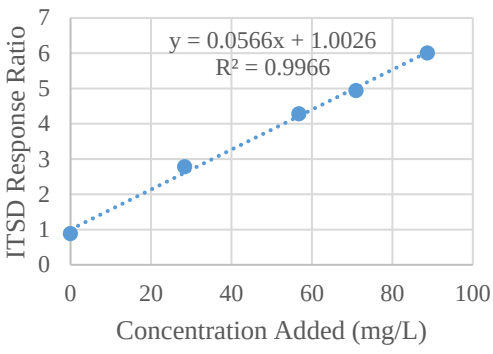
p-Cresol
y = 0.0566x + 1.0026
R² = 0.9966
ITSD Response Ratio
Concentration Added (mg/L)

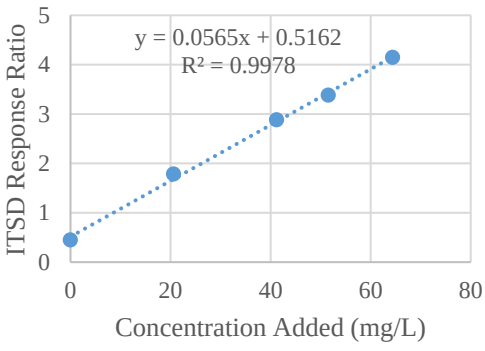
m-Cresol
y = 0.0565x + 0.5162
R² = 0.9978
ITSD Response Ratio
Concentration Added (mg/L)

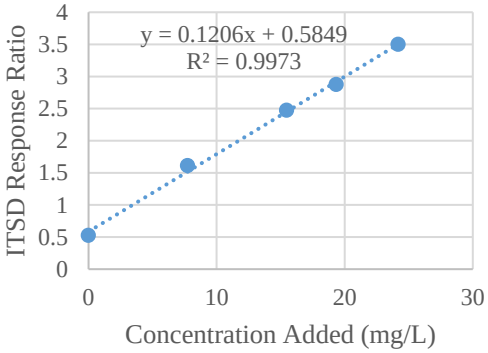
4-Ethylphenol
y = 0.1206x + 0.5849
R² = 0.9973
ITSD Response Ratio
Concentration Added (mg/L)

Continued

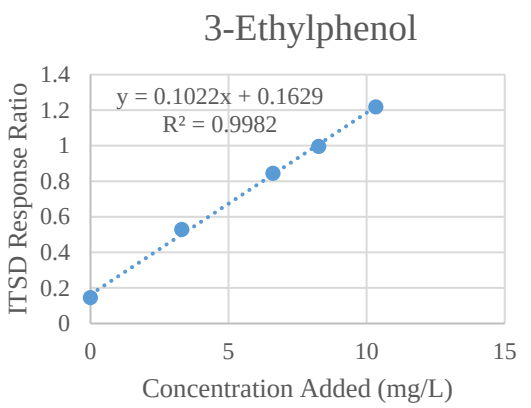
3-Ethylphenol
y = 0.1022x + 0.1629
R² = 0.9982
ITSD Response Ratio
Concentration Added (mg/L)
0
0.2
0.4
0.6
0.8
1
1.2
1.4
0
5
10
15

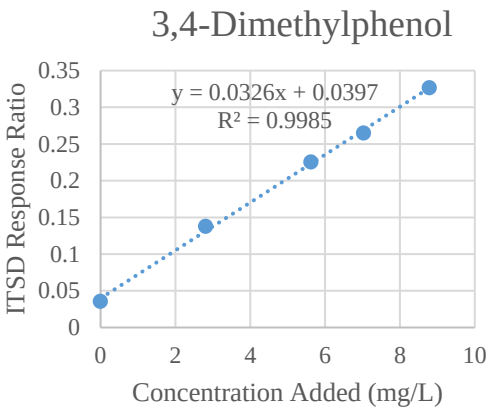
3,4-Dimethylphenol
y = 0.0326x + 0.0397
R² = 0.9985
ITSD Response Ratio
Concentration Added (mg/L)
0
0.05
0.1
0.15
0.2
0.25
0.3
0.35
0
2
4
6
8
10

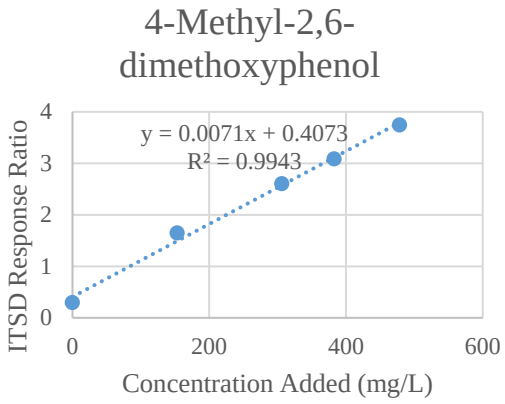
4-Methyl-2,6-dimethoxyphenol
y = 0.0071x + 0.4073
R² = 0.9943
ITSD Response Ratio
Concentration Added (mg/L)
0
1
2
3
4
0
200
400
600

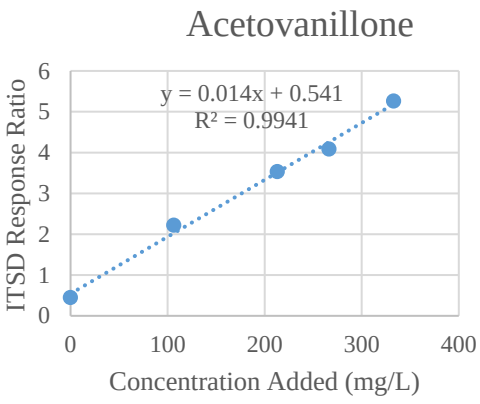
Acetovanillone
y = 0.014x + 0.541
R² = 0.9941
ITSD Response Ratio
Concentration Added (mg/L)
0
1
2
3
4
5
6
0
100
200
300
400

Continued

# Chapter 4. The impact of hardwood cell wall structure on the formation of aroma compounds in condensed smoke

*Vazquez, T., Tello E., Klein M., Peterson D.G. 2022.*
*Manuscript in preparation.*

## **4.1** Abstract

The relationship between hardwood cell-wall structure and the aroma profile of condensed smoke flavorings generated by pyrolysis was investigated. Six hardwood samples were utilized to generate condensed smoke samples, with aroma profiles characterized by sensory Descriptive Analysis (DA) and quantified by Gas Chromatography/Mass Spectrometry/Mass Spectrometry (GC/MS/MS). The cell-wall structures of hardwood samples were also characterized by Heteronuclear Single Quantum Coherence (HSQC) analysis. Sensory DA revealed significant differences among the samples for six out of the eight aroma attributes, including ashy, creosote, green-woody, smoky, spice-sweet, and woody. The wood NMR chemical profiles were modeled against the concentrations of 27 aroma compounds by Orthogonal Partial Least Squares Regression (OPLS-R) models with good fit and predictive ability ($R^2Y$: 0.88-0.99, $Q^2$: 0.73-0.97). Predictive NMR spectra revealed changes in hemicellulose, cellulose, and the methoxylation of the wood lignin were key components during pyrolysis that impacted the generation of the aroma composition in condensed smoke.

Key Words: Liquid smoke, Hardwood cell-wall, Aroma descriptive analysis, Heteronuclear Single Quantum Coherence (HSQC) experiment, Untargeted metabolomics approach

**4.2** Introduction

For thousands of years, smoking of food has been used to not only inhibit microbial growth for food safety,[17,120] but to impart a unique and desirable flavor[4,35,37] to many culturally meaningful foods. These processes are time-consuming and result in variable quality due to factors such as smoking methodology, wood composition, water content, and temperature[3,121–123]. To provide consistency, the food industry commonly relies on condensed smoke, also known as liquid smoke[1,35]. Condensed smoke is produced from the smoke aerosol generated by pyrolysis of woody material, such as sawdust, which is then cooled and condensed into a liquid. Due to the inherent differences in smoking methodology, condensed smoke often has different flavor[15], color[124], and textural properties[35,124] as compared to a conventional smokehouse application. Currently, there is an inadequate understanding of the pathways of flavor generation of condensed smoke limiting optimization by the industry.

Traditionally, hardwood species have been chosen for their preferred flavor[35], the most common species include hickory, mesquite, maple, oak, apple, and cherry[4]. Smoked foods are frequently marketed toward consumers utilizing the hardwood species names in the product name.

The perceived difference in flavor profiles is thought to be impacted by the molecular structure of hardwoods, which pyrolyzes to form aroma compounds[76]. Hardwood is composed of three cell-wall polymers: lignin (23-30%), cellulose (38-49%), and hemicellulose (19-26%)[4,5,61,103]. Lignin comprises three types of phenyl-propane subunits: guaiacyl (G), syringyl (S), and hydroxyphenyl (H), which are bonded by a variety

of carbon-carbon, ether, and ester linkages[56]. Pyrolysis of lignin has been reported to be responsible for the formation of phenolic aroma compounds such as guaiacol and syringol.[8] Cellulose is a well characterized polymer composed of glucose subunits bound by a β-1,4-glycosdic bond[70]. Conversely, hemicellulose is less well characterized and more heterogeneous in structure. Hemicellulose is comprised of a variety of monosaccharide units and uronic acid subunits[103], and are 70-80% xylose units in hardwood. Together, hemicellulose and cellulose comprise "holocellulose", and are linked to the formation of aroma compounds including acids, alcohols, carbonyls, lactones, and furans[58,66].

Wood cell-wall polymers are typically analyzed by a series of "wet" chemical methods, which are destructive in nature[103,125]. Recent advances in methodology for Nuclear Magnetic resonance (NMR) have allowed for liquid-state or solid-state characterization of lignin and hollocellulose, which minimizes sample degradation and allows for comprehensive analysis of the wood structure. Heteronuclear Single Quantum Coherence (HSQC) NMR is specifically well-suited for the 'untargeted' cell-wall profiling analysis of wood due to its high resolution.

This study aimed to correlate hardwood cell-wall structures to the subsequent aroma profile of condensed smoke. The first objective was to characterize the aroma profiles of six hardwood condensed smoke samples generated by identical conditions on a pilot-scale smoke generator using Sensory Descriptive Analysis (DA). Second, twenty-seven aroma compounds, previously identified in chapter 3, were quantified in each condensed smoke sample via tandem Gas-Chromatography/Mass Spectrometry/Mass Spectrometry (GC/MS/MS). Finally, the key cell-wall components correlated to the

enhancement or inhibition of aroma-active volatile compounds in each wood sample were analyzed via an untargeted bidimensional NMR approach using an HSQC experiment.

## **4.3** Materials and methods

### **4.3.1** Chemicals

High purity dichloromethane (DCM), dimethylsulfoxide (DMSO), 1-methylimidazole (NMI), acetic anhydride, ethanol, acetone, propylene glycol, and dimethysulfoxide-d6 were purchased from Thermo Fisher Scientific (Waltham, MA). The compounds 2,3-butanedione, 2,3-pentanedione, 1-hydroxyacetone, 2-methyl-cyclopentenone, acetic acid, 1-acetoxyacetone, 2-furaldehyde (furfural), 2-acetylfuran, butyric acid, 3-methyl-2(5H)-furanone, 2-methoxyphenol (guaiacol), 2,6-dimethylphenol, 2-methoxy-4-methylphenol (creosol), maltol, 2-methylphenol (o-cresol), 2-methoxy-4-ethylphenol, 2-ethylphenol, 2,5-dimethylphenol, 2,4-dimethylphenol, 4-methylphenol (p-cresol), 3-methylphenol (m-cresol), 4-ethylphenol, 3-ethylphenol, 3,4-dimethylphenol, 2,6-dimethoxyphenol (syringol), 3,5-dimethoxytoluene (4-methylsyringol), and acetovanillone were purchased from Sigma Aldrich (St. Louis, MO). Alkane ladder (C7-C30) was purchased from Agilent Technologies (Santa Clara, CA).

### **4.3.2** Wood and condensed smoke samples

Six hardwood sawdust samples were obtained by Kerry Ingredients (Beloit, WI) from lumber sources in central Wisconsin, and stored at ambient temperature until analysis. The hardwood species were maple, red oak, apple, hickory, mesquite, and beech.

Condensed smoke samples were generated from the same six lots of hardwood species on a pilot-scale rapid thermal pyrolysis smoke generator at Kerry Ingredients. All condensed smoke samples were 70˚ Brix with a pH of 3.4.

### **4.3.3** Sensory Descriptive Analysis

#### **4.3.3.1** Lexicon development and panel training

Sensory DA was conducted by an expert external panel at Kerry Ingredients (Beloit, WI), with each panelist having >1000 hours total DA experience, of which >100 hours were focused on condensed smoke products (ages 28-65, 2 males and 7 females). The lexicon was established in section 3.3.8, and attribute definitions are reported in Table 4-1.

**Table 4-1**. Aroma attributes with definitions and references used for descriptive analysis.

| Attribute | Definition | Reference |
|---|---|---|
| Ashy | Aromatics associated with the residual of burnt products and dirty ashtrays. | Ghirardelli 100% cocoa |
| Burnt – sulfurous | The dark, heavy, slightly sharp and pungent notes of burning, skunk, or rubber or with the charring or burning of food. | Starbucks dark roast whole bean coffee, espresso roast, 100% Arabica |
| Creosote | Tarry and phenolic aroma associated with smoke and solvents. | Medicasp coal tar gel shampoo |
| Green – woody | Aromatics associated with green wood, unseasoned wood, young branches or saplings. | Grape stems, red seedless table grapes |
| Pungent | A strong, penetrating aroma or flavor resulting in a physically penetrating sensation in the nasal cavity. | Nakano rice vinegar |
| Smoky | Mellow and well-balanced, hardwood smoke notes. | McCormick Grill Mates mesquite seasoning |
| Spice – sweet | Brown spice or sweet spice; sweet, brown, such as clove, cinnamon, nutmeg, and allspice; baking spices. | Tones ground allspice |
| Woody | Wood notes characteristic of bark, pits, seeds, or trees. | Great Value chopped walnuts |
| Overall | Intensity of overall aroma from the sample | None |

**4.3.3.2** Sample preparation

Sample preparation was adapted from Wang and Chamber IV[9]. The six condensed smoke samples were diluted 1:20 with propylene glycol. Aroma strips were then dipped to a depth of 2 cm and placed in a 60 mL amber bottle for analysis. Samples were stored at 4 ˚C for no more than 48 hours and equilibrated to room temperature for 15 minutes prior to aroma evaluation.

**4.3.3.3** Sample Evaluation

Condensed smoke samples were labeled with three-digit codes and presented in randomized order. Panelists evaluated each sample for the orthonasal aroma intensity of the nine attributes using a 15-point scale anchored with 1 as “just recognizable” and 15 as “extremely intense”, responses were recorded using EyeQuestion (Logic8 B.V., Elst, Netherlands). Sample evaluation was performed in duplicate during four separate sessions occurring over 2 days.

**4.3.3.4** Sensory data analysis

The condensed smoke samples had significant differences in overall aroma intensity ($p = 0.046$; range 3.5-4.3). To adjust for these differences, the attribute intensity ratings for each sample were transformed according to wood-type:

$$Adjusted\ rating = \frac{O_S}{O_A} * Original\ rating$$

$O_S$ = Average overall intensity for a single wood-type
$O_A$ = Average overall intensity across all wood-types

Sensory DA data and statistics of panelist performance were evaluated using a 3-way ANOVA in the IBM SPSS Statistics program version 28 (IBM, Armonk, NY). In the case of observed significant sample effects, a Fisher’s LSD post-hoc test was performed ($\alpha = 0.05$). Two panelists were removed from the data set for creosote, and one panelist for smoky, due to a lack of alignment on those attributes.

**4.3.4** Quantification of aroma compounds

GC/MS/MS was used to quantify the aroma-active compounds previously identified by GC/MS/O in chapter 3, section 3.3.4. Quantification was performed by standard addition

using a five-point calibration curve generated in triplicate built in a linear concentration range ($r^2 > 0.97$) (See Supplemental Figure 1). Ten milliliters of DCM spiked with authentic standards for each of the analytes ranging from 1 to 5 times the approximate concentration were added to 250 mg of condensed smoke with 1 uL of 10 mg/L of 2-methyl-3-heptanone as an internal standard. Samples were held at 4 ˚C.

One microliter of each sample was injected onto an Agilent 7010B GC-QQQ system equipped with a DB-5MS or DB-WAX column depending on analyte performance. A split/splitless injector was used and set to split 10:1. Inlet temperature was set to 250 ˚C. Helium gas was used as a carrier gas with a flow rate of 1.2 mL/min. Depending on compound concentration and to avoid detector saturation, samples were either diluted 1:10 or 1:100 in DCM before injection. The DB-5 MS column (60 m x 0.25 mm x 0.25 μm; Agilent Technologies Santa Clara, CA) used an initial oven temperature of 40 ˚C which was held for 1 min, then ramped to 200˚C (3 ˚C/min), 275 ˚C (10 ˚C/min) and held for 2 min. MSD transfer line was set to 275 ˚C. The DB-WAX column (60 m x 0.25 mm x 0.25 μm; Agilent Technologies) used an initial temperature of 40 ˚C which was ramped to 180 ˚C (7 ˚C/min), 225 ˚C (3 ˚C/min), 250 ˚C (10 ˚C/min), and held for 5 min. MSD capillary transfer line was set to 250 ˚C.

In the case of both columns, the MSD conditions were as follows. Agilent 7010B GC-QQQ was used in multiple reaction monitoring (MRM) mode. Quadrupole temperatures were set at 150 ˚C and source temperature was 250 ˚C. MRM methods were optimized by injection of pure standards (see Table 4-2). First, each standard was analyzed in scan mode (30-350 amu) to identify precursor ions. Next, each precursor ion for each

standard was fragmented in the second quadrupole using multiple collision energies (5, 10, 15, 20, and 25 eV). Optimal product ions were then selected based on abundance and selectivity. In the case of 2,3-butanedione, a single ion monitoring method was used because of a lack of unique product ions. Compounds were quantified using a 5-point standard addition curve in triplicate ($r^2 > 0.97$).

**Table 4-2**. GC-MS-MRM quantification parameters for aroma compounds in condensed liquid smoke.

| Identified Compounds | Precursor Ion (*m/z*) | Product Ion (*m/z*) | | Collision Energy (eV) |
|---|---|---|---|---|
| | | Quantifier | Qualifier | |
| **2,3-Butanedione*** | - | 86 | 43 | - |
| **2,3-Pentanedione** | 100 | 57 | 43 | 5 |
| **Acetol** | 74 | 43 | - | 5 |
| **2-Methyl-2-cyclopentenone** | 96 | 67 | 53 | 5 |
| **Acetic acid** | 60 | 45 | 43 | 10 |
| **Acetoxyacetone** | 86 | 43 | - | 5 |
| **Furfural** | 96 | 39 | 67 | 25 |
| **2-Acetylfuran** | 110 | 95 | 39 | 5 |
| **Butyric acid** | 73 | 55 | 45 | 5 |
| **3-Methyl-2(5H)-furanone** | 98 | 69 | 41 | 5 |
| **Guaiacol** | 124 | 109 | 81 | 15 |
| **2,6-Dimethylphenol** | 122 | 107 | 77 | 15 |
| **4-Methylguaiacol** | 138 | 123 | 95 | 15 |
| **Maltol** | 126 | 71 | 97 | 25 |
| **o-Cresol** | 108 | 107 | 79 | 15 |
| **4-Ethylguaiacol** | 152 | 137 | 122 | 15 |
| **2-Ethylphenol** | 107 | 77 | 79 | 15 |
| **2,5-Dimethylphenol** | 122 | 107 | 77 | 15 |
| **2,4-Dimethylphenol** | 122 | 107 | 77 | 15 |
| **p-Cresol** | 108 | 107 | 79 | 15 |
| **m-Cresol** | 108 | 107 | 79 | 15 |
| **4-Ethylphenol** | 107 | 77 | 79 | 15 |
| **3-Ethylphenol** | 107 | 77 | 79 | 15 |
| **3,4-Dimethylphenol** | 122 | 107 | 77 | 15 |
| **2,6-Dimethoxyphenol** | 154 | 139 | 111 | 15 |
| **4-Methylsyringol** | 168 | 153 | 125 | 5 |
| **Acetovanillone** | 166 | 151 | 123 | 15 |

*Analyzed in single ion monitoring mode

**4.3.5** Hardwood sawdust preparation for NMR analysis

Preparation of cell-wall materials of wood sawdust samples was adapted from the methodologies published in Mansfield et al 2012[56]. In short, hardwood sawdust samples were prepared in triplicate for each of the 6 samples, with cell walls isolated by sequential extractions. Two grams of each sample was added to a 50-mL conical centrifuge tubes containing 40 mL of nanopure water and the samples were sonicated for 20 minutes. Samples were then centrifuged for 10 minutes at 10,000 rpm at room temperature, and the supernatant was discarded. Extraction and sonication were repeated two additional times with nanopure water, then three times with 80% (vol/vol) ethanol/water, and one time with acetone. Extracted cell-wall material was washed once with nanopure water to remove residual acetone and lyophilized for 24 hours.

Cell wall material was milled using a Geno/Grinder 2010 (SPEX Sample Prep, Metuchen, NJ). Two-hundred milligrams were added to a 4 mL polyethylene vial with 3/8 inch diameter stainless steel grinding media. Samples were milled at 1000 rpm for 10 minutes, followed by 5 minutes of rest to avoid excess heat generation. This was repeated ten times until a fine powder was acquired.

For cell wall dissolution, 100 mg of milled cell wall powder was suspended in 2 mL of DMSO in a 20 mL glass vial, then 1 mL of NMI was subsequently added and the samples were stirred on a shaking table for 4 hours. Acetylation of cell walls was accomplished by adding 0.5 mL of acetic anhydride and stirring for an additional 1.5 hours. The solutions were then added to 500 mL of nanopure water and samples were left to

precipitate for 3 hours at room temperature. The precipitate was washed three times with 50 mL of water and dried by lyophilization for 24 hours. Eighty milligrams of dry acetylated cell-wall material was then added to 0.5 mL of DMSO-d6, sonicated for 15 minutes, and then transferred to 5 mm NMR tubes for analysis.

**4.3.5.1** Mono- and bidimensional NMR experiments

NMR spectra were acquired on a Bruker Avance III HD 850 MHz spectrometer (Bruker Billerica, MA) equipped with a TCI cryoprobe. Two-dimensional HSQC spectra were acquired with a gradient-selective pulse sequence using adiabatic pulses for inversion, refocusing, and bi-level decoupling and an INEPT transfer delay optimized for 145 Hz 1-bond C-H couplings. The proton and carbon carriers were set to 6 ppm and 90 ppm, respectively, with sweep widths of 40 ppm and 220 ppm. A recovery delay of 5 seconds was used with acquisition times of 30 ms and 6.8 ms, amounting to 1024 and 320 complex points, in proton and carbon dimensions respectively. The large sweep width and short acquisition time in the proton dimension were chosen to improve the sensitivity of signals with short T2 relaxation times that are observed in the samples. The spectra were processed using Topspin 3.6.4 (Bruker Billerica, MA). Spectral alignment was done using the residual DMSO peak at $\delta_H$ = 2.50 ppm and $\delta_C$ = 40.0 ppm before analysis.

**4.3.6** Multivariate Analysis

The “mrbin” package version 1.6.1 (Klein 2021) in R version 3.2.4 (The R Foundation for Statistical Computing, Vienna, Austria) was utilized for the spectral binning of raw HSQC data. Spectra was divided into bins with a width of 0.02 ppm ($^1$H) and a

height of 1 ppm ($^{13}C$). Residual solvent regions from NMI (7.1/121, 6.9/129, 7.6/138) and DMSO (2.5/40) (chemical shift ppm $^{1}H/^{13}C$) were removed. Mrbin features for noise removal (signal/noise cutoff ratio of 3 and 75% noise threshold), HSQC cropping, PQN scaling, Pareto scaling and removal of negative values were employed. Data set contained 834 bins.

Data were further processed with SIMCA Version 14.1 (umetrics, Umeå, Sweden). Orthogonal Partial Least Squares-Regression (OPLS-R) models were developed using compound concentration of condensed smoke samples as Y-variables, and binned HSQC data as X-variables. Twenty-seven OPLS-R models were developed using cross-validation to ensure overfitting was minimized. The generated predictive variable of importance scores (VIPpred) and correlation values were used to evaluate bins that were predictive of compound concentration. Bins were then assigned to their respective NMR features which were identified by comparison with available HSQC data of acetylated cell-wall samples as well as literature on isolated model compounds[72,126–128].

## **4.4** Results and Discussion

### **4.4.1** Sensory descriptive analysis of condensed smoke samples

Sensory descriptive analysis of the six condensed smoke samples is reported in Table 4-3. Six of the eight attributes assessed were found to have significant differences in the perceived intensity indicating that hardwood species impacted the flavor profile of the condensed smoke. Beech was significantly higher in woody, green/woody, and creosote intensity than the majority of the other samples. In contrast, apple was significantly lower

in ashy and woody compared to most other hardwoods. Maple, although not statistically different than beech, received the highest intensity score for creosote. Red oak, hickory, and mesquite were not significantly different for the majority of attributes, however, mesquite was significantly lower in green/woody than hickory and significantly lower in sweet/spice than red oak. The replicate effect and panelist by sample interaction was only significant for creosote, indicating overall good concept alignment and reproducibility.

**Table 4-3**. Sensory profiles of condensed smoke samples made from different hardwood samples normalized by overall intensity.

| | Attribute Mean Sensory Score | | | | | | | |
|---|---|---|---|---|---|---|---|---|
| **Wood-type** | **Ashy** | **Burnt - sulfurous** | **Creosote** | **Green - woody** | **Pungent** | **Smoky** | **Spice - sweet** | **Woody** |
| Red Oak | $2.1^{a}$ | 2.1 | $2.5^{b}$ | $1.5^{bc}$ | 1.0 | $2.7^{b}$ | $1.6^{ab}$ | $2.7^{b}$ |
| Maple | $2.3^{a}$ | 2.2 | $3.0^{a}$ | $1.4^{bc}$ | 1.4 | $3.3^{a}$ | $1.5^{abc}$ | $2.8^{b}$ |
| Hickory | $2.0^{ab}$ | 1.9 | $2.5^{b}$ | $1.6^{ab}$ | 1.2 | $3.1^{ab}$ | $1.6^{abc}$ | $2.8^{b}$ |
| Beech | $2.2^{a}$ | 2.3 | $2.8^{ab}$ | $1.9^{a}$ | 1.5 | $3.3^{a}$ | $1.9^{a}$ | $3.2^{a}$ |
| Mesquite | $2.3^{a}$ | 2.3 | $2.6^{b}$ | $1.1^{c}$ | 1.1 | $3.1^{ab}$ | $1.2^{cd}$ | $2.5^{bc}$ |
| Apple | $1.8^{b}$ | 2.0 | $2.6^{b}$ | $1.4^{bc}$ | 1.0 | $2.7^{b}$ | $1.3^{bc}$ | $2.4^{c}$ |
| **Effect/Interaction** | **P Value** | | | | | | | |
| sample | 0.008 | 0.065 | 0.029 | 0.010 | 0.136 | 0.007 | 0.017 | <0.001 |
| replicate | 0.385 | 0.870 | 0.001 | 0.666 | 0.115 | 0.842 | 0.771 | 0.824 |
| panelist | <0.001 | <0.001 | <0.001 | <0.001 | <0.001 | <0.001 | <0.001 | <0.001 |
| sample*panelist | 0.450 | 0.181 | 0.007 | 0.541 | 0.234 | 0.105 | 0.307 | 0.240 |
| panelist*rep | 0.542 | 0.796 | 0.470 | 0.967 | 0.394 | 0.503 | 0.440 | 0.600 |
| product*rep | 0.146 | 0.593 | 0.155 | 0.532 | 0.489 | 0.602 | 0.470 | 0.752 |

Statistics are based on a three-way analysis of variance (ANOVA). Letters indicate statistical groupings based on a Fisher's LSD post-hoc test $\alpha = 0.05$. Samples were analyzed in duplicate. N = 9

Currently, there is no general consensus in the literature on the characteristic sensory attributes of smoke produced by different hardwood species. Researchers have utilized sensory DA to characterize smoke fractions[129] or smoked foods[14,130], but results

are inconsistent across studies, likely due to the differences in wood source, smoke generation conditions, and sensory methodology. To further understand the observed differences in the sensory profiles of the condensed smoke samples from the different wood types, the aroma compounds were quantified and investigated.

### **4.4.2** Quantification of aroma compounds in condensed smoke

The concentrations of the aroma compounds in the six condensed smoke samples were reported to range from 20μg/g for 2,3-pentanedione to 200,000 μg/g for acetic acid (Table 4-4). The condensed smoke samples are highly concentrated at 70% soluble solids, which are typically diluted to less than 1% strength in food applications and when calculated at this dosage, were within typical compound ranges reported condensed smoke food samples[2,104–113].

**Table 4-4**. Concentration of aroma compounds in condensed smoke generated from different wood sources.

| | Compound concentration (ug/g) by Wood Type* | | | | | | |
|---|---|---|---|---|---|---|---|
| **Compound** | **Hickory** | **Maple** | **Red Oak** | **Beech** | **Apple** | **Mesquite** | **Average** |
| 2,3-Butanedione | 1267 ± 108 ab | 1273 ± 20 a | 1295 ± 53 a | 1184 ± 59 ab | 1097 ± 70 b | 140 ± 14 c | 1043 ± 54 |
| 2,3-Pentanedione | 149 ± 13 a | 152 ± 4 a | 164 ± 4 a | 151 ± 11 a | 103 ± 7 b | 22 ± 0 c | 123 ± 7 |
| Acetol | 99409 ± 6265 a | 87772 ± 1546 bc | 88007 ± 2962 bc | 91196 ± 3966 b | 86121 ± 4569 c | 96801 ± 747 bc | 91551 ± 3342 |
| 2-Methyl-2-cyclopentenone | 676 ± 50 a | 623 ± 18 a | 647 ± 19 a | 669 ± 37 a | 535 ± 32 c | 576 ± 5 b | 621 ± 27 |
| Acetic acid | 193037 ± 18186 a | 207051 ± 5255 a | 217593 ± 6473 a | 244455 ± 14516 a | 217217 ± 12183 a | 154750 ± 1669 b | 205684 ± 9714 |
| Acetoxyacetone | 1343 ± 87 b | 1257 ± 26 bc | 1340 ± 47 b | 1541 ± 71 a | 1383 ± 86 b | 1225 ± 7 c | 1348 ± 54 |
| Furfural | 16960 ± 1237 a | 17364 ± 576 a | 17498 ± 373 a | 17673 ± 1138 a | 16124 ± 893 a | 6255 ± 42 b | 15312 ± 710 |
| 2-Acetylfuran | 278 ± 21 a | 267 ± 10 a | 264 ± 3 a | 282 ± 22 a | 263 ± 15 a | 226 ± 2 b | 263 ± 12 |
| Butyric acid | 665 ± 85 a | 756 ± 16 ab | 804 ± 28 b | 658 ± 30 ab | 699 ± 49 ab | 502 ± 5 c | 681 ± 35 |
| 3-Methyl-2(5H)-furanone | 953 ± 64 a | 931 ± 30 a | 914 ± 26 a | 933 ± 65 a | 854 ± 56 a | 532 ± 5 b | 853 ± 41 |
| Guaiacol | 2006 ± 172 a | 1921 ± 137 ab | 2177 ± 56 abc | 2419 ± 203 cd | 1127 ± 66 e | 2676 ± 42 d | 2054 ± 113 |
| 2,6-Dimethylphenol | 113 ± 9 ab | 125 ± 9 a | 119 ± 5 ab | 120 ± 11 a | 97 ± 6 b | 61 ± 1 c | 106 ± 7 |
| 4-Methylguaiacol | 1028 ± 136 b | 1056 ± 61 b | 1310 ± 20 a | 1191 ± 104 ab | 588 ± 41 c | 1063 ± 57 b | 1039 ± 70 |
| Maltol | 1116 ± 48 a | 1022 ± 66 a | 1007 ± 14 a | 973 ± 73 a | 1005 ± 67 a | 682 ± 30 b | 967 ± 50 |
| o-Cresol | 899 ± 76 | 824 ± 40 | 805 ± 16 | 832 ± 52 | 832 ± 57 | 801 ± 19 | 832 ± 43 |
| 4-Ethylguaiacol | 429 ± 39 c | 465 ± 30 bc | 536 ± 21 ab | 547 ± 51 ab | 243 ± 16 d | 555 ± 12 a | 463 ± 28 |
| 2-Ethylphenol | 77 ± 5 a | 76 ± 4 a | 72 ± 1 a | 80 ± 7 a | 73 ± 5 a | 57 ± 1 b | 73 ± 4 |
| 2,5-Dimethylphenol | 56 ± 6 bc | 37 ± 5 d | 49 ± 2 bc | 61 ± 8 b | 50 ± 3 bc | 103 ± 3 a | 59 ± 4 |
| 2,4-Dimethylphenol | 1131 ± 84 a | 1233 ± 88 a | 1083 ± 19 a | 1076 ± 99 a | 1040 ± 75 a | 800 ± 8 b | 1061 ± 62 |
| p-Cresol | 787 ± 50 c | 478 ± 20 d | 449 ± 12 d | 567 ± 41 d | 886 ± 49 b | 1235 ± 15 a | 734 ± 31 |
| m-Cresol | 461 ± 29 a | 412 ± 15 a | 445 ± 13 a | 457 ± 29 a | 467 ± 27 a | 688 ± 10 b | 488 ± 21 |
| 4-Ethylphenol | 172 ± 10 b | 125 ± 5 c | 109 ± 4 c | 178 ± 11 b | 257 ± 19 b | 295 ± 3 a | 189 ± 9 |
| 3-Ethylphenol | 74 ± 4 b | 71 ± 3 b | 70 ± 2 b | 80 ± 5 b | 74 ± 5 b | 100 ± 1 a | 78 ± 4 |
| 3,4-Dimethylphenol | 68 ± 5 b | 58 ± 4 b | 61 ± 2 b | 65 ± 4 b | 64 ± 5 b | 80 ± 1 a | 66 ± 4 |
| Syringol | 10547 ± 994 abc | 8981 ± 999 c | 10816 ± 719 ab | 12137 ± 1068 a | 8319 ± 542 c | 9244 ± 513 bc | 10007 ± 806 |
| 4-Methylsyringol | 3384 ± 412 abc | 2714 ± 166 c | 3664 ± 77 ab | 4073 ± 540 a | 2860 ± 154 c | 3107 ± 141 c | 3300 ± 248 |
| Acetovanillone | 1982 ± 189 a | 2157 ± 178 a | 2002 ± 84 a | 1943 ± 230 ab | 1572 ± 91 bc | 1411 ± 28 c | 1845 ± 133 |

*Mean values ± standard deviation (n=3) letters indicate significance by ANOVA with a Tukey post-hoc test

To investigate linear relationships between sensory DA scores and compound concentration, a Pearson correlation matrix was generated (**Table 4-5**). The correlations revealed significant associations between aroma concentration and the perceived intensity of the sensory attributes. The guaiacol derivative 4-ethylguaiacol was significantly positively correlated to the ashy aroma, indicating its importance to ashy character in condensed smoke. Apple condensed smoke had the lowest mean sensory score in ashy and was 48% lower in 4-ethylguaiacol as compared to the average (Table 4-3).

Similarly, the green-woody attribute had a significant positive correlation to acetic acid, acetoxyacetone, 2-acetylfuran, and 2-ethylphenol, indicating that these compounds may contribute to green-woody perception or have related formation pathways during pyrolysis. Mesquite smoke had the lowest green-woody sensory score and was 25% lower in acetic acid, 9% lower in acetoxyacetone, 14% lower in acetylfuran, and 22% lower in 2-ethylphenol compared to the average. In contrast, beech smoke was 18% higher in acetic acid, 14% higher in acetoxyacetone, and 10% higher in 2-ethylphenol compared to the average, which was in alignment with the reported higher green-woody score for beech among all attributes except hickory.

The spice-sweet and woody intensities were significantly correlated to 2-methyl-2-cyclopentenone and syringol, which again would suggest a contribution of these compounds to both attributes in the context of condensed smoke. For woody, beech was significantly higher than all other woods and apple was significantly lower than all other woods except mesquite. Beech had 8% higher 2-methyl-2-cyclopentenone concentration

and 21% higher syringol concentration, while apple had the lowest concentration of both compounds (14% and 17% lower respectively).

The analysis of the smoky attribute did not yield significant correlations by a two-tailed Pearson test, however guaiacol and 4-ethylguaiacol are known smoky compounds.[9] Upon closer examination, both compounds would yield a p-value close to 0.10 (0.098 and 0.106 respectively) in a one-tailed test. It is likely that a sample set with more variation and thus more power would yield a significant result at $\alpha = 0.05$.

The analysis creosote attribute did not yield significant correlations, suggesting that their character is not related to any single compound, despite significant differences in sensory DA data among condensed smoke samples. A lack of concept alignment on the creosote attribute could also be a contributing factor. For burnt-sulfurous and pungent attributes, no significant correlations were found, as to be expected with no significant differences in sensory scores (data not shown).

**Table 4-5**. Correlation matrix of aroma attribute intensity ratings versus aroma compound concentration.

| Compound | Concentration Range (µg/g condensed smoke) | Pearson correlation coefficients (r) | | | | | |
|---|---|---|---|---|---|---|---|
| | | Ashy | Creosote | Green-woody | Smoky | Spice-sweet | Woody |
| 2,3-Butanedione | 140-1295 | -0.314 | -0.083 | 0.720 | 0.063 | 0.646 | 0.395 |
| 2,3-Pentanedione | 22-164 | -0.101 | 0.024 | 0.779 | 0.229 | 0.783 | 0.570 |
| Acetol | 71600-99400 | 0.221 | 0.025 | -0.124 | 0.315 | -0.024 | 0.091 |
| 2-Methyl-2-cyclopentenone | 523-675 | 0.364 | 0.231 | 0.705 | 0.639 | .864* | .822* |
| Acetic acid | 155000-244000 | -0.242 | 0.028 | .853* | 0.148 | 0.735 | 0.565 |
| Acetoxyacetone | 1150-1540 | -0.272 | -0.048 | .859* | 0.226 | 0.726 | 0.612 |
| Furfural | 6260-17500 | -0.311 | -0.049 | 0.778 | 0.097 | 0.686 | 0.447 |
| Acetylfuran | 247-282 | -0.262 | 0.041 | .908* | 0.298 | 0.797 | 0.607 |
| Butyric_acid | 502-804 | -0.238 | -0.169 | 0.414 | -0.175 | 0.416 | 0.160 |
| 3-Methyl-2(5H)-furanone | 532-953 | -0.270 | -0.013 | 0.791 | 0.171 | 0.711 | 0.484 |
| Guaiacol | 1130-2680 | 0.810 | 0.406 | 0.002 | 0.597 | 0.272 | 0.497 |
| 2,6-Dimethylphenol | 61.3-125.3 | -0.021 | 0.170 | 0.785 | 0.315 | 0.771 | 0.602 |
| 4-Methylguaiacol | 588-1310 | 0.696 | 0.275 | 0.309 | 0.528 | 0.613 | 0.668 |
| Maltol | 682-1120 | -0.448 | -0.183 | 0.633 | -0.005 | 0.524 | 0.258 |
| o-Cresol | 664-899 | -0.378 | -0.139 | 0.394 | 0.154 | 0.273 | 0.149 |
| 4-Ethylguaiacol | 243-555 | .848* | 0.431 | 0.119 | 0.612 | 0.417 | 0.598 |
| 2-Ethylphenol | 57.4-80.3 | -0.227 | 0.129 | .890* | 0.320 | 0.763 | 0.595 |
| 2,5-Dimethylphenol | 23.4-103 | 0.304 | 0.010 | -0.514 | 0.039 | -0.413 | -0.193 |
| 2,4-Dimethylphenol | 800-1230 | -0.072 | 0.223 | 0.605 | 0.261 | 0.543 | 0.398 |
| p-Cresol | 434-1240 | -0.109 | -0.183 | -0.693 | -0.275 | -0.743 | -0.591 |
| m-Cresol | 323-688 | 0.269 | -0.018 | -0.691 | -0.088 | -0.597 | -0.377 |
| 4-Ethylphenol | 109-295 | -0.207 | -0.149 | -0.561 | -0.291 | -0.689 | -0.543 |
| 3-Ethylphenol | 56.9-99.6 | 0.399 | 0.192 | -0.518 | 0.140 | -0.442 | -0.165 |
| 3,4-Dimethylphenol | 43.7-80.3 | 0.167 | -0.075 | -0.537 | -0.019 | -0.473 | -0.283 |
| Syringol | 5960-12100 | 0.271 | 0.098 | 0.768 | 0.536 | .897* | .858* |
| 4-Methylsyringol | 1800-4070 | 0.126 | -0.086 | 0.682 | 0.341 | 0.792 | 0.724 |
| Acetovanillone | 1360-2160 | 0.247 | 0.327 | 0.654 | 0.474 | 0.731 | 0.635 |

Negative correlation — Positive correlation

*Significant Pearson correlation (α=0.05, two-tailed)

**4.4.3** Untargeted NMR flavoromics analysis of hardwood sawdust samples

The influence of wood structure on the aroma composition of condensed smoke was investigated using an untargeted NMR chemical profiling approach. HSQC provides the $^{1}H$ and $^{13}C$ crosspeak correlations for enhanced resolution of the chemical constituents as compared to monodimensional NMR analysis. In addition, HSQC analysis has been established as a suitable method for the comprehensive analysis of cell-wall material.[56,70,72,131–133] In hardwood sawdust, the majority of the material is sapwood[102] that consists of heat-resistant cell wall material such as cellulose, hemicellulose, and lignin, which is generally considered to be the source of volatile compounds in smoke.[4]

The HSQC analysis revealed two main spectral regions of the wood chemical composition that are characteristic of wood cell-wall material that consisted of the aromatic region containing aromatic lignin signals and the polysaccharide region containing cellulose and hemicellulose signals (**Figure 4-1**).

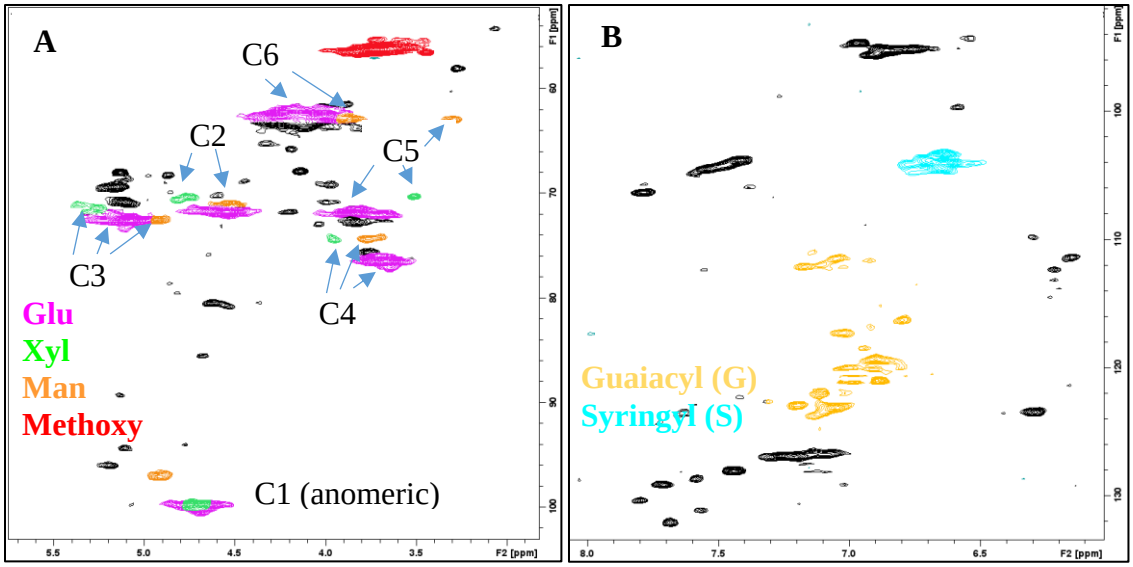


**Figure 4-1.** Representative HSQC spectra of hardwood cell wall material (Beech hardwood). A) Lignin aromatic region B) Polysaccharide and lignin linkage region

The spectral region from $\delta_H$ 7.5 ppm to $\delta_H$ 6.5 ppm correlated with a $^{13}C$ region from $\delta_C$ 140 ppm to $\delta_C$ 105 ppm that is characteristic of aromatic signals attributed to lignin (Figure 4-2). Among these signals, three types of lignin subunits can be differentiated by the number of methoxy groups on the benzene ring: zero (hydroxyphenyl lignin), one (guaiacyl lignin), and two (syringyl lignin) (**Figure 4-2**).[72]

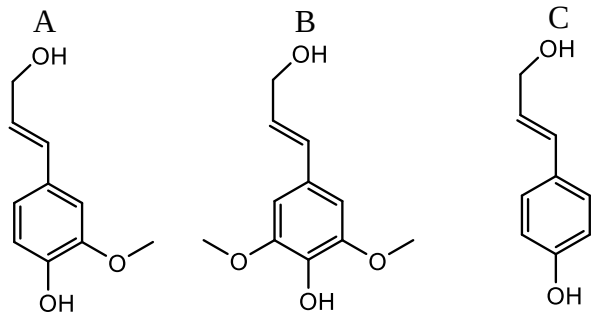


**Figure 4-2.** Phenylpropene monomer units of lignin. A) Guaiacyl lignin, precursor to guaiacol B) Syringyl lignin, precursor to syringol; C) Hydroxyphenyl lignin, precursor to phenol

The second spectral region was characteristic of polysaccharides that were established from the signals resonating at $\delta_H$ 6 ppm to $\delta_H$ 3 ppm and correlated with a $^{13}C$ region between $\delta_C$ 105 ppm to $\delta_C$ 50 ppm (**Figure 4-2**, B). This polysaccharide region was complex due to the diversity of monosaccharide units present, in addition to the lignin linkages. However, the high resolution of the experiments acquired allowed the identification of the anomeric protons of the monosaccharide subunits present in the hardwood cell-wall materials. Additionally, $^{1}H$-$^{1}H$ COSY spectra were acquired in the hardwood samples, allowing the correlation of anomeric protons with the other protons present in each saccharide moiety, referred to as a shared spin system. Three main spin systems for different saccharide monomer units were identified in COSY spectra: 2,3,6-O-triacetyl-glucose (C1-4.69 ppm, C2-4.53 ppm , C3-5.08 ppm, C4-3.67 ppm, and C5-3.84 ppm), 2,3-O-diacetyl-xylose (C2-4.76 ppm, C3-5.28 ppm, C4-3,95 ppm, C5-3.50 ppm), and 2,3,6-O-triacetyl-mannose (C1-4.92 ppm, C2-4.50 ppm , C3-4.92 ppm, C4-3.77 ppm, C5-3.31 ppm and C6-3.87 ppm). Missing residues had too low of signals in COSY to be

confirmed, but these signals correspond well to COSY spectra of acetylated cellulose and hemicellulose samples.[126,127] **Figure 4-3** shows the structures of these saccharide subunits.

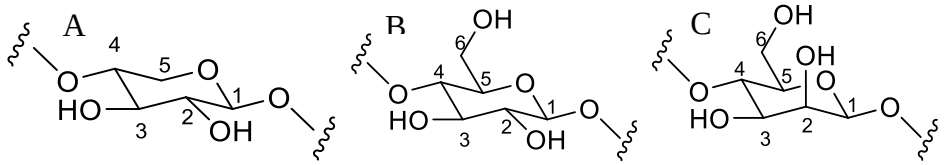


**Figure 4-3.** Chemical structures found in the polysaccharide components of cell walls.A) Xylose found in hemicellulose. B) Glucose found in cellulose C) Mannose found in hemicellulose.

Additionally, a methoxy signal was established near the polysaccharide region from $\delta_H$ 4.0 ppm to $\delta_H$ 3.3 ppm and correlated with the $^{13}C$ region between $\delta_C$ 55 ppm to $\delta_C$ 57 ppm which correspond to the methoxy groups associated primarily with lignin.[56]

**4.4.3.1** Multivariate models of select condensed smoke volatiles

The HSQC spectral data was "binned" into 834 bins for parameterization. An initial unsupervised multivariate principal component analysis (PCA) was performed to evaluate the data structure and quality (**Figure 4-4**). The replicates of the same species were in close agreement indicating good reproducibility of the data. Further examination of wood species samples indicates inherent differences with three general groupings of the samples observed based on the similarities of the chemical composition with maple, beech, apple (group 1), hickory, red oak (group 2), and mesquite (group 3).

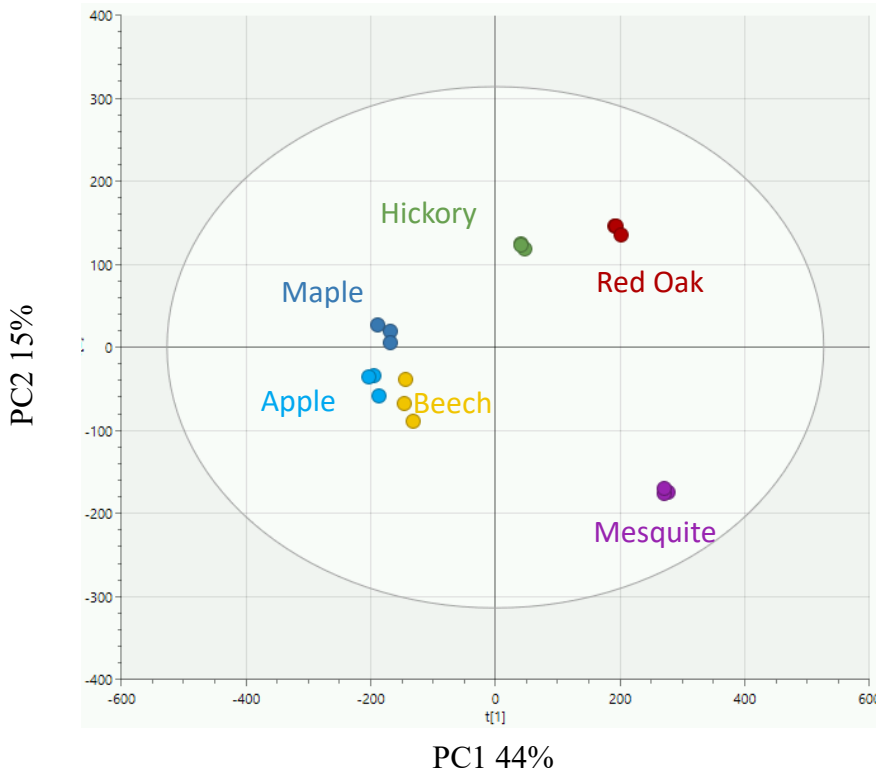


**Figure 4-4.** Scores plot for principal component analysis (PCA) of HSQC spectra from hardwood sawdust samples.

Subsequently, OPLS regression analysis was conducted to model the connection between the HSQC spectra of the wood structure and chemical composition of the condensed smoke. OPLS is a multivariate modeling technique similar to PLS that is suitable for statistical regressions in which there is a large number of variables and a low sample size. OPLS allows for better interpretability as compared to PLS because the model is able to distinguish variance that is predictive of the *y*-variable, and orthogonal variance[134]. OPLS-DA modeling has been previously used in combination with HSQC data as a method to understand differences in cell-wall composition in poplar[72].

To identify regions on the HSQC spectra that were predictive of the condensed smoke aroma compound concentrations, an OPLS-R model was constructed with each of the 27 compounds as the predictive components (*y*-variables), and the HSQC spectra as the independent variables (*x*-variables). This resulted in 27 different models with good predictive ability ($R^2Y$: 0.88-0.99, $Q^2$: 0.73-0.97). A representative OPLS model for guaiacol, a well known smoke aroma compound, is shown in **Figure 4-5**. $R^2Y$ represents the model correlation of the HSQC spectral bin intensities to the variable Y which is the aroma compound concentration and $Q^2$ represents the predictive relevance by cross-validation. $R^2$ and $Q^2$ should be <0.3 apart to avoid overfitting and minimize the correlation of irrelevant data, or noise[135]

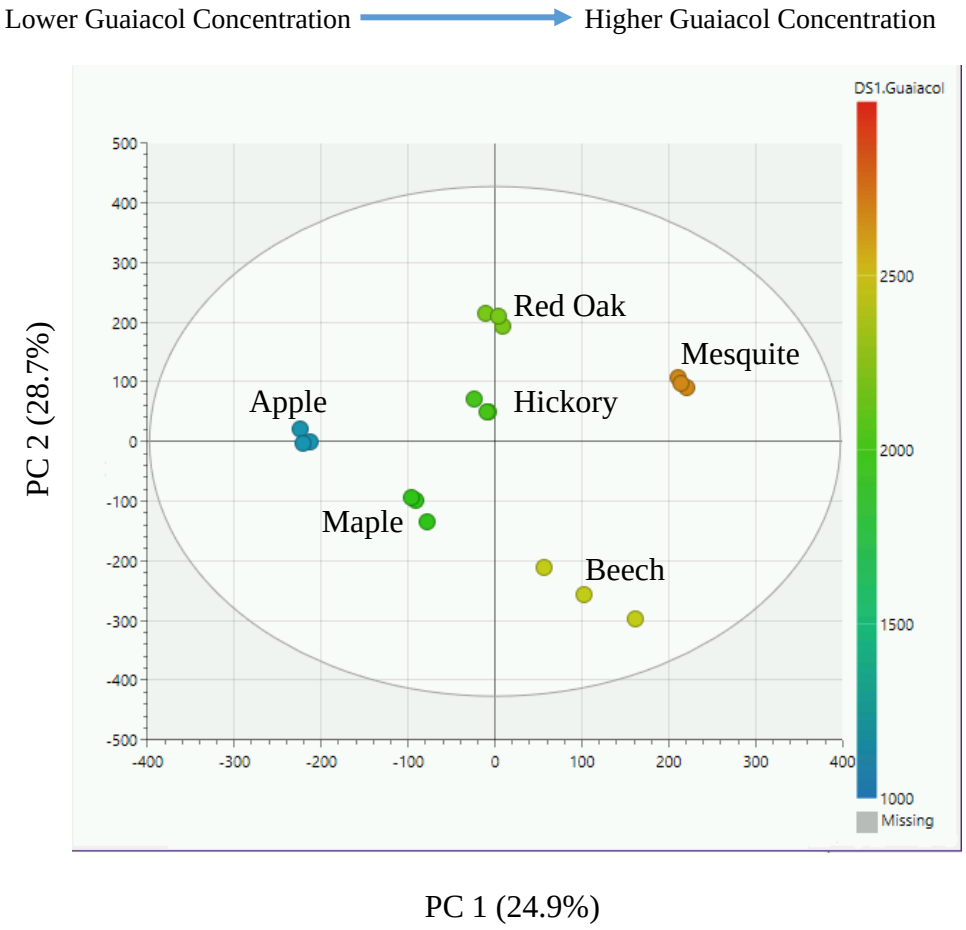


**Figure 4-5**. OPLS regression model scores scatter plot for guaiacol concentration of condensed smoke samples (n = 18) modeled with binned HSQC spectra of hardwood sawdust samples (n = 834). The X-axis represents variability explained by guaiacol concentration, and the Y-axis represents variability orthogonal to guaiacol concentration. Samples are colored by guaiacol concentration (µg/g smoke).

**4.4.3.2** Interpretation of OPLS modeling data

The OPLS model predictive variable importance in projection (VIPpred) score, which is the ability of the *x*-variable (HSQC) to predict the *y*-variable (aroma compound

concentrations) was used to identify relevant connections between wood structure and smoke aroma composition. VIPpred scores >1.0 are considered to be significant.[136] Additionally the correlation values between the *x* and *y*-variables were reported from the Y-axis of S-plot generated in the OPLS modeling, also known as p(corr), Corr(t,X), or the reliability[137]. All HSQC spectra (bins) with VIPpred score > 2.0 were compiled for each of the 27 aroma compounds and reported in **Table 4-6**.

**Table 4-6.** OPLS model wood substructures predictive of condensed smoke aroma concentrations.

| | | | Hardwood Substructure* | | | | | | | | | | | |
|---|---|---|---|---|---|---|---|---|---|---|---|---|---|---|
| | | | Glucose (cellulose) | | Xylose (hemicellulose) | | Mannose (hemicellulose) | | Methoxy (lignin) | | Syringyl lignin | | Guaiacyl lignin | |
| **Compound (Y)** | **R2Y** | **Q2** | VIPpred | P(corr) | VIPpred | p(corr) | VIPpred | p(corr) | VIPpred | p(corr) | VIPpred | p(corr) | VIPpred | p(corr) |
| 2,3-Butanedione | 0.98 | 0.96 | 3.2 | 0.8 | 3.2 | -0.97 | - | - | - | - | - | - | 2.33 | -0.97 |
| 2,3-Pentanedione | 0.96 | 0.90 | 3.4 | 0.76 | 3.4 | -0.92 | - | - | 3 | 0.45 | - | - | 2.5 | -0.96 |
| Acetol | 0.96 | 0.88 | 3.3 | -0.85 | 2.0 | 0.52 | 2.2 | -0.94 | 2.1 | 0.76 | - | - | - | - |
| 2-Methyl-2-cyclopenten-1-one | 0.91 | 0.80 | 2.1 | 0.85 | 2.2 | -0.48 | - | - | 7 | 0.82 | 2.1 | 0.82 | 2.2 | -0.64 |
| Acetic acid | 0.90 | 0.74 | 2.5 | 0.76 | 2.1 | -0.81 | - | - | 2.4 | -0.68 | - | - | 2.1 | -0.92 |
| Acetoxyacetone | 0.91 | 0.68 | 3.4 | 0.88 | - | - | - | - | 2.2 | -0.57 | | | 2.1 | 0.49 |
| Furfural | 0.97 | 0.94 | 3.2 | 0.81 | 3.1 | -0.96 | - | - | - | - | - | - | 2.3 | 0.98 |
| 2-Acetylfuran | 0.97 | 0.91 | 3.6 | 0.91 | 2.8 | -0.87 | - | - | - | - | - | - | 2.2 | -0.93 |
| Butyric acid | 0.96 | 0.93 | 2.5 | 0.61 | 3.7 | -0.94 | 2 | 0.69 | 2.4 | 0.33 | | | 2.2 | -0.91 |
| 3-Methyl-2(5H)-furanone | 0.98 | 0.95 | 3.3 | 0.84 | 3.1 | -0.95 | - | - | - | - | - | - | 2.3 | -0.97 |
| Guaiacol | 0.92 | 0.76 | 2.3 | -0.87 | 2.2 | 0.82 | 2.0 | -0.75 | 3.5 | 0.75 | - | - | - | - |
| 2,6-Dimethylphenol | 0.94 | 0.87 | 3.2 | 0.76 | 3.2 | -0.94 | - | - | 2.2 | 0.35 | - | - | - | - |
| 4-Methylguaiacol | 0.90 | 0.72 | 2.4 | -0.56 | - | - | - | - | 6.7 | 0.96 | 2.4 | 0.67 | - | - |
| Maltol | 0.99 | 0.97 | 3.5 | 0.84 | 3.2 | -0.96 | - | - | - | - | - | - | 2.3 | -0.95 |
| o-Cresol | 0.92 | 0.82 | 3.9 | 0.89 | 2.2 | -0.60 | - | - | 2.9 | 0.34 | - | - | 2.5 | 0.52 |
| 4-Ethylguaiacol | 0.95 | 0.74 | 4.0 | -0.81 | 2.2 | 0.57 | - | - | 4.3 | 0.83 | - | - | - | - |
| 2-Ethylphenol | 0.97 | 0.93 | 4.1 | 0.91 | 2.5 | -0.91 | - | - | - | - | - | - | 2.0 | -0.93 |
| 2,5-Dimethylphenol | 0.97 | 0.93 | 2.2 | -0.85 | 3.1 | 0.99 | - | - | - | - | - | - | 2.1 | 0.94 |
| 2,4-Dimethylphenol | 0.95 | 0.89 | 2.2 | 0.83 | 3.1 | -0.97 | - | - | - | - | - | - | - | - |
| p-Cresol | 0.90 | 0.80 | 2.8 | -0.61 | 3.4 | 0.90 | - | - | 3.1 | -0.45 | - | - | 2.6 | 0.94 |
| m-Cresol | 0.98 | 0.96 | 2.1 | -0.82 | 3.0 | 0.97 | - | - | - | - | - | - | 2.2 | 0.97 |
| 4-Ethylphenol | 0.90 | 0.81 | 2.4 | -0.58 | 2.6 | 0.82 | - | - | 5.1 | -0.65 | 2.2 | -0.92 | 2.6 | 0.84 |
| 3-Ethylphenol | 0.99 | 0.98 | 2.2 | -0.79 | 3.4 | 0.99 | - | - | - | - | - | - | 2.3 | 0.95 |
| 3,4-Dimethylphenol | 0.96 | 0.92 | 2.1 | -0.82 | 3.2 | 0.97 | 2.1 | -0.79 | - | - | - | - | 2.2 | 0.94 |
| Syringol | 0.91 | 0.73 | 2.4 | 0.84 | 2.3 | -0.59 | - | - | 7.2 | 0.85 | 2.0 | 0.84 | 2.0 | 0.37 |
| 4-Methylsyringol | 0.89 | 0.65 | 2.1 | 0.76 | - | - | - | - | 7.1 | 0.84 | 2.1 | 0.73 | 2.0 | -0.55 |
| Acetovanillone | 0.88 | 0.73 | 3.2 | 0.67 | 2.6 | -0.89 | - | - | 3.9 | 0.55 | - | - | 2.1 | -0.87 |

*Selected based on VIPpred score > 2 from OPLS regression model (Pareto scaling) for aroma concentration (y-variable) and NMR chemical profiling data (x-variable, n = 834) from six samples in triplicate.

Review of the VIPpred scores across the 27 OPLS models revealed six main wood substructures that were predictive of the aroma concentration in the condensed smoke samples. Two wood polysaccharides, glucose moieties from cellulose and xylose from the

xylan in hemicellulose were reported to be predictive (VIPpred scores 2.0-4.1) for 27 and 24 aroma compounds, respectively. Mannose in hemicellulose was also predictive for 4 of the 27 aroma compounds. Additionally, methoxy groups associated with lignin frequently had high VIPpred scores (2.1-7.2). Methoxy functional groups are primarily associated with lignin, but are not specific to the lignin subunit (**Figure 4-2**). Signals associated with aromatic signals on the phenolic rings of lignin (guaiacyl and syringyl) generally had lower VIPpred scores (2.0-2.6) and syringyl lignin signals were only above VIPpred score of 2.0 in 5 of the 27 models.

Interestingly, all OPLS models indicated cellulose structures (glucose subunits) were positively correlated whereas hemicellulose structures (xylose subunits) were negatively correlated or cellulose structures are negatively correlated in models where hemicellulose is positively correlated (**Table 4-6**). While both are carbohydrates, the portion of each material would be anticipated to impact the thermodynamics during the cell-wall pyrolysis. The pyrolysis of cellulose is endothermic, forming anhydrosugars, and would decrease energy availability for compound generation, whereas pyrolysis of hemicellulose is exothermic, that would increase reaction rates[50]. During holocellulose pyrolysis, increased downstream reactions have been shown to increase the yield of 2 or 3-carbon linear carbonyls. Increased downstream pyrolysis reactions of lignin have been reported to favor the formation of phenolic compounds without side-chains and methoxy groups, as well as increased alkylation[138] which would alter flavor formation. Thus, cellulose and hemicellulose can impact the degradation pathways of lignin derivatives as well as polysaccharide derivatives.

Analysis of alkylated phenolic aroma compounds reveals most were positively correlated to hemicellulose, with the exception of o-cresol, 2-ethylphenol, 2,6-dimethylphenol, and 2,4-dimethylphenol, which were positively correlated with cellulose (**Table 4-6**). The latter four phenolic compounds are substituted in the ortho-position, which is the methoxylated position of guaiacyl and syringyl lignin. The generation of ortho-methoxylated phenolic compounds is favored compared to the meta-position due to the relative stability of the ortho-quinine methide intermediate.[59] In addition decreased energy from the endothermic pyrolysis of cellulose likely contributed to the selective alkylation for ortho-substituted phenols. Other studies have corroborated the thermodegradative effects lignin, hemicellulose, and cellulose pyrolysis in model systems when studied independently rather than as a complete lignocellulosic material[5].

Presence of one or two methoxy groups on phenolic aromatic compounds in lignin is known to impact the generation of syringol or guaiacol derivatives. In addition, it is a major source of methylene radicals that can further react with carbohydrate and lignin intermediate compounds in radical-based reaction mechanisms that are common during cell-wall pyrolysis[47,60,61,139]. These findings explain the noted predictivity of methoxy regions in lignin on aroma formation (**Table 4-6**).

The final substructure, guaiacyl lignin specifically in the aromatic signal region, was reported to be predictive of aroma generation. Guaiacyl lignin is a known direct precursor to many aroma phenolic compounds. Generally this region was positively correlated to most phenolic compounds monitored, with the exception of 2-ethylphenol and the syringol derivatives 4-methylsyringol and acetovanillone (Table 4-6). The guaiacyl

lignin region was not predictive of guaiacol, 4-methylguaiacol, and 4-ethylguaiacol, but the methoxy region was highly predictive (VIPpred >4) and positively correlated. Guaiacol and related compounds could plausibly form from both guaiacyl and syringyl lignin if a demethoxylation occurs on any syringyl derivative compounds.

Overall, the results reveal the importance of intermolecular interactions during pyrolysis in the formation of condensed smoke. Polysaccharide composition was suggested to influence the selectivity of compound formation through the enthalpy effects on pyrolysis pathways[50], and thus was suggested as an parameter on the aroma profile of condensed smoke. In addition to the aforementioned mechanistic explanations, cellulose and hemicellulose are also known H-donors to radical volatile phenolics derived from lignin, which can stabilize alkylated phenols after they are formed.[140] Additionally, the methoxy region was reported to be predictive of phenolic compound generation that was derived from methoxylated lignin. The degree of lignin methoxylation has been known to impact competitive reactions that can occur in the pyrolysis of lignocellulosic materials.[140]

### **4.4.4** Limitations and Future Research

Pilot-scale smoke generation that accurately simulates commercial condensed smoke is expensive and time-consuming to operate. As such, samples were limited to only one series which consisted of the 6 samples studied. Model quality could be greatly enhanced by the expansion of the sample set to include a new series of samples with the same or similar hardwood species, which will be attained in a continuation of this study.

HSQC provides high-resolution data for mixtures of compounds but is still low resolution for solution-state analysis of cell-wall materials. Dissolution of cell walls may have been incomplete as a gel-type sample may result in preferentially high signals of more soluble components. Acetylation was done to alleviate some of the solubility issues, but information about native acetylation could also be useful for understanding pyrolysis behavior.

As in any untargeted analysis, the interpretation must consider biases that are associated with the analysis as well. Binning of HSQC spectra can result in some bins on the edges of large or broad signals having a bias toward greater VIP scores. Large signals contain more bins and they broaden with increased concentration, thus the bins on the edges would have inherently more variability. Some cell-wall structures may also have an increased range of signals that correspond to the same moiety, as seen in the large range in $^{13}C$ shift of aromatic guaiacyl carbons, which is due to the variety of lignin sidechains present and the asymmetry of the molecule as compared to syringyl lignin. The broader range could result in a smaller variation of bin intensities, and thus a smaller VIP score.

If consideration of reaction energies are driving volatile selectivity, as these data would suggest, carbohydrate and lignin substructure ratios may be important to consider in order to select appropriate smoke generation parameters, such as temperature and water content. Increased exothermic activity would require a decreased pyrolysis temperature to match the flavor components generated in a different type of wood. Additionally, manipulation of the acid content in the wood could result in increased selectivity due the

importance of hemicellulose as a proton donor. These changes would allow for more consistency in processing or the ability to selectively generate specific aroma compounds.

## **4.5** Conclusion

Six hardwood condensed smoke samples and their source hardwood sawdusts were analyzed by combining sensory descriptive analysis, quantification of 27 aroma-active compounds in the samples, and untargeted NMR HSQC analysis. It was found that sensory differences in wood smoke samples could be explained by variations in their volatile profile, which was subsequently connected to the differences in wood structure. Variation in wood structures such as hemicellulose, cellulose, and lignin impacted the OPLS-R models. This combinatory approach has promise in the understanding of wood pyrolysis to drive the formation of desirable aroma compounds.

## Bibliography


(1) Simon, R.; de la Calle, B.; Palme, S.; Meier, D.; Anklam, E. Composition and Analysis of Liquid Smoke Flavouring Primary Products. *J. Sep. Science* **2005**, *28* (9–10), 871–882. https://doi.org/10.1002/jssc.200500009.

(2) Giri, A.; Zelinkova, Z.; Wenzl, T. Experimental Design-Based Isotope-Dilution SPME-GC/MS Method Development for the Analysis of Smoke Flavouring Products. *Food Additives & Contaminants: Part A* **2017**, *34* (12), 2069–2084. https://doi.org/10.1080/19440049.2017.1374564.

(3) Guillén, M. D.; Ibargoitia, M. L. Influence of the Moisture Content on the Composition of the Liquid Smoke Produced in the Pyrolysis Process of *Fagus Sylvatica* L. Wood. *J. Agric. Food Chem.* **1999**, *47* (10), 4126–4136. https://doi.org/10.1021/jf990122e.

(4) Maga, J. A. The Flavor Chemistry of Wood Smoke. *Food Reviews International* **1987**, *3* (1–2), 139–183. https://doi.org/10.1080/87559128709540810.

(5) Jakab, E. Analytical Techniques as a Tool to Understand the Reaction Mechanism. In *Recent Advances in Thermo-Chemical Conversion of Biomass*; Elsevier, 2015; pp 75–108. https://doi.org/10.1016/B978-0-444-63289-0.00003-X.

(6) Paravisini, L.; Gourrat-Pernin, K.; Gouttefangeas, C.; Moretton, C.; Nigay, H.; Dacremont, C.; Guichard, E. Identification of Compounds Responsible for the Odorant Properties of Aromatic Caramel: Identification of the Odorant Compounds in Aromatic Caramel. *Flavour Fragr. J.* **2012**, *27* (6), 424–432. https://doi.org/10.1002/ffj.3111.

(7) Buttery, R. G.; Orts, W. J.; Takeoka, G. R.; Nam, Y. Volatile Flavor Components of Rice Cakes. *J. Agric. Food Chem.* **1999**, *47* (10), 4353–4356. https://doi.org/10.1021/jf990140w.

(8) Sequeiros, A.; Labidi, J. Characterization and Determination of the S/G Ratio via Py-GC/MS of Agricultural and Industrial Residues. *Industrial Crops and Products* **2017**, *97*, 469–476. https://doi.org/10.1016/j.indcrop.2016.12.056.

(9) Wang, H.; Chambers IV, E. Sensory Characteristics of Various Concentrations of Phenolic Compounds Potentially Associated with Smoked Aroma in Foods. *Molecules* **2018**, *23* (4), 780. https://doi.org/10.3390/molecules23040780.

(10) Guillen, M. D.; Manzanos, M. J.; Zabala, L. Study of a Commercial Liquid Smoke Flavoring by Means of Gas Chromatography/Mass Spectrometry and Fourier Transform Infrared Spectroscopy. *J. Agric. Food Chem.* **1995**, *43* (2), 463–468. https://doi.org/10.1021/jf00050a039.

(11) Söllner, K.; Schieberle, P. Decoding the Key Aroma Compounds of a Hungarian-Type Salami by Molecular Sensory Science Approaches. *J. Agric. Food Chem.* **2009**, *57* (10), 4319–4327. https://doi.org/10.1021/jf900402e.

(12) Cardinal, M.; Cornet, J.; Serot, T.; Baron, R. Effects of the Smoking Process on Odour Characteristics of Smoked Herring and Relationships with Phenolic

Compound Content. *Food Chemistry* **2006**, *96* (1), 137–146. https://doi.org/10.1016/j.foodchem.2005.02.040.
(13) Curioni, P. M. G.; Bosset, J. O. Key Odorants in Various Cheese Types as Determined by Gas Chromatography-Olfactometry. *International Dairy Journal* **2002**, *12* (12), 959–984. https://doi.org/10.1016/S0958-6946(02)00124-3.
(14) Del Toro-Gipson, R. S.; Rizzo, P. V.; Hanson, D. J.; Drake, M. Sensory Characterization of Specific Wood Smoke Aromas and Their Contributions to Smoked Cheddar Cheese Flavor. *J Sens Stud* **2020**, *35* (3). https://doi.org/10.1111/joss.12564.
(15) Martinez, C. C.; Machado, T. J. Consumer Evaluation of Cold Smoked Fat in Beef Sausages. *International Food Research Journal* **2016**, *23* (4), 1782–1786.
(16) Möhler, K. *Das Räuchern*; Fleischforschung und Praxis; Verlag der Rheinhess. Druckwerkstätte, 1978.
(17) Lingbeck, J. M.; Cordero, P.; O'Bryan, C. A.; Johnson, M. G.; Ricke, S. C.; Crandall, P. G. Functionality of Liquid Smoke as an All-Natural Antimicrobial in Food Preservation. *Meat Science* **2014**, *97* (2), 197–206. https://doi.org/10.1016/j.meatsci.2014.02.003.
(18) Kim, S. P.; Kang, M. Y.; Park, J. C.; Nam, S. H.; Friedman, M. Rice Hull Smoke Extract Inactivates Salmonella Typhimurium in Laboratory Media and Protects Infected Mice against Mortality. *Journal of Food Science* **2012**, *77* (1), M80–M85. https://doi.org/10.1111/j.1750-3841.2011.02478.x.
(19) Van Loo, E. J.; Babu, D.; Crandall, P. G.; Ricke, S. C. Screening of Commercial and Pecan Shell–Extracted Liquid Smoke Agents as Natural Antimicrobials against Foodborne Pathogens. *Journal of Food Protection* **2012**, *75* (6), 1148–1152. https://doi.org/10.4315/0362-028X.JFP-11-543.
(20) Gedela, S.; Gamble, R. K.; Macwana, S.; Escoubas, J. R.; Muriana, P. M. Effect of Inhibitory Extracts Derived from Liquid Smoke Combined with Postprocess Pasteurization for Control of Listeria Monocytogenes on Ready-to-Eat Meats†. *Journal of Food Protection* **2007**, *70* (12), 2749–2756. https://doi.org/10.4315/0362-028X-70.12.2749.
(21) Guilbaud, M.; Chafsey, I.; Pilet, M.-F.; Leroi, F.; Prévost, H.; Hébraud, M.; Dousset, X. Response of Listeria Monocytogenes to Liquid Smoke. *J Appl Microbiol* **2008**, *104* (6), 1744–1753. https://doi.org/10.1111/j.1365-2672.2008.03731.x.
(22) Martin, E. M.; O'Bryan, C. A.; Lary, R. Y.; Griffis, C. L.; Vaughn, K. L. S.; Marcy, J. A.; Ricke, S. C.; Crandall, P. G. Spray Application of Liquid Smoke to Reduce or Eliminate Listeria Monocytogenes Surface Inoculated on Frankfurters. *Meat Science* **2010**, *85* (4), 640–644. https://doi.org/10.1016/j.meatsci.2010.03.017.
(23) Montazeri, N.; Oliveira, A. C. M.; Himelbloom, B. H.; Leigh, M. B.; Crapo, C. A. Chemical Characterization of Commercial Liquid Smoke Products. *Food Sci Nutr* **2013**, *1* (1), 102–115. https://doi.org/10.1002/fsn3.9.

(24) Morey, A.; Bratcher, C. L.; Singh, M.; McKee, S. R. Effect of Liquid Smoke as an Ingredient in Frankfurters on Listeria Monocytogenes and Quality Attributes. *Poultry Science* **2012**, *91* (9), 2341–2350. https://doi.org/10.3382/ps.2012-02251.
(25) Dibner, J. J.; Buttin, P. Use of Organic Acids as a Model to Study the Impact of Gut Microflora on Nutrition and Metabolism. *Journal of Applied Poultry Research* **2002**, *11* (4), 453–463. https://doi.org/10.1093/japr/11.4.453.
(26) Milly, P. J.; Toledo, R. T.; Ramakrishnan, S. Determination of Minimum Inhibitory Concentrations of Liquid Smoke Fractions. *Journal of Food Science* **2005**, *70* (1), M12–M17. https://doi.org/10.1111/j.1365-2621.2005.tb09040.x.
(27) Milly, P. J. ANTIMICROBIAL PROPERTIES OF LIQUID SMOKE FRACTIONS, The University of Georgia, Athens, Georgia, 2003.
(28) Guillén, M. D.; Ibargoitia, M. L. New Components with Potential Antioxidant and Organoleptic Properties, Detected for the First Time in Liquid Smoke Flavoring Preparations. *J. Agric. Food Chem.* **1998**, *46* (4), 1276–1285. https://doi.org/10.1021/jf970952x.
(29) Soldera, S.; Sebastianutto, N.; Bortolomeazzi, R. Composition of Phenolic Compounds and Antioxidant Activity of Commercial Aqueous Smoke Flavorings. *J. Agric. Food Chem.* **2008**, *56* (8), 2727–2734. https://doi.org/10.1021/jf072117d.
(30) Riha, W. E.; Wendorff, W. L. Browning Potential of Liquid Smoke Solutions: Comparison of Two Methods. *J Food Science* **1993**, *58* (3), 671–674. https://doi.org/10.1111/j.1365-2621.1993.tb04353.x.
(31) Yost, M.; Abu-Ali, J. M.; Barringer, S. A. Kinetics of Potato Color and Texture Development during Baking, Frying, and Microwaving with the Addition of Liquid Smoke. *J Food Science* **2006**, *71* (9), E364–E369. https://doi.org/10.1111/j.1750-3841.2006.00171.x.
(32) Fox, J. B.; Ackerman, S. A. Formation of Nitric Oxide Myoglobin: Mechanisms of the Reaction with Various Reductants. *J Food Science* **1968**, *33* (4), 364–370. https://doi.org/10.1111/j.1365-2621.1968.tb03631.x.
(33) Pathare, P. B.; Opara, U. L.; Al-Said, F. A.-J. Colour Measurement and Analysis in Fresh and Processed Foods: A Review. *Food Bioprocess Technol* **2013**, *6* (1), 36–60. https://doi.org/10.1007/s11947-012-0867-9.
(34) *Liquid Smoke Market Size, Share & Trends Analysis Report By Application (Meat Products, Sauces, Dairy Products, Pet Food), By Region, And Segment Forecasts, 2019 - 2025*; GVR-2-68038-936-4; Grand View Research, 2018.
(35) Maga, J. A. *Smoke in Food Processing*, 1st ed.; CRC Press, 1988.
(36) *Ingredients in Meat Products*; Tarté, R., Ed.; Springer New York: New York, NY, 2009. https://doi.org/10.1007/978-0-387-71327-4.
(37) Cadwallader, K. Wood Smoke Flavor. In *Handbook of Meat, Poultry, and Seafood Quality*; Blackwell Pub: Ames, Iowa, 2007; pp 201–210.
(38) IARC Working Group on the Evaluation of Carcinogenic Risks to Humans. *IARC Monographs on the Evaluation of Carcinogenic Risks to Humans, Volume 114 ; Red Meat and Processed Meat*; IARC monographs on the evaluation of carcinogenic risks to humans; IARC Press: Lyon, 2018.

(39) EU. Commission Regulation (EU) No 836/2011 of 19 August 2011 Amending Regulation (EC) No 333/2007 Laying down the Methods of Sampling and Analysis for the Official Control of the Levels of Lead, Cadmium, Mercury, Inorganic Tin, 3-MCPD and Benzo(a)Pyrene in FoodstuffsText with EEA Relevance. **2011**, 8.
(40) Compilation of Air Pollutant Emissions Factors (AP-42); Enivronmental Protection Agency: Reserach Triangle Park, NC, 1995; Vol. 1, p 9.5.2-1-9.5.2-6.
(41) Kawamoto, H.; Saka, Shiro. Pyrolysis Mechanism of Woody Biomass Relating to Product Selectivity. *ACS Symp. Ser.* **2007**, *954* , 363–376. https://doi.org/10.1021/bk-2007-0954.ch023.
(42) Manyà, J. J.; Velo, E.; Puigjaner, L. Kinetics of Biomass Pyrolysis: A Reformulated Three-Parallel-Reactions Model. *Ind. Eng. Chem. Res.* **2003**, *42* (3), 434–441. https://doi.org/10.1021/ie020218p.
(43) Raveendran, K. Pyrolysis Characteristics of Biomass and Biomass Components. *Fuel* **1996**, *75* (8), 987–998. https://doi.org/10.1016/0016-2361(96)00030-0.
(44) Ben, H.; Ragauskas, A. J. Heteronuclear Single-Quantum Correlation-Nuclear Magnetic Resonance (HSQC-NMR) Fingerprint Analysis of Pyrolysis Oils. *Energy Fuels* **2011**, *25* , 5791–5801. https://doi.org/10.1021/ef201376w.
(45) Dieguez-Alonso, A.; Anca-Couce, A.; Zobel, N.; Behrendt, F. Understanding the Primary and Secondary Slow Pyrolysis Mechanisms of Holocellulose, Lignin and Wood with Laser-Induced Fluorescence. *Fuel* **2015**, *153*, 102–109. https://doi.org/10.1016/j.fuel.2015.02.097.
(46) Evans, R. J.; Milne, T. A. Molecular Characterization of the Pyrolysis of Biomass. *Energy Fuels* **1987**, *1* (2), 123–137. https://doi.org/10.1021/ef00002a001.
(47) Sharma, R. K.; Wooten, J. B.; Baliga, V. L.; Lin, X.; Geoffrey Chan, W.; Hajaligol, M. R. Characterization of Chars from Pyrolysis of Lignin. *Fuel* **2004**, *83* (11–12), 1469–1482. https://doi.org/10.1016/j.fuel.2003.11.015.
(48) Timell, T. E. Recent Progress in the Chemistry of Wood Hemicelluloses. *Wood Sci.Technol.* **1967**, *1* (1), 45–70. https://doi.org/10.1007/BF00592255.
(49) Ibn Yaich, A.; Edlund, U.; Albertsson, A.-C. Transfer of Biomatrix/Wood Cell Interactions to Hemicellulose-Based Materials to Control Water Interaction. *Chem. Rev.* **2017**, *117* (12), 8177–8207. https://doi.org/10.1021/acs.chemrev.6b00841.
(50) Yang, H.; Yan, R.; Chen, H.; Lee, D. H.; Zheng, C. Characteristics of Hemicellulose, Cellulose and Lignin Pyrolysis. *Fuel* **2007**, *86* (12–13), 1781–1788. https://doi.org/10.1016/j.fuel.2006.12.013.
(51) Ball, R.; Mcintosh, A. C.; Brindley, J. Feedback Processes in Cellulose Thermal Decomposition: Implications for Fire-Retarding Strategies and Treatments. *Combustion Theory and Modelling* **2004**, *8* (2), 281–291. https://doi.org/10.1088/1364-7830/8/2/005.
(52) Wang, S.; Ru, B.; Lin, H.; Sun, Wuxing. Pyrolysis Behaviors of Four O-Acetyl-Preserved Hemicelluloses Isolated from Hardwoods and Softwoods. *Fuel* **2015**, *150* , 243–251. https://doi.org/10.1016/j.fuel.2015.02.045.

(53) Lupoi, J. S.; Singh, S.; Parthasarathi, R.; Simmons, B. A.; Henry, R. J. Recent Innovations in Analytical Methods for the Qualitative and Quantitative Assessment of Lignin. *Renewable and Sustainable Energy Reviews* **2015**, *49*, 871–906. https://doi.org/10.1016/j.rser.2015.04.091.

(54) Adler, E. Lignin Chemistry: Past, Present and Future. *Wood Sci. Technol.* **1977**, *11* (3), 169–218. https://doi.org/10.1007/BF00365615.

(55) Bunzel, M.; Ralph, J. NMR Characterization of Lignins Isolated from Fruit and Vegetable Insoluble Dietary Fiber. *J. Agric. Food Chem.* **2006**, *54* (21), 8352–8361. https://doi.org/10.1021/jf061525z.

(56) Mansfield, S. D.; Kim, H.; Lu, F.; Ralph, J. Whole Plant Cell Wall Characterization Using Solution-State 2D NMR. *Nat Protoc* **2012**, *7* (9), 1579–1589. https://doi.org/10.1038/nprot.2012.064.

(57) Wang, H.-M.; Wang, B.; Wen, J.-L.; Yuan, T.-Q.; Sun, R.-C. Structural Characteristics of Lignin Macromolecules from Different *Eucalyptus* Species. *ACS Sustainable Chem. Eng.* **2017**, *5* (12), 11618–11627. https://doi.org/10.1021/acssuschemeng.7b02970.

(58) Ohra-aho, T.; Gomes, F. J. B.; Colodette, J. L.; Tamminen, T. S/G Ratio and Lignin Structure among Eucalyptus Hybrids Determined by Py-GC/MS and Nitrobenzene Oxidation. *Journal of Analytical and Applied Pyrolysis* **2013**, *101*, 166–171. https://doi.org/10.1016/j.jaap.2013.01.015.

(59) Kawamoto, H. Lignin Pyrolysis Reactions. *J Wood Sci* **2017**, *63* (2), 117–132. https://doi.org/10.1007/s10086-016-1606-z.

(60) Hosoya, T.; Kawamoto, H.; Saka, Shiro. Role of Methoxyl Group in Char Formation from Lignin-Related Compounds. *J. Anal. Appl. Pyrolysis* **2009**, *84* , 79–83. https://doi.org/10.1016/j.jaap.2008.10.024.

(61) Dieguez-Alonso, A.; Anca-Couce, A.; Zobel, N.; Behrendt, Frank. Understanding the Primary and Secondary Slow Pyrolysis Mechanisms of Holocellulose, Lignin and Wood with Laser-Induced Fluorescence. *Fuel* **2015**, *153* , 102–109. https://doi.org/10.1016/j.fuel.2015.02.097.

(62) Kawamoto, H.; Watanabe, T.; Saka, S. Strong Interactions during Lignin Pyrolysis in Wood – A Study by in Situ Probing of the Radical Chain Reactions Using Model Dimers. *Journal of Analytical and Applied Pyrolysis* **2015**, *113*, 630–637. https://doi.org/10.1016/j.jaap.2015.04.009.

(63) Zhang, T.; Li, X.; Guo, L.; Guo, Xin. Reaction Mechanisms in Pyrolysis of Hardwood, Softwood, and Kraft Lignin Revealed by ReaxFF MD Simulations. *Energy Fuels* **2019**, *33* , 11210–11225. https://doi.org/10.1021/acs.energyfuels.9b02843.

(64) Yuan, S.; Chen, X.; Li, J.; Wang, F. CO 2 Gasification Kinetics of Biomass Char Derived from High-Temperature Rapid Pyrolysis. *Energy Fuels* **2011**, *25* (5), 2314–2321. https://doi.org/10.1021/ef200051z.

(65) Zanzi, R.; Sjostrom, K.; Bjornbom, E. Rapid Pyrolysis of Agricultural Residues at High Temperature. *Biomass and Bioenergy* **2002**, 10.

(66) Gu, X.; Ma, X.; Li, L.; Liu, C.; Cheng, K.; Li, Zhongzheng. Pyrolysis of Poplar Wood Sawdust by TG-FTIR and Py-GC/MS. *J. Anal. Appl. Pyrolysis* **2013**, *102* , 16–23. https://doi.org/10.1016/j.jaap.2013.04.009.

(67) Dong, C.; Zhang, Z.; Lu, Q.; Yang, Y. Characteristics and Mechanism Study of Analytical Fast Pyrolysis of Poplar Wood. *Energy Conversion and Management* **2012**, *57*, 49–59. https://doi.org/10.1016/j.enconman.2011.12.012.

(68) Becker, E. D. *High Resolution NMR: Theory and Chemical Applications*, 3rd. ed.; Academic Press: San Diego, CA, 2000.

(69) Chang, H.; Cowling, E. B.; Brown, W. Comparative Studies on Cellulolytic Enzyme Lignin and Milled Wood Lignin of Sweetgum and Spruce. *Holzforschung* **1975**, *29* (5), 153–159. https://doi.org/10.1515/hfsg.1975.29.5.153.

(70) Cheng, K.; Sorek, H.; Zimmermann, H.; Wemmer, D. E.; Pauly, M. Solution-State 2D NMR Spectroscopy of Plant Cell Walls Enabled by a Dimethylsulfoxide- $d_6$ /1-Ethyl-3-Methylimidazolium Acetate Solvent. *Anal. Chem.* **2013**, *85* (6), 3213–3221. https://doi.org/10.1021/ac303529v.

(71) Ben, H.; Hao, N.; Liu, Q.; Ragauskas, A. J. Solid-State NMR Investigation of Bio-Chars Produced from Biomass Components and Whole Biomasses. *Bioenerg. Res.* **2017**, *10* (4), 1036–1044. https://doi.org/10.1007/s12155-017-9863-2.

(72) Hedenström, M.; Wiklund-Lindström, S.; Öman, T.; Lu, F.; Gerber, L.; Schatz, P.; Sundberg, B.; Ralph, J. Identification of Lignin and Polysaccharide Modifications in Populus Wood by Chemometric Analysis of 2D NMR Spectra from Dissolved Cell Walls. *Molecular Plant* **2009**, *2* (5), 933–942. https://doi.org/10.1093/mp/ssp047.

(73) Alonso, A.; Marsal, S.; JuliÃ, A. Analytical Methods in Untargeted Metabolomics: State of the Art in 2015. *Front. Bioeng. Biotechnol.* **2015**, *3*. https://doi.org/10.3389/fbioe.2015.00023.

(74) Nicholson, J. K.; Holmes, E.; Kinross, J.; Burcelin, R.; Gibson, G.; Jia, W.; Pettersson, S. Host-Gut Microbiota Metabolic Interactions. *Science* **2012**, *336* (6086), 1262–1267. https://doi.org/10.1126/science.1223813.

(75) Wikoff, W. R.; Anfora, A. T.; Liu, J.; Schultz, P. G.; Lesley, S. A.; Peters, E. C.; Siuzdak, G. Metabolomics Analysis Reveals Large Effects of Gut Microflora on Mammalian Blood Metabolites. *Proceedings of the National Academy of Sciences* **2009**, *106* (10), 3698–3703. https://doi.org/10.1073/pnas.0812874106.

(76) Wang, L.; Zhang, R.; Li, J.; Guo, L.; Yang, H.; Ma, F.; Yu, H. Comparative Study of the Fast Pyrolysis Behavior of Ginkgo, Poplar, and Wheat Straw Lignin at Different Temperatures. *Industrial Crops and Products* **2018**, *122*, 465–472. https://doi.org/10.1016/j.indcrop.2018.06.038.

(77) Kim, K.; Kurata, T.; Fujimaki, M. Identification of Flavor Constituents in Carbonyl, Non-Carbonyl Neutral and Basic Fractions of Aqueous Smoke Condensates. *Agricultural and Biological Chemistry* **1974**, *38* (1), 53–63. https://doi.org/10.1080/00021369.1974.10861117.

(78) Guillén, M. D.; Manzanos, M. J.; Ibargoitia, M. L. Carbohydrate and Nitrogenated Compounds in Liquid Smoke Flavorings. *J. Agric. Food Chem.* **2001**, *49* (5), 2395–2403. https://doi.org/10.1021/jf000760t.
(79) REGULATION (EC) No 2065/2003 on Smoke Flavourings Used or Intended for Use in or on Foods. European Comission.
(80) Simon, R.; Palme, S.; Anklam, E. Single-Laboratory Validation of a Gas Chromatography–Mass Spectrometry Method for Quantitation of 15 European Priority Polycyclic Aromatic Hydrocarbons in Spiked Smoke Flavourings. *Journal of Chromatography A* **2006**, *1103* (2), 307–313. https://doi.org/10.1016/j.chroma.2005.11.020.
(81) Kostyra, E.; Baryłko-Pikielna, N. Volatiles Composition and Flavour Profile Identity of Smoke Flavourings. *Food Quality and Preference* **2006**, *17* (1–2), 85–95. https://doi.org/10.1016/j.foodqual.2005.06.008.
(82) Meilgaard, M.; Civille, G. V.; Carr, B. T. *Sensory Evaluation Techniques*, 2nd ed.; CRC Press: Boca Raton, 1991.
(83) Acree, T. E.; Barnard, J.; Cunningham, D. G. A Procedure for the Sensory Analysis of Gas Chromatographic Effluents. *Food Chemistry* **1984**, *14* (4), 273–286. https://doi.org/10.1016/0308-8146(84)90082-7.
(84) Ullrich, F.; Grosch, W. Identification of the Most Intense Volatile Flavour Compounds Formed during Autoxidation of Linoleic Acid. *Z Lebensm Unters Forch* **1987**, *184* (4), 277–282. https://doi.org/10.1007/BF01027663.
(85) Grosch, W. Determination of Potent Odourants in Foods by Aroma Extract Dilution Analysis (AEDA) and Calculation of Odour Activity Values (OAVs). *Flavour Fragr. J.* **1994**, *9* (4), 147–158. https://doi.org/10.1002/ffj.2730090403.
(86) Kosowska, M.; Majcher, M. A.; Jeleń, H. H.; Fortuna, T. Key Aroma Compounds in Smoked Cooked Loin. *J. Agric. Food Chem.* **2018**, *66* (14), 3683–3690. https://doi.org/10.1021/acs.jafc.7b05996.
(87) Poisson, L.; Schieberle, P. Characterization of the Key Aroma Compounds in an American Bourbon Whisky by Quantitative Measurements, Aroma Recombination, and Omission Studies. *J. Agric. Food Chem.* **2008**, *56* (14), 5820–5826. https://doi.org/10.1021/jf800383v.
(88) Schoenauer, S.; Schieberle, P. Characterization of the Key Aroma Compounds in the Crust of Soft Pretzels by Application of the Sensomics Concept. *J. Agric. Food Chem.* **2019**, *67* (25), 7110–7119. https://doi.org/10.1021/acs.jafc.9b02601.
(89) Straßer, S.; Schieberle, P. Characterization of the Key Aroma Compounds in Roasted Duck Liver by Means of Aroma Extract Dilution Analysis: Comparison with Beef and Pork Livers. *Eur Food Res Technol* **2014**, *238* (2), 307–313. https://doi.org/10.1007/s00217-013-2095-6.
(90) Escudero, A.; Gogorza, B.; Melús, M. A.; Ortín, N.; Cacho, J.; Ferreira, V. Characterization of the Aroma of a Wine from Maccabeo. Key Role Played by Compounds with Low Odor Activity Values. *J. Agric. Food Chem.* **2004**, *52* (11), 3516–3524. https://doi.org/10.1021/jf035341l.

(91) Peterson, D. G.; Reineccius, G. A. Characterization of the Volatile Compounds That Constitute Fresh Sweet Cream Butter Aroma. *Flavour Fragr. J.* **2003**, *18* (3), 215–220. https://doi.org/10.1002/ffj.1192.
(92) Atanasova, B.; Thomas-Danguin, T.; Langlois, D.; Nicklaus, S.; Chabanet, C.; Etiévant, P. Perception of Wine Fruity and Woody Notes: Influence of Peri-Threshold Odorants. *Food Quality and Preference* **2005**, *16* (6), 504–510. https://doi.org/10.1016/j.foodqual.2004.10.004.
(93) Bult, J. H. F. The Influence of Olfactory Concept on the Probability of Detecting Sub- and Peri-Threshold Components in a Mixture of Odorants. *Chemical Senses* **2001**, *26* (5), 459–469. https://doi.org/10.1093/chemse/26.5.459.
(94) Pino, J. A. Characterisation of Volatile Compounds in a Smoke Flavouring from Rice Husk. *Food Chemistry* **2014**, *153*, 81–86. https://doi.org/10.1016/j.foodchem.2013.12.041.
(95) Pu, D.; Zhang, Y.; Zhang, H.; Sun, B.; Ren, F.; Chen, H.; Tang, Y. Characterization of the Key Aroma Compounds in Traditional Hunan Smoke-Cured Pork Leg (Larou, THSL) by Aroma Extract Dilution Analysis (AEDA), Odor Activity Value (OAV), and Sensory Evaluation Experiments. *Foods* **2020**, *9* (4), 413. https://doi.org/10.3390/foods9040413.
(96) Kawamoto, H.; Murayama, M.; Saka, S. Pyrolysis Behavior of Levoglucosan as an Intermediate in Cellulose Pyrolysis: Polymerization into Polysaccharide as a Key Reaction to Carbonized Product Formation. *J Wood Sci* **2003**, *49* (5), 469–473. https://doi.org/10.1007/s10086-002-0487-5.
(97) Guillen, M. D.; Ibargoitia, M. L. GC/MS Analysis of Lignin Monomers, Dimers and Trimers in Liquid Smoke Flavourings. *J Sci Food Agric* **1999**, 15.
(98) Majcher, M. A.; Jeleń, H. H. Key Odorants of Oscypek, a Traditional Polish Ewe's Milk Cheese. *J. Agric. Food Chem.* **2011**, *59* (9), 4932–4937. https://doi.org/10.1021/jf2002602.
(99) E18 Committee. *Practice for Determination of Odor and Taste Thresholds By a Forced-Choice Ascending Concentration Series Method of Limits*; ASTM International. https://doi.org/10.1520/E0679-19.
(100) Jaffe, T. R.; Wang, H.; Chambers, E. Determination of a Lexicon for the Sensory Flavor Attributes of Smoked Food Products: JAFFE et Al. *J Sens Stud* **2017**, *32* (3), e12262. https://doi.org/10.1111/joss.12262.
(101) Shigeto, A.; Hachisuka, S.; Kumazawa, K. Characterization of Potent Odorants in Three Different Cultivars (Madagascar, Comoro and Tahiti) of Vanilla Bean by Aroma Extract Dilution Analysis (AEDA). *FSTR* **2016**, *22* (6), 811–816. https://doi.org/10.3136/fstr.22.811.
(102) Bamber, R. K. Sapwood & Heartwood. *Forestry Commision of New South Wales* **1963**, No. 2, 8.
(103) Rowell, R.; Pettersen, R.; Tshabalala, M. Cell Wall Chemistry. In *Handbook of Wood Chemistry and Wood Composites, Second Edition*; CRC Press, 2012; pp 33–72. https://doi.org/10.1201/b12487-5.

(104) EFSA Panel on Food Contact Materials, Enzymes, Flavourings and Processing Aids (CEF). Scientific Opinion on Safety of Smoke Flavour - Primary Product – AM 01. *EFS2* **2010**, *8* (1). https://doi.org/10.2903/j.efsa.2009.1396.
(105) EFSA Panel on Food Contact Materials, Enzymes, Flavourings and Processing Aids (CEF). Scientific Opinion on the Safety of Smoke Flavour Primary Product Scansmoke R909. *EFS2* **2010**, *8* (1). https://doi.org/10.2903/j.efsa.2009.1395.
(106) EFSA Panel on Food Contact Materials, Enzymes, Flavourings and Processing Aids (CEF). Scientific Opinion on Safety of Smoke Flavour Primary Product – TRADISMOKE™ A MAX. *EFS2* **2010**, *8* (1). https://doi.org/10.2903/j.efsa.2009.1394.
(107) EFSA Panel on Food Contact Materials, Enzymes, Flavourings and Processing Aids (CEF). Scientific Opinion on the Safety of Smoke Flavour Primary Product Zesti Smoke Code 10 - 2011 Update. *EFS2* **2011**, *9* (7). https://doi.org/10.2903/j.efsa.2011.2307.
(108) European Food Safety Authority (EFSA). Safety of Smoke Flavour Primary Product - Scansmoke PB 1110. *EFS2* **2009**, *7* (4). https://doi.org/10.2903/j.efsa.2009.1056.
(109) European Food Safety Authority (EFSA). Safety of Smoke Flavour Primary Product - Scansmoke SEF7525. *EFS2* **2009**, *7* (6). https://doi.org/10.2903/j.efsa.2009.1093.
(110) European Food Safety Authority (EFSA). Safety of Smoke Flavour Primary Product Smoke Concentrate 809045. *EFS2* **2009**, *7* (4). https://doi.org/10.2903/j.efsa.2009.981.
(111) European Food Safety Authority (EFSA). Safety of Smoke Flavour Primary Product – SmokEz C-10. *EFS2* **2009**, *7* (6). https://doi.org/10.2903/j.efsa.2009.1091.
(112) European Food Safety Authority (EFSA). Safety of Smoke Flavour Primary Product – SmokEz Enviro 23. *EFS2* **2009**, *7* (6). https://doi.org/10.2903/j.efsa.2009.1092.
(113) European Food Safety Authority (EFSA). Safety of Smoke Flavour Primary Product Unismoke. *EFS2* **2009**, *7* (4). https://doi.org/10.2903/j.efsa.2009.983.
(114) Fagerson, I. S. Thermal Degradation of Carbohydrates; a Review. *J. Agric. Food Chem.* **1969**, *17* (4), 747–750. https://doi.org/10.1021/jf60164a019.
(115) Ginz, M.; Balzer, H. H.; Bradbury, A. G. W.; Maier, H. G. Formation of Aliphatic Acids by Carbohydrate Degradation during Roasting of Coffee. *European Food Research and Technology* **2000**, *211* (6), 404–410. https://doi.org/10.1007/s002170000215.
(116) Fricke, K.; Schieberle, P. Characterization of the Key Aroma Compounds in a Commercial Milk Chocolate by Application of the Sensomics Approach. *J. Agric. Food Chem.* **2020**, *68* (43), 12086–12095. https://doi.org/10.1021/acs.jafc.0c05787.
(117) Akiyama, M.; Murakami, K.; Hirano, Y.; Ikeda, M.; Iwatsuki, K.; Wada, A.; Tokuno, K.; Onishi, M.; Iwabuchi, H. Characterization of Headspace Aroma Compounds of Freshly Brewed Arabica Coffees and Studies on a Characteristic

Aroma Compound of Ethiopian Coffee. *J Food Science* **2008**, *73* (5), C335–C346. https://doi.org/10.1111/j.1750-3841.2008.00752.x.
(118) Grosch, W. Flavour of Coffee. A Review. *Nahrung* **1998**, *42* (06), 344–350. https://doi.org/10.1002/(SICI)1521-3803(199812)42:06<344::AID-FOOD344>3.0.CO;2-V.
(119) Wang, H.; Chambers, E.; Kan, J. Sensory Characteristics of Combinations of Phenolic Compounds Potentially Associated with Smoked Aroma in Foods. *Molecules* **2018**, *23* (8), 1867. https://doi.org/10.3390/molecules23081867.
(120) Holley, R. A.; Patel, D. Improvement in Shelf-Life and Safety of Perishable Foods by Plant Essential Oils and Smoke Antimicrobials. *Food Microbiology* **2005**, *22* (4), 273–292. https://doi.org/10.1016/j.fm.2004.08.006.
(121) Diebold, J. P. *A Review of the Chemical and Physical Mechanisms of the Storage Stability of Fast Pyrolysis Bio-Oils*; NREL/SR-570-27613, 753818; 1999; p NREL/SR-570-27613, 753818. https://doi.org/10.2172/753818.
(122) Zhang, Y.; Silcock, P.; Jones, J. R.; Eyres, G. T. Changes in Wood Smoke Volatile Composition by Manipulating the Smoke Generation Conditions. *Journal of Analytical and Applied Pyrolysis* **2020**, 104769. https://doi.org/10.1016/j.jaap.2019.104769.
(123) Xin, X.; Bissett, A.; Wang, J.; Gan, A.; Dell, K.; Baroutian, S. Production of Liquid Smoke Using Fluidised-Bed Fast Pyrolysis and Its Application to Green Lipped Mussel Meat. *Food Control* **2021**, *124*, 107874. https://doi.org/10.1016/j.foodcont.2021.107874.
(124) Sink, J. D.; Hsu, L. A. Chemical Effects of Smoke Processing on Frankfurter Quality and Palatability Characteristics. *Meat Science* **1979**, *3* (4), 247–253. https://doi.org/10.1016/0309-1740(79)90001-9.
(125) Wen, J.-L.; Sun, S.-L.; Xue, B.-L.; Sun, R.-C. Recent Advances in Characterization of Lignin Polymer by Solution-State Nuclear Magnetic Resonance (NMR) Methodology. *Materials* **2013**, *6* (1), 359–391. https://doi.org/10.3390/ma6010359.
(126) Kono, H. Chemical Shift Assignment of the Complicated Monomers Comprising Cellulose Acetate by Two-Dimensional NMR Spectroscopy. *Carbohydrate Research* **2013**, *375*, 136–144. https://doi.org/10.1016/j.carres.2013.04.019.
(127) Naran, R.; Black, S.; Decker, S. R.; Azadi, P. Extraction and Characterization of Native Heteroxylans from Delignified Corn Stover and Aspen. *Cellulose* **2009**, *16* (4), 661–675. https://doi.org/10.1007/s10570-009-9324-y.
(128) Ralph, S.; Ralph, J. NMR Database of Lignin and Cell Wall Model Compounds. 2009.
(129) Maga, J. A.; Fapojuwo, O. O. AROMA INTENSITIES OF VARIOUS WOOD SMOKE FRACTIONS. *J Sensory Studies* **1986**, *1* (1), 9–13. https://doi.org/10.1111/j.1745-459X.1986.tb00155.x.
(130) Swaney-Stueve, M.; Talavera, M.; Jepsen, T.; Severns, B.; Wise, R.; Deubler, G. Sensory and Consumer Evaluation of Smoked Pulled Pork Prepared Using Different Smokers and Different Types of Wood: Evaluation of Smoked Pulled

Pork…. *Journal of Food Science* **2019**, *84* (3), 640–649. https://doi.org/10.1111/1750-3841.14469.
(131) Koso, T.; Rico del Cerro, D.; Heikkinen, S.; Nypelö, T.; Buffiere, J.; Perea-Buceta, J. E.; Potthast, A.; Rosenau, T.; Heikkinen, H.; Maaheimo, H.; Isogai, A.; Kilpeläinen, I.; King, A. W. T. 2D Assignment and Quantitative Analysis of Cellulose and Oxidized Celluloses Using Solution-State NMR Spectroscopy. *Cellulose* **2020**, *27* (14), 7929–7953. https://doi.org/10.1007/s10570-020-03317-0.
(132) Wen, J.-L.; Sun, S.-L.; Xue, B.-L.; Sun, R.-C. Recent Advances in Characterization of Lignin Polymer by Solution-State Nuclear Magnetic Resonance (NMR) Methodology. *Materials* **2013**, *6* (1), 359–391. https://doi.org/10.3390/ma6010359.
(133) Pettolino, F. A.; Walsh, C.; Fincher, G. B.; Bacic, A. Determining the Polysaccharide Composition of Plant Cell Walls. *Nat Protoc* **2012**, *7* (9), 1590–1607. https://doi.org/10.1038/nprot.2012.081.
(134) Sadeghi-Bazargani, H.; Fathi; Savadi-Oskouei; Farhoudi, M.; Mehdizadeh Esfanjani. OPLS Statistical Model versus Linear Regression to Assess Sonographic Predictors of Stroke Prognosis. *NDT* **2012**, 387. https://doi.org/10.2147/NDT.S33991.
(135) Veerasamy, R.; Rajak, H.; Jain, A.; Sivadasan, S.; Varghese, C. P.; Agrawal, R. K. Validation of QSAR Models - Strategies and Importance. 10.
(136) Galindo-Prieto, B.; Eriksson, L.; Trygg, J. Variable Influence on Projection (VIP) for Orthogonal Projections to Latent Structures (OPLS): Variable Influence on Projection for OPLS. *J. Chemometrics* **2014**, *28* (8), 623–632. https://doi.org/10.1002/cem.2627.
(137) Wiklund, S.; Johansson, E.; Sjöström, L.; Mellerowicz, E. J.; Edlund, U.; Shockcor, J. P.; Gottfries, J.; Moritz, T.; Trygg, J. Visualization of GC/TOF-MS-Based Metabolomics Data for Identification of Biochemically Interesting Compounds Using OPLS Class Models. *Anal. Chem.* **2008**, *80* (1), 115–122. https://doi.org/10.1021/ac0713510.
(138) Dong, C.; Zhang, Z.; Lu, Q.; Yang, Y. Characteristics and Mechanism Study of Analytical Fast Pyrolysis of Poplar Wood. *Energy Convers. Manage.* **2012**, *57* , 49–59. https://doi.org/10.1016/j.enconman.2011.12.012.
(139) Bradbury, A. G. W.; Sakai, Y.; Shafizadeh, F. A Kinetic Model for Pyrolysis of Cellulose. *J. Appl. Polym. Sci.* **1979**, *23* (11), 3271–3280. https://doi.org/10.1002/app.1979.070231112.
(140) Hosoya, T.; Kawamoto, H.; Saka, S. Solid/Liquid- and Vapor-Phase Interactions between Cellulose- and Lignin-Derived Pyrolysis Products. *Journal of Analytical and Applied Pyrolysis* **2009**, *85* (1–2), 237–246. https://doi.org/10.1016/j.jaap.2008.11.028.